



Norwegian University  
of Life Sciences

**Master's Thesis 2019 30 ECTS**  
Faculty of Science and Technology

# **Valorization of glycerol into new bulk chemicals: hydrogen, propylene glycol and propanols.**

Federico Muscolino  
Mechanics and Process Technology



# Preface

The subject of this thesis was proposed by Professor Jorge Mario Marchetti, leader of the Reaction Engineering and Catalysis Group at Norwegian University of Life Sciences.

The increasing quantities of glycerol released during processing of biodiesel have saturated its global market. This by-product is nowadays a waste that needs to be disposed and can compromise the sustainability of biodiesel processing, environmentally and economically. To address this issue, it is necessary to find routes that convert glycerol into valuable commodities.

This thesis has studied two processes, steam reforming and hydrogenolysis, to valorize glycerol respectively in three products: hydrogen, propylene glycol and propanols. The analysis is performed at chemical, process and economical level; the most profitable conversion route is identified.

A special thank is expressed to Professor Marchetti for the interesting proposal and valuable supervision during the semester.

Oslo, May 10<sup>th</sup>, 2019

---

Federico Muscolino

# Sammendrag

I prosessering av biodiesel er glycerol omtrent 10% av det totale produktet som er frigjort. Hvis dette var en merverdi i den tidlige industrialiseringen av prosessen, er det i dag et problem. Ved den økende produksjonsraten av biodiesel, overskrider den totale glycerol frigjort sitt globale markedet. Dette overskuddet har redusert verdien av bioglycerol, noe som gjør at det ikke er et biprodukt lenger, men et avfall som er kostbart å avhende. Denne situasjonen kan compromittere miljøbegrepet av biodiesel og gjøre hans produksjonen dyrere.

Formålet med denne masteroppgaven er å finne ruter for å omdanne glycerol til verdifulle varer, for å beholde biodieselsprosess bærekraftig. En litteraturforskning av vitenskapelige artikler har identifisert tre produkter som kan oppnås ved katalytisk omdannelse av bioglycerol: hydrogen, propylenglykol og propanoler. Disse kjemikaliene har store bruksområder og viser en økende etterspørsel: bioproduksjonen av hvert av dem alene kunne lett absorbere all glycerol frigjort i biodieselsprosessering. Hydrogen kan oppnås ved dampreforming, den mest anvendte prosessen for tiden i bruk for produksjon av denne varen fra metan. Propylenglykol og propanoler kan oppnås gjennom en prosess som kalles hydrogenolyse.

De fleste artikler som er funnet, er relatert til dampreforming av glycerol til hydrogen og hydrogenolyse av glycerol til propylenglykol. Studier om omdannelse av glycerol til propanoler er i stedet fortsatt begrenset. Det er interessant at analysen viser felles mønstre. Katalysatoren er det kritiske elementet i alle konverteringsprosesser. De mest effektive er basert på edle metaller, men deres kostnadene hindrer omfanget av applikasjonen fra laboratorium til industrielt nivå. Katalysatorer basert på overgangsmetaller er lettere tilgjengelige og billigere, men de er mer påvirket av forgiftning og deaktivering. Derfor undersøker forskningen hvordan de skal gjøres mer effektive og resistente. Kombinasjonen av kjemiske forbindelser som alumina, silika og zirkonium tilsatt i katalytisk støtte viser seg å være en lovende løsning.

Flere katalysatorer, basert på nikkel og kobber, er blitt testet henholdsvis i dampreforming til hydrogen og hydrogenolyse til propylenglykol. Selv om problemene av deaktivering ikke er fullstendig løst, viser økonomiske vurderinger at det kan oppnås fortjeneste med den tilgjengelige teknologien, ved å erstatte katalysatoren som vedlikeholdsoperasjon når det trengs. Produksjon av hydrogen fører til litt høyere fortjeneste enn produksjon av propylenglykol; likevel er investeringen for bygging av en dampreformeringsanlegg 31 ganger høyere. Dette arbeidet vurderer derfor hydrogenolyse til propylenglykol som den beste prosessen for å verdsette glycerol, ved å føre til fortjeneste på laveste investering.

Videre arbeid kan utvide resultatene funnet gjennom denne masteroppgaven. En interessant casestudie som kan vurderes teknisk og økonomisk sett, er konvertering til glycerol av en eksisterende dampreformeringsanlegg basert på metan. Dette alternativet kan være rimeligere med hensyn til investeringskostnader og føre til høyere fortjeneste enn å bygge et nytt anlegg. Ytterligere studier kunne vurdere lønnsomheten i produksjon av hydrogen og propylenglykol ved å bruke de nyeste katalysatorene som ble utviklet.

# Abstract

In processing of biodiesel, about 10% of the total product released is glycerol. If this was an added value in the early industrialization of the process, nowadays it's an issue. At the increasing production rates of biodiesel, the total quantities of glycerol released exceed its global market. This oversupply has reduced the value of bio-glycerol, making it not a by-product anymore, but a waste that is costly to dispose. This situation can compromise the environmental concept of biodiesel and make its production more expensive.

The purpose of this thesis is to find routes to convert glycerol into valuable commodities, so to keep the biodiesel processing sustainable. A literature research of scientific articles has identified three products that can be obtained through catalytic conversion of bio-glycerol: hydrogen, propylene glycol and propanols. These chemicals have wide applications and show an increasing demand: the bio-production of any of them alone could easily absorb all glycerol released in biodiesel processing. Hydrogen can be obtained by steam reforming, the most applied process currently in use for production of this commodity from methane. Propylene glycol and propanols can be obtained through a process called hydrogenolysis.

Most of articles found are related to steam reforming of glycerol into hydrogen and hydrogenolysis of glycerol into propylene glycol. Studies on conversion of glycerol into propanols are instead still limited. Interestingly, the analysis shows common patterns. The catalyst is the critical element in all conversion processes. The most performing ones are based on noble metals, whose cost however hinder the scale up of the application from laboratory to industrial level. Catalysts based on transition metals are more easily available and cheaper, but they are more affected by poisoning and deactivation. Therefore, research is investigating how to make them more performing and resistant. The combination of chemical compounds like alumina, silica and zirconia added in the catalytic support is showing to be a promising solution.

Several catalysts, based on nickel and copper, have been tested respectively in steam reforming to hydrogen and hydrogenolysis to propylene glycol. Even if the issues of deactivation are not completely solved, economic assessments show that profit can be achieved with the available technology, by replacing the catalyst as maintenance operation when required. Production of hydrogen leads to a slightly higher profit than production of propylene glycol; however, the investment required for the construction of a steam reforming plant is 31 times higher. Therefore, this work does assess hydrogenolysis to propylene glycol as the best process to valorize glycerol, by making profit at the lowest investment.

Further work could extend the results found in this thesis. An interesting case study to be assessed technically and economically is the conversion to glycerol of an existing steam reforming plant based on methane. This option might be more affordable in terms of investment costs and lead to higher profits than constructing a new plant. Additional studies could assess the profitability of hydrogen and propylene glycol production using the latest catalysts developed.



# Table of Contents

Preface.....	i
Sammendrag.....	ii
Abstract.....	iii
1 Introduction.....	1
1.1 Scope of work.....	2
2 Hydrogen and other bulk chemicals from glycerol.....	3
3 Valorization of glycerol into hydrogen.....	5
3.1 Steam reforming - Reactions.....	5
3.2 Steam reforming - Catalysts.....	7
3.3 Latest catalytic development.....	8
3.3.1 Ni catalysts supported on Silica-Zirconia.....	8
3.3.2 Ni catalysts supported on Zirconia-Alumina.....	13
3.3.3 Transition metal catalysts supported on Attapulgite.....	15
3.3.4 Ni catalysts supported on Niobia-Alumina.....	23
3.3.5 Comparison of catalysts analysed.....	30
3.4 Techno-economic assessment of steam reforming plant.....	31
3.4.1 Technical assessment.....	34
3.4.2 Economic assessment.....	38
3.4.3 Conclusions.....	40
4 Valorization of glycerol into propylene glycol.....	41
4.1 Hydrogenolysis - Reactions.....	42
4.2 Hydrogenolysis - Catalysts.....	42
4.3 Catalytic development.....	44
4.4 Techno-economic assessment of hydrogenolysis plant.....	45
4.4.1 Process description.....	45
4.4.2 Technical assessment.....	49
4.4.3 Economic assessment.....	50
4.4.4 Conclusions.....	51
5 Valorization of glycerol into propanols.....	53
5.1 Introduction.....	53
5.2 Double layer catalysts.....	54
5.3 Noble metal-based catalysts.....	56

6	Discussion of literature review .....	59
6.1	Potential of bio-processes.....	59
6.2	Catalytic development of bio-processes.....	59
6.3	Comparison of techno-economic assessments .....	61
6.4	Suggestions for future work .....	63
7	Conclusion .....	65
8	Appendix .....	67
9	References .....	73

## Abbreviations

ASU: Air Separation Unit

ATP: Attapulgate

BAU: Business as Usual (route)

COP: Coefficient of Performance

EP: Economic Potential

GB: Glycerol Based (route)

LHSV: Liquid Hourly Space Velocity

Mt: million tonnes

O&M: Operational and Maintenance

1,2-PD: propylene glycol (1,2-propanediol)

PFD: Process Flow Diagram

PSA: Pressure Swing Adsorption unit

S: Selectivity

SPECCA: Specific Primary Energy Consumption for CO<sub>2</sub> Avoided

TAC: Total Annualized Cost

WHSV: Weight Hourly Space Velocity

wt: weight

X: Conversion

Y: Yield



# List of figures

<b>Figure 1.</b> Biodiesel produced and glycerol released in period 2000-2025. ....	1
<b>Figure 2.</b> Commercial applications of glycerol. ....	2
<b>Figure 3.</b> Conversion of glycerol into hydrogen: scientific articles by process. ....	4
<b>Figure 4.</b> Different reactions to convert glycerol into valuable products. ....	4
<b>Figure 5.</b> Ni catalysts supported on SiZr: glycerol conversion. ....	9
<b>Figure 6.</b> Ni catalysts supported on SiZr: H <sub>2</sub> selectivity and yield. ....	10
<b>Figure 7.</b> Ni catalysts supported on SiZr: selectivity to CO <sub>2</sub> and CO. ....	10
<b>Figure 8.</b> Ni catalysts supported on SiZr: selectivity to CH <sub>4</sub> . ....	11
<b>Figure 9.</b> Ni catalysts supported on SiZr: molar ratios H <sub>2</sub> /CO and CO/CO <sub>2</sub> . ....	12
<b>Figure 10.</b> Metal catalysts supported on ATP: glycerol conversion. ....	16
<b>Figure 11.</b> Metal catalysts supported on ATP: hydrogen selectivity. ....	17
<b>Figure 12.</b> Metal catalysts supported on ATP: CO selectivity. ....	18
<b>Figure 13.</b> Metal catalysts supported on ATP: CO <sub>2</sub> selectivity. ....	18
<b>Figure 14.</b> Metal catalysts supported on ATP: CH <sub>4</sub> selectivity. ....	19
<b>Figure 15.</b> Metal catalysts supported on ATP: molar ratio H <sub>2</sub> /CO. ....	19
<b>Figure 16.</b> Ni/ATP catalyst: performance during stability test. ....	20
<b>Figure 17.</b> Co/ATP catalyst: performance during stability test. ....	21
<b>Figure 18.</b> Cu/ATP catalyst: performance during stability test. ....	21
<b>Figure 19.</b> Fe/ATP catalyst: performance during stability test. ....	22
<b>Figure 20.</b> Nb supported catalysts: glycerol conversion. ....	24
<b>Figure 21.</b> Nb supported catalysts: glycerol conversion into gas. ....	24
<b>Figure 22.</b> Nb supported catalysts: H <sub>2</sub> yield. ....	25
<b>Figure 23.</b> Nb supported catalysts: H <sub>2</sub> production. ....	26
<b>Figure 24.</b> Nb supported catalysts: selectivity to H <sub>2</sub> . ....	26
<b>Figure 25.</b> Nb supported catalysts: yields to CO. ....	27
<b>Figure 26.</b> Nb supported catalysts: yields to CO <sub>2</sub> . ....	27
<b>Figure 27.</b> Nb supported catalysts: yields to CH <sub>4</sub> . ....	28
<b>Figure 28.</b> Schematic of steam reforming plant: H <sub>2</sub> production with CO <sub>2</sub> capture. ....	32
<b>Figure 29.</b> Schematic of steam reforming plant: power generation with CO <sub>2</sub> capture. ....	32
<b>Figure 30.</b> Schematic of steam reforming plant: H <sub>2</sub> and power cogeneration with CO <sub>2</sub> capture. ....	33
<b>Figure 31.</b> Glycerol reforming plants: specific investment costs. ....	38
<b>Figure 32.</b> Glycerol reforming plants: specific O&M costs. ....	39
<b>Figure 33.</b> Glycerol reforming plants: cumulative cash flow analysis of H <sub>2</sub> production cases. ....	40
<b>Figure 34.</b> Commercial applications of propylene glycol. ....	41
<b>Figure 35.</b> Hydrolysis reaction of propylene oxide into propylene glycol. ....	41
<b>Figure 36.</b> Hydrogenolysis reaction of glycerol into propylene glycol. ....	42
<b>Figure 37.</b> PFD: non-catalytic hydrolysis of propylene oxide. ....	45
<b>Figure 38.</b> PFD: isothermal hydrogenolysis at high pressure with external H <sub>2</sub> . ....	46
<b>Figure 39.</b> PFD: non-isothermal hydrogenolysis at ambient pressure with external H <sub>2</sub> . ....	47
<b>Figure 40.</b> PFD: isothermal hydrogenolysis at high pressure with H <sub>2</sub> generated in situ. ....	48
<b>Figure 41.</b> Production of propylene glycol: specific TAC and EP per route. ....	50
<b>Figure 42.</b> Production of propylene glycol: specific TAC and EP under uncertainty. ....	51
<b>Figure 43.</b> Synthetic routes to propanols: fossil and glycerol based. ....	53
<b>Figure 44.</b> Hydrogenolysis into propanols: performance by ratio H <sub>2</sub> /NiAl <sub>2</sub> O <sub>3</sub> . ....	55
<b>Figure 45.</b> Specific TAC and EP: hydrogen vs propylene glycol. ....	62

## List of tables

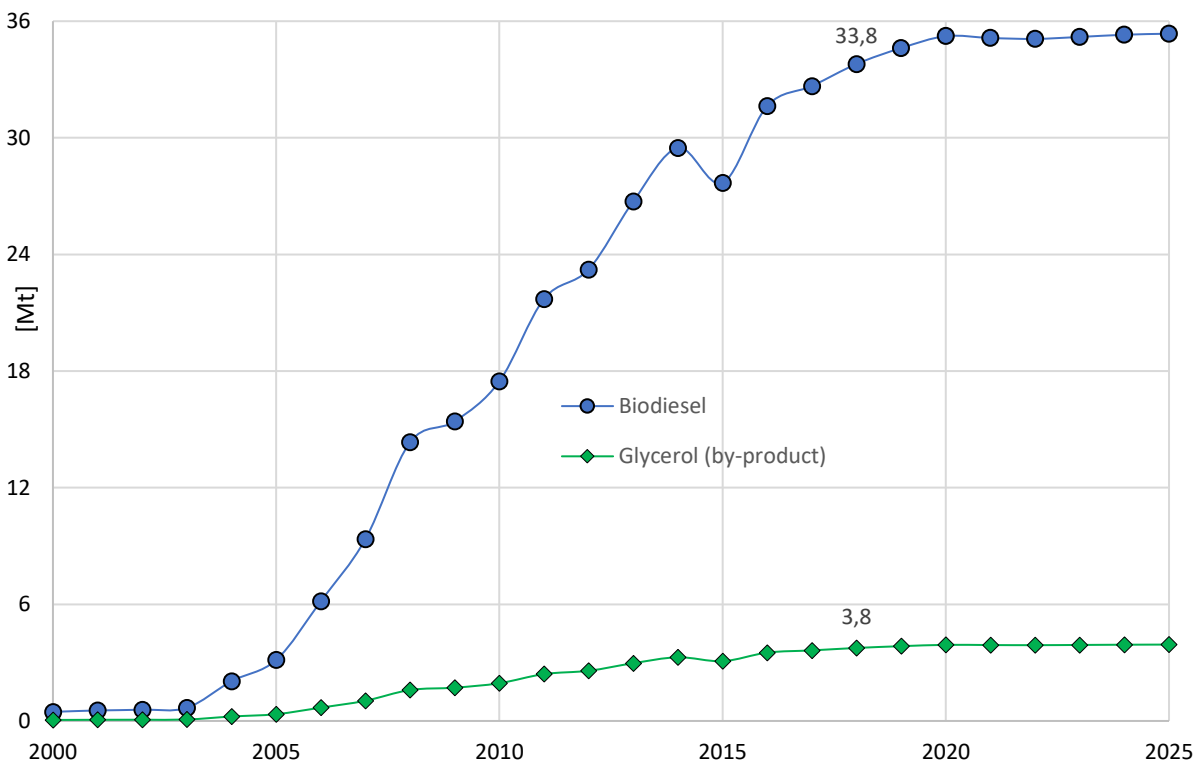
<b>Table 1.</b> Main characteristics of glycerol.....	3
<b>Table 2.</b> Reactions involved in steam reforming of glycerol.....	6
<b>Table 3.</b> Steam reforming of glycerol into hydrogen: performance of Ni based catalysts. ....	8
<b>Table 4.</b> Ni catalysts supported on SiZr: performance during stability test.....	12
<b>Table 5.</b> Textural properties of NiZr <sub>x</sub> Al catalysts.....	13
<b>Table 6.</b> Performance of NiZr <sub>x</sub> Al catalysts.....	14
<b>Table 7.</b> Quantification of deposited coke on the spent NiZr <sub>x</sub> Al catalysts. ....	15
<b>Table 8.</b> Carbon deposition and particle size of spent ATP supported catalysts. ....	23
<b>Table 9.</b> Carbon deposition and particle size of spent Nb supported catalysts.....	29
<b>Table 10.</b> Performance of latest catalysts for steam reforming of glycerol. ....	30
<b>Table 11.</b> Design cases of glycerol reforming plants.....	31
<b>Table 12.</b> Glycerol reforming plants: main design parameters.....	34
<b>Table 13.</b> Plants performance indicators: H <sub>2</sub> production. ....	35
<b>Table 14.</b> Plants performance indicators: power production. ....	36
<b>Table 15.</b> Plant performance indicators: flexible H <sub>2</sub> and power co-generation. ....	37
<b>Table 16.</b> Production costs of H <sub>2</sub> and electricity and capture costs of CO <sub>2</sub> . ....	39
<b>Table 17.</b> Hydrogenolysis to propylene glycol: performance of catalysts by preparation method.....	43
<b>Table 18.</b> Production of propylene glycol: specific mass and energy balances per route. ....	49
<b>Table 19.</b> Hydrogenolysis into propanols: performance of single and double layer catalysts.....	54
<b>Table 20.</b> Hydrogenolysis into propanols: performance over time of H-β/NiO/Al <sub>2</sub> O <sub>3</sub> .....	56
<b>Table 21.</b> Hydrogenolysis into propanols: performance of noble metal-based catalysts.....	56

# 1 Introduction

Statistics made by Organisation for Economic Co-operation and Development - Food and Agriculture Organization, report that the worldwide production of biodiesel has increased from 0,5 million tonnes in the year 2000 to 33,8 Mt in 2018. Projections for the near future foresee that the production will settle to 35,4 million tonnes in 2025 (OECD-FAO, 2017).

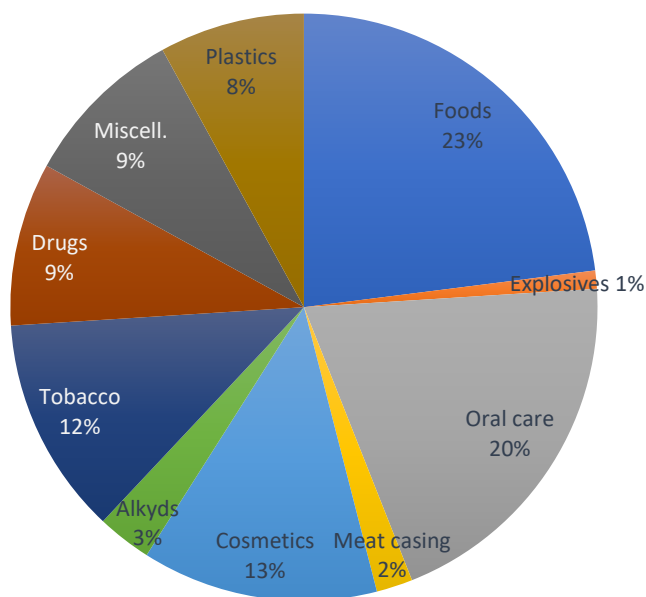
Biodiesel is produced by transesterification of vegetable oil or animal fats with an alcohol, typically methanol. The product of this reaction is about 90% weight biodiesel and 10% wt glycerol (Schwengber et al., 2016), (Zhao et al., 2019).

Figure 1 shows the quantities of biodiesel produced and the related glycerol released as by-product from year 2000 to 2025 (period 2019-2025 is projected). In 2018 as example, the production of biodiesel accounted for 33,8 million tonnes and 3,8 Mt of glycerol were released as by-product.



*Figure 1. Biodiesel produced and glycerol released in period 2000-2025.*

Glycerol finds several commercial applications, reported in figure 2; however, its global consumption is less than 0,5 million tonnes per year. The rising demand for biodiesel as renewable fuel has therefore created a surplus of glycerol, causing an oversupply crisis worldwide (Lin, 2013).



Reprinted (adapted) from (Lin, 2013), Copyright (2013), with permission from Elsevier.

**Figure 2.** Commercial applications of glycerol.

The market's saturation was evident in 2006, when Procter & Gamble Chemicals closed its glycerol's refinery in England, and in 2007 when Dow Chemical shut down its production of synthetic glycerol in Texas (Anitha et al., 2016).

The glycerol released from biodiesel production is called "crude" glycerol: in addition to water, it contains impurities left from its processing, like alcohol and salts. It is therefore less valuable than refined glycerol that could be sold for applications i.e. in pharmaceutical industry. The equipment for purification of crude glycerol is expensive, reason why it is usually available at large biodiesel plants but not at smaller producers. Nowadays, with the oversupply crisis, the cost of purification might be not sustainable anymore, and the crude glycerol ends up as waste that needs to be disposed. This is both an environmental and economic issue, because the disposal service increases the production costs. In order to maintain biodiesel production sustainable, it is necessary to find technologies to transform this crude glycerol in added value products that don't saturate the market (Anitha et al., 2016).

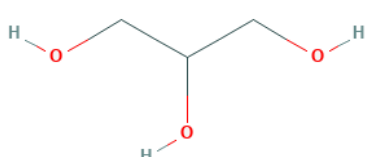
## 1.1 Scope of work

This thesis shall identify one or more valuable products that can be obtained from glycerol and study the related conversion processes. The commodities shall have a significant market, so that using bio-glycerol as feedstock for their production could absorb relevant part of the quantities released from biodiesel processing. The study shall analyse the level of development of conversion processes, to understand if they are close to their industrialization stage.

## 2 Hydrogen and other bulk chemicals from glycerol

Glycerol, also called glycerine, is a tri-hydroxy alcohol. At ambient conditions it appears as a hygroscopic viscous liquid, colourless to brown. Its main characteristics are reported in table 1 (NCBI, 2019<sup>a</sup>).

*Table 1. Main characteristics of glycerol.*

IUPAC name:	propane-1,2,3-triol
Structure:	
Formula:	$C_3H_8O_3$ or $CH_2OH-CHOH-CH_2OH$
Molar mass:	92,1 g/mol
Boiling point:	290 °C
Melting point:	18 °C
Density:	1260 kg/m <sup>3</sup>
Viscosity:	954 cP at 25 °C

The glycerol's molecule is made of 14 atoms of three different elements: carbon, hydrogen and oxygen. Hydrogen is present with 8 atoms accounting for 57% of the total. This suggests that glycerol can be used as feedstock to produce hydrogen gas.

Hydrogen has a growing potential as biofuel both in combustion engines and in fuel cells applications, therefore it represents a valuable valorization of glycerol. Conversion of glycerol into hydrogen is possible through several processes; however, the most widely applied is steam reforming (Anitha et al., 2016).

A literature research on valorization of glycerol has been conducted. The research has resulted in almost 200 scientific articles found about conversion into hydrogen, describing more than 10 different processes to produce hydrogen gas from glycerol. The result is presented in figure 3: the Pareto chart shows that 97 scientific articles, 52% of total, focus on steam reforming, suggesting it as the most promising method. Steam reforming is followed by photocatalytic reforming, supercritical water reforming and aqueous phase reforming. These 4 methods collect the 80% of total documentation found.

The literature research has suggested other products obtainable from glycerol. Figure 4 shows an overview of several reactions to valorize glycerol into bulk chemicals. Hydrogenolysis leads to propylene glycol, a commodity of increasing importance (Nanda et al., 2016): after hydrogen, it is the second chemical with most scientific articles found on conversion from glycerol. A deeper hydrogenolysis of glycerol produces further commodities of growing demand: propanols (Samudrala and B., 2018).

This thesis will study the catalytic steam reforming of glycerol into hydrogen, and the catalytic hydrogenolysis of glycerol into propylene glycol and propanols.

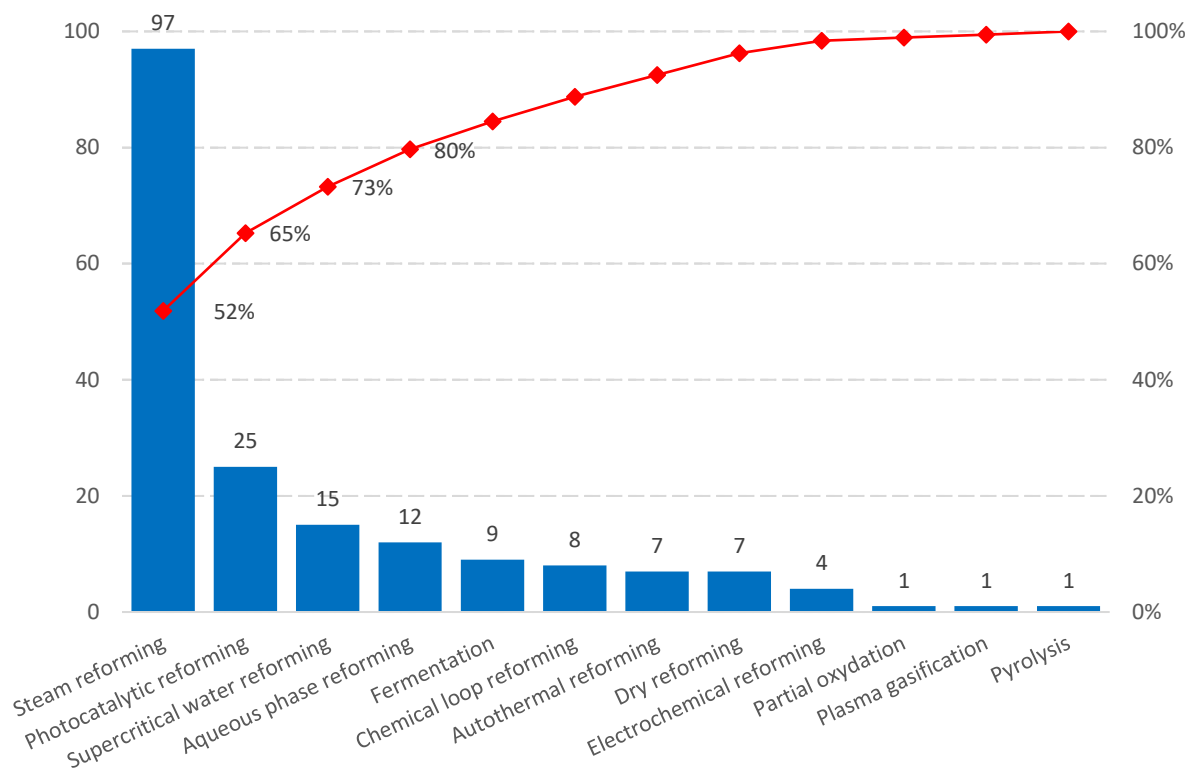
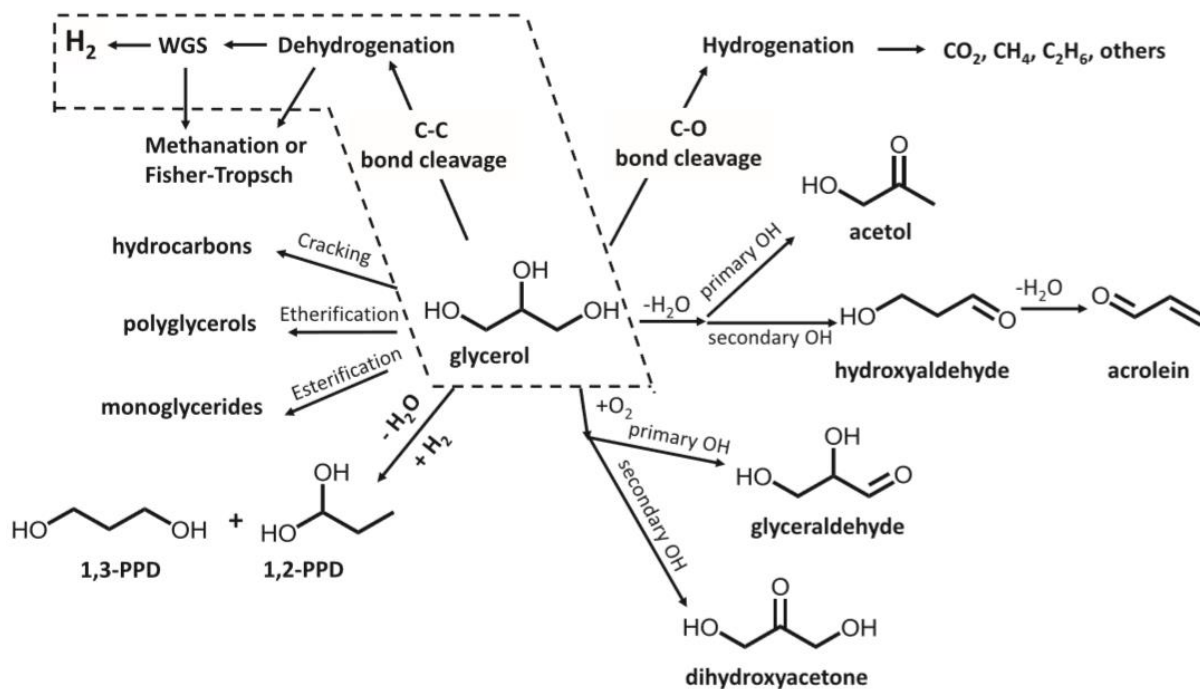


Figure 3. Conversion of glycerol into hydrogen: scientific articles by process.



Reprinted from (Sad et al., 2015), Copyright (2015), with permission from Elsevier.

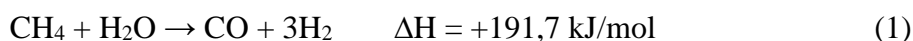
Figure 4. Different reactions to convert glycerol into valuable products.

## 3 Valorization of glycerol into hydrogen

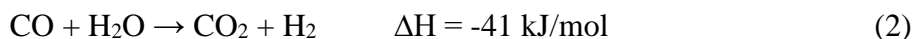
### 3.1 Steam reforming - Reactions

The worldwide production of hydrogen accounts for 57 million tonnes per year (Badwal et al., 2013). Almost the whole, 95% of the total, is derived from fossil fuels: natural gas (48%), heavy oils (30%) and coal (17%). The remaining 5% is produced by electrolysis of water (4%) and from biomass (1%). Overall, steam reforming of methane is the dominant route (Menezes et al., 2018).

During reforming of natural gas, methane reacts with steam at atmospheric pressure and high temperatures in the range of 700-1100 °C. In a first stage, the reaction is endothermic and it yields syngas, a mix of hydrogen and carbon monoxide:



In a second stage, carbon monoxide reacts with water vapour at lower temperature, ~130 °C generating carbon dioxide and further hydrogen:



This reaction is called water shift gas and it is exothermic, releasing about 21% of the heat required by the first one. The total process is therefore endothermic and needs heat supply. The major part of it is generally provided by burning a portion of methane, while some heat is generated by side reactions, where carbon monoxide is oxidized into carbon dioxide (Avasthi et al., 2013).

Steam reforming can be utilized to valorize glycerol into hydrogen. It is considered the most promising process because its scale up to industrial level would not require significant changes in the current infrastructure employed for reforming of methane. Moreover, during steam reforming the hydrogen produced is simultaneously removed from the steam: this increases the yield of the reaction, making it preferable to other conversion processes (Schwengber et al., 2016).

There are several main and side reactions involved in steam reforming of glycerol: they are reported in table 2.

**Table 2.** Reactions involved in steam reforming of glycerol.

Chemical equation <sup>a</sup>	$\Delta H_{298}^0$ [kJ/mol]	Type of reaction	Reference
$C_3H_8O_3(g) + 3H_2O(g) \rightarrow 3CO_2(g) + 7H_2(g)$ (3)	+128	Global reaction	(Charisiou et al., 2019)
$C_3H_8O_3(g) \rightarrow 3CO(g) + 4H_2(g)$ (4)	+245	Glycerol decomposition	
$CO(g) + H_2O(g) \rightleftharpoons CO_2(g) + H_2(g)$ (2)	-41	Water-gas shift	
$CO(g) + 3H_2(g) \rightleftharpoons CH_4(g) + H_2O(g)$ (5)	-206	Methanation	(Schwengber et al., 2016)
$CO_2(g) + 4H_2(g) \rightleftharpoons CH_4(g) + 2H_2O(g)$ (6)	-165	Methanation	(Charisiou et al., 2019)
$CH_4(g) + H_2O(g) \rightleftharpoons 3H_2(g) + CO(g)$ (1)	+191,7	Methane steam reforming	
$CH_4(g) + CO_2(g) \rightarrow 2H_2(g) + 2CO(g)$ (7)	+247	Methane dry reforming	
$CO(g) + H_2(g) \rightleftharpoons C(s) + H_2O(g)$ (8)	-131	Coke formation	(Schwengber et al., 2016)
$CH_4(g) \rightarrow 2H_2(g) + C(s)$ (9)	+75,6	Coke formation	(Charisiou et al., 2019)
$2CO(g) \rightleftharpoons CO_2(g) + C(s)$ (10)	-172	Coke formation	(Schwengber et al., 2016)
$CO_2(g) + 2H_2(g) \rightleftharpoons 2H_2O(g) + C(s)$ (11)	-90	Coke formation	(Menezes et al., 2018)

<sup>a</sup> (g): gas phase, (s): solid phase.

Glycerol's steam reforming is described by the global reaction 3, which is mainly a combination of thermal decomposition of glycerol (eq. 4) and water gas shift reactions (eq. 2). It can be noted comparing equation 3 vs equations 1 and 2, that the molar ratio of hydrogen to the feedstock is 7:1 by reacting glycerol, and 4:1 by reacting methane. Therefore, the stoichiometric analysis shows that reforming of glycerol is more attractive than reforming of methane, because 7 moles of hydrogen are formed per each mole of glycerol, instead of 4. Moreover, glycerol's reforming requires a temperature range of 800-1000 K, lower than reforming of methane (Avasthi et al., 2013).

However, real operation shows that the moles of hydrogen obtained in glycerol's steam reforming range from a minimum of 4 to a maximum of 6 (Avasthi et al., 2013). In fact, several side reactions are usually present: methanation, methane steam and dry reforming, and carbon formation; their entity depending on the operating conditions. The main side reactions are methanation and coke formation, shown by equations 5-6 and 8-11, respectively. During methanation, carbon monoxide and carbon dioxide react with hydrogen to produce methane. During coke formation, carbon atoms are released from carbon monoxide, carbon dioxide or methane. Both phenomena have a negative effect on reforming performance: the first by reducing the available moles of hydrogen, the second by releasing carbon that tends to deposit into the catalyst, blocking and deactivating its active sites (Schwengber et al., 2016).



In general, coke formation does increase with increasing temperatures of reaction (Avasthi et al., 2013), but it is also triggered by high concentration of glycerol and low reaction temperatures (Charisiou et al., 2019). Coke formation can be prevented by use of large amount of water: according Le Chatelier's principle, this would promote the water gas shift reaction, facilitating the gasification of carbon and hydrogen production (Schwengber et al., 2016).

Methanation is promoted by low temperatures and therefore can be prevented by increasing temperature of reaction (Schwengber et al., 2016); at temperatures higher than 650 °C, formation of CH<sub>4</sub> is inhibited by the reaction of methane steam reforming. In general, with rising temperatures, the reactions of water gas shift and methanation are promoted in backward direction, leading to an increase of CO gas (Charisiou et al., 2019).

According to several studies, the optimal conditions for steam reforming are with a molar ratio water to glycerol 6:1 and 9:1 (the choice depending on catalyst and temperature: refer to table 3), and at a temperature range of 525-725 °C. However, this would cost higher consumption of energy to vaporize the excess of water, more complexity in process control to maintain the temperature in the correct range and higher capital cost for the construction of the reactor. An alternative would be to operate in vacuum conditions instead of atmospheric, so to allow for lower reaction temperatures (Schwengber et al., 2016).

## 3.2 Steam reforming - Catalysts

A suitable catalyst for steam reforming of glycerol shall fulfil two main tasks. It shall cleave the different bonds of its molecule: C-C, C-H and H-O. Simultaneously, it shall catalyse the water gas shift reaction to remove the CO adsorbed on the metallic surface (Zhao et al., 2019).

Catalytic steam reforming of glycerol into hydrogen is a combination of pyrolysis of glycerol and water gas shift reaction of the resulting carbon monoxide. Thermal cracking reactions occur first, before the reactants enter the catalyst bed. Then, acid-base reactions take place at the acid and basic sites of the catalyst's support. The nature of the support is crucial to achieve suitable conditions for the process. In chemical terms, it provides the required acid-base characteristics for the reactions. In mechanical terms, it promotes dispersion of nanoparticles of the active metal on itself, enhancing its active surface. Overall, it's the interface between metal and support which features the active region of the catalyst, by presenting new characteristics, different from those of the metal and the support alone. Pyrolysis would take place even without catalyst, decomposing glycerol into a mixture of H<sub>2</sub>, CO, CO<sub>2</sub>, CH<sub>4</sub>, C<sub>2</sub>H<sub>4</sub> and C<sub>2</sub>H<sub>6</sub>. However, the catalyst steers the product distribution in favour of H<sub>2</sub>, reducing the concentration of C1-C2 hydrocarbons (Charisiou et al., 2019).

The main catalysts reported in literature are based on noble metals like iridium (Ir), palladium (Pd), platinum (Pt), rhenium (Re), rhodium (Rh) and ruthenium (Ru), and base metals like cobalt (Co) and nickel (Ni). Noble metals are preferable in terms of performance: the corresponding catalysts show higher activity and lower tendency to coke formation. However, the higher cost limits their application to laboratory level. Base metals like nickel are instead cheap due to their high availability, and for this reason they are used for industrial catalysts on large scale. Therefore, recent research is focusing on nickel-based catalysts on different supports and promoters (Schwengber et al., 2016).

Table 3 reports the performance of different nickel-based catalysts in steam reforming of glycerol (all processes are carried out in fixed bed reactors).

**Table 3.** Steam reforming of glycerol into hydrogen: performance of Ni based catalysts.

Reprinted (adapted) from (Schwengber et al., 2016), Copyright (2016), with permission from Elsevier.

Temperature [°C]	Molar ratio C <sub>3</sub> H <sub>8</sub> O <sub>3</sub> :H <sub>2</sub> O	Spatial vel. [g <sub>glyc</sub> /h-g <sub>cat</sub> ]	Pressure	Catalyst	Max H <sub>2</sub> prod. [%]	Max C <sub>3</sub> H <sub>8</sub> O <sub>3</sub> X [%]
300, 500, 700	1:9	—	atm.	Ni-Cu-Al	54,3-70,4	100
500-600	1:9	7,7	0,4 MPa	Ni,Pt,Pt-Ni + $\gamma$ -Al <sub>2</sub> O <sub>3</sub> ,La <sub>2</sub> O <sub>3</sub>	90	100
600-700	1:16	3,4-10,0	atm.	Ni/Al <sub>2</sub> O <sub>3</sub>	76-99	99,7
400-700	1:3	—	atm.	Ni/Al <sub>2</sub> O <sub>3</sub>	80	100
650	1:6	0,04	—	Ni/MgO	65,6	100
				Ni/CeO <sub>2</sub>	53,9	100
				Ni/TiO <sub>2</sub>	62,2	98
500-600	1:3	7,7	0,4 MPa	ZrO <sub>2</sub> /Ni/Al <sub>2</sub> O <sub>3</sub>	70	80

Nickel shows good intrinsic activity in reforming reactions, especially when it is highly dispersed over the support. The most common material used for supports is alumina (Charisiou et al., 2019), thanks to its mechanical and chemical resistance under reaction conditions, and its high surface area that enhances metal dispersion (Charisiou et al., 2017).

However, when nickel is dispersed on an acid support like Al<sub>2</sub>O<sub>3</sub>, it promotes coke formation and sintering of metallic sites, that affect negatively its stability, leading to deactivation (Zhao et al., 2019). Carbon deposition is due to reactions of dehydration, cracking and polymerization, occurring at the acid sites of the alumina. Sintering is associated with a transition of alumina to crystalline phase during steam reforming; it creates larger metal aggregates that increase carbon deposition further. A way to limit these issues is to neutralize the acidity of alumina. This can be achieved with additives or promoters that support water adsorption and mobility of O-H surface (Charisiou et al., 2017).

### 3.3 Latest catalytic development

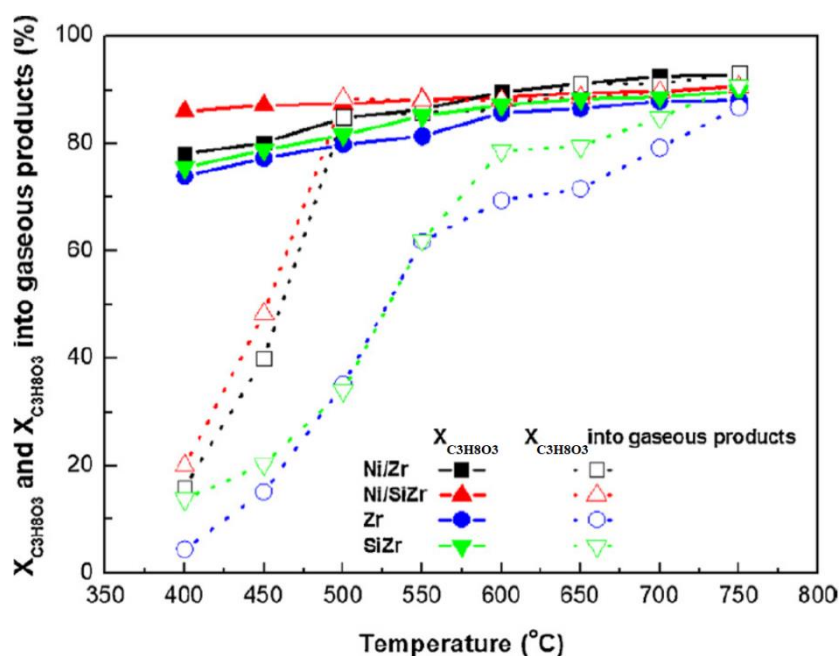
The four latest catalysts developed for steam reforming of glycerol into hydrogen are object of deeper review in the following paragraphs.

#### 3.3.1 Ni catalysts supported on Silica-Zirconia

Zirconium dioxide is a promising material to be used as support of a nickel catalyst. It shows acid/basic character, oxidizing and reducing properties and a high capability in stabilizing the nickel active phase. Dopants like SiO<sub>2</sub> can enhance the thermal stability further by delaying the loss of surface area and the structure transformation that normally occur upon heating. Furthermore, zirconia has the ability of first adsorbing, then dissociating the water. During steam reforming of glycerol, this property can enhance the adsorption of steam on its surface, activating gasification of hydrocarbons and water gas shift reactions (Charisiou et al., 2019).

In their study, Charisiou and co-workers compared the catalytic activity and stability of nickel catalysts supported on zirconia ( $ZrO_2$ ) and zirconia doped with silica ( $SiO_2-ZrO_2$ ). The catalysts, with a Ni loading of circa 8% weight, were prepared via wet impregnation of zirconia and silica-zirconia powders followed by calcination or reduction (Charisiou et al., 2019). The catalytic performance was investigated with two different tests: the first, to study the activity and selectivity of the catalysts at steady state conditions, the second to study their stability over time. In both tests, the steam reforming of glycerol was carried out in a fixed bed reactor, at atmospheric pressure, with a liquid feed of 0,12 mL/min and 200 mg of each catalyst. In the first test, the glycerol's concentration was 20% vol. in water, and the temperature was increased from 400 to 750 °C by 50 °C steps of 50 minutes. In the second, to promote deactivation, the glycerol concentration was increased to 31% vol. in water and the reforming reaction was maintained for 20 hours, at a constant temperature of 600 °C. The performances are calculated with equations A.1-A.5 (Charisiou et al., 2019).

Glycerol's conversion (global and into gaseous products) as function of reaction temperature is shown in figure 5 for the different catalysts and supports.

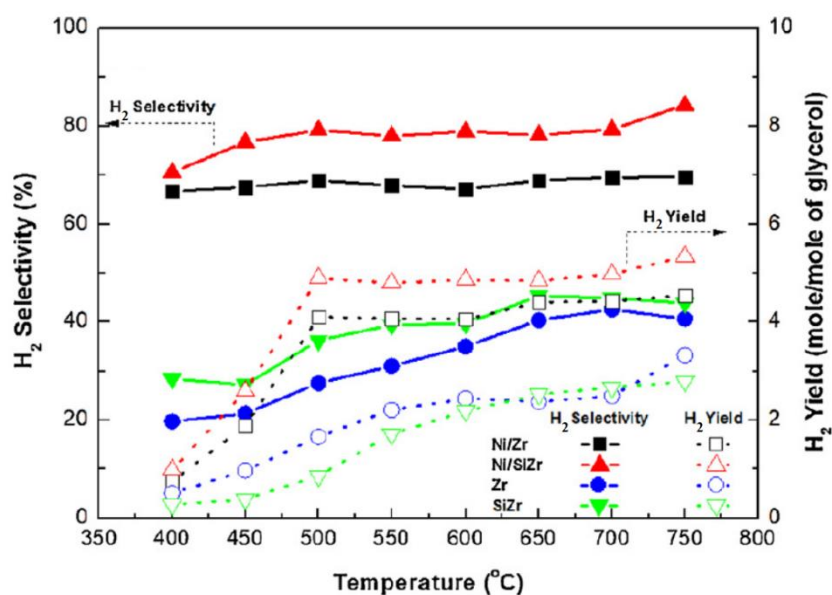


Reprinted (adapted) from (Charisiou et al., 2019), Copyright (2019), with permission from Elsevier.

**Figure 5.** Ni catalysts supported on SiZr: glycerol conversion.

Ni/SiZr catalyst performs a high global conversion of ~90% through the entire temperature range. Ni/Zr catalyst and the single supports (Zr, SiZr) instead, reach the same value only at high temperatures (600-750°C), while showing a lower conversion of 70-75% at beginning of reaction (400°C). Both catalysts show a similar conversion into gaseous products, with a steep increase from 20% at 400 °C to 85% at 500 °C. The supports behave much worse than catalysts, especially at low temperatures. The highest gap in conversion is at 500 °C, and it's reduced only towards the highest temperatures (Charisiou et al., 2019).

Figure 6 shows hydrogen's selectivity and yield as function of reaction temperature.

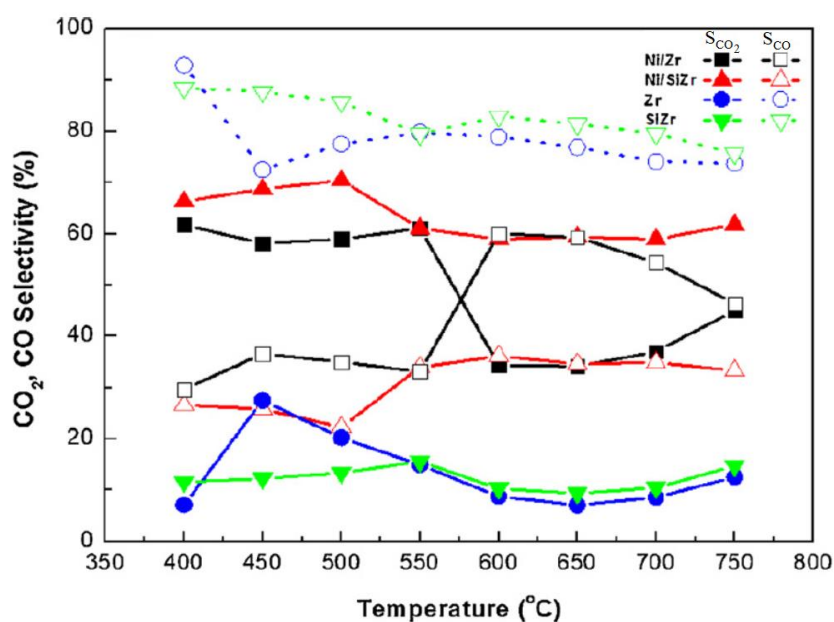


Reprinted (adapted) from (Charisiou et al., 2019), Copyright (2019), with permission from Elsevier.

**Figure 6.** Ni catalysts supported on SiZr: H<sub>2</sub> selectivity and yield.

Ni/SiZr catalyst has higher hydrogen's selectivity and yield than Ni/Zr in the entire temperature range. The highest values, 85% and 5.5 respectively, are approached at 750 °C and they are very close to those predicted by thermodynamics. Compared to the catalysts, the supports have a significantly lower selectivity and yield, at most ~45% and 3. Doping with Si has a beneficial effect on H<sub>2</sub> selectivity, especially at lower temperatures (400-600 °C) where SiZr support shows higher performance than Zr one. Their behaviour gets closer at higher temperatures (600-750 °C) (Charisiou et al., 2019).

Selectivities to carbon dioxide and carbon monoxide are shown in figure 7.

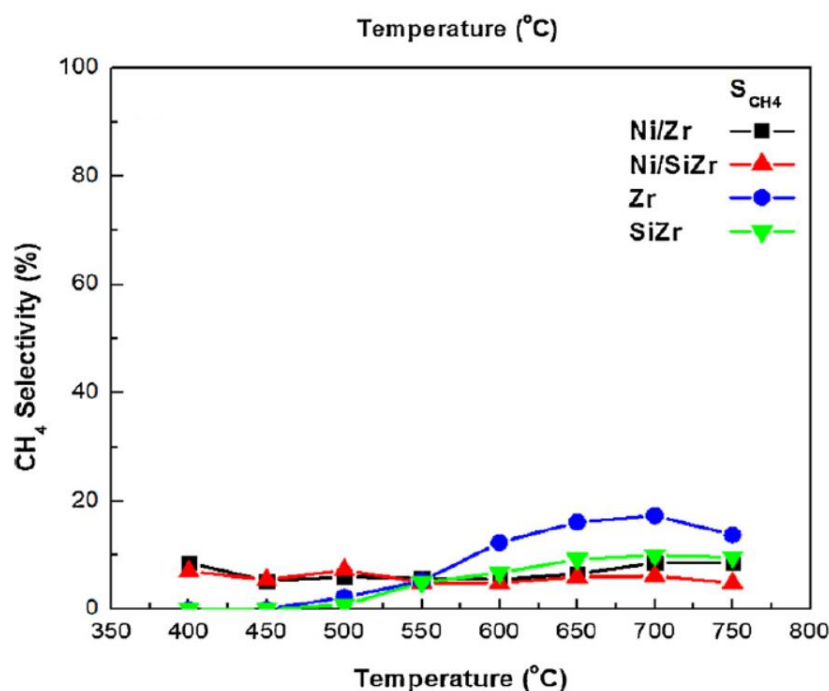


Reprinted (adapted) from (Charisiou et al., 2019), Copyright (2019), with permission from Elsevier.

**Figure 7.** Ni catalysts supported on SiZr: selectivity to CO<sub>2</sub> and CO.

Ni/SiZr catalyst has higher selectivity to CO<sub>2</sub> than CO in the entire temperature range. Ni/Zr catalyst shows a similar behaviour at lower temperatures, while above 550 °C the selectivity to CO<sub>2</sub> drops and the one to CO increases steeply, for then converging to the same value at 750 °C. The supports are both much more selective towards CO (~80%) than CO<sub>2</sub> (~10%) (Charisiou et al., 2019).

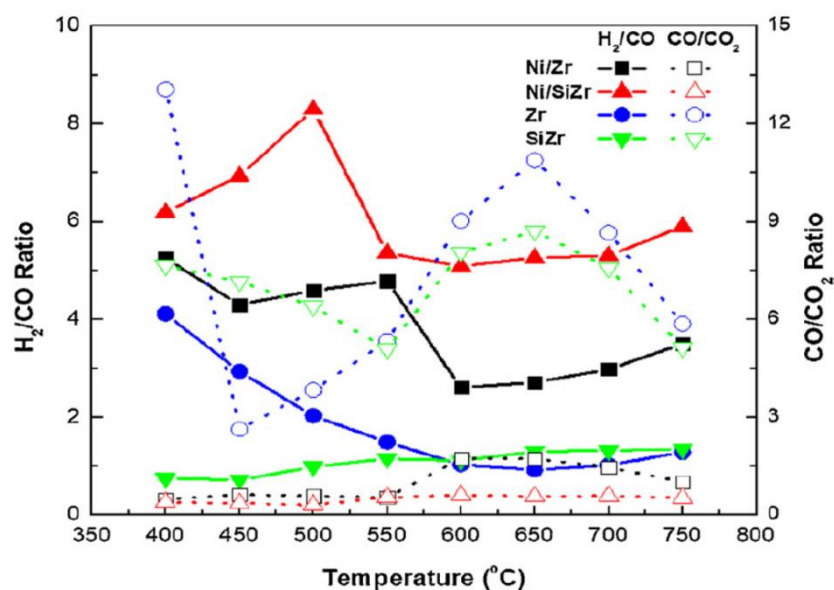
Figure 8 shows the selectivity to methane. Both Ni/SiZr and Ni/Zr catalysts have low selectivity to CH<sub>4</sub>, about 5-10% in the entire temperature range. The support in SiZr has a selectivity null until 500 °C, but increasing to almost 10% from 650 °C. The one made of pure ZrO<sub>2</sub> shows a stronger increase with temperature, and a peak close to 20% at 700 °C (Charisiou et al., 2019).



Reprinted from (Charisiou et al., 2019), Copyright (2019), with permission from Elsevier.

**Figure 8.** Ni catalysts supported on SiZr: selectivity to CH<sub>4</sub>.

The molar ratios H<sub>2</sub>/CO and CO/CO<sub>2</sub> are shown in figure 9. For Ni/SiZr catalyst, the ratio CO/CO<sub>2</sub> is always close to zero. The ratio H<sub>2</sub>/CO at first increases with temperature from 6 to a maximum of ~8,5 at 500 °C; then, it lowers to ~5-6 in the range 550-750 °C. The ratio CO/CO<sub>2</sub> of Ni/Zr is close to zero at low temperatures and increases to ~1,5 at 600 °C. The ratio H<sub>2</sub>/CO instead decreases with temperature from about 5 in the range 400-550 °C to circa 3 in the range 600-750 °C. Regarding the supports in Zr and SiZr, even if they alternate decreasing and increasing trends, they both have a high CO/CO<sub>2</sub> ratio with an average of about 7. Their H<sub>2</sub>/CO ratio is instead low: for Zr it decreases with temperature from 4 to circa 1; for SiZr is between 1-1,5 (Charisiou et al., 2019).



Reprinted from (Charisiou et al., 2019), Copyright (2019), with permission from Elsevier.

**Figure 9.** Ni catalysts supported on SiZr: molar ratios  $H_2/CO$  and  $CO/CO_2$ .

From these results, it can be concluded that the catalysts promote the production of hydrogen, increasing its selectivity and yield already from low temperatures. At temperatures higher than 500 °C, they provide a high conversion into gaseous products of ~80%; the hydrogen content reaches its thermodynamic value with Ni/SiZr. Doping the  $ZrO_2$  support with  $SiO_2$  not only promotes  $H_2$  production, but also prevents the reverse water gas shift reaction, limiting the transformation of  $CO_2$  in  $CO$ . This results in a high mole ratio  $H_2/CO$  while  $CO/CO_2$  is negligible (Charisiou et al., 2019).

Table 4 reports relevant parameters of the catalysts during the second test, at the beginning and after 20 hours.

**Table 4.** Ni catalysts supported on SiZr: performance during stability test.

Reprinted (adapted) from (Charisiou et al., 2019), Copyright (2019), with permission from Elsevier.

Reaction parameter	Ni/Zr		Ni/SiZr	
	1 <sup>st</sup> measure	Last measure	1 <sup>st</sup> measure	Last measure
$X_{C_3H_8O_3}$ [%]	80,25	64,90	83,10	68,16
$X_{C_3H_8O_3}$ gaseous products [%]	44,88	38,60	48,59	37,89
$Y_{H_2}$	2,33	1,50	2,88	2,08
$S_{H_2}$ [%]	74,25	55,72	87,88	76,67
$S_{CO_2}$ [%]	50,89	39,48	67,94	57,67
$S_{CO}$ [%]	45,44	52,31	30,05	39,98
$S_{CH_4}$ [%]	3,66	8,20	1,99	2,33
$H_2/CO$	3,81	2,48	6,82	4,59
$CO/CO_2$	0,89	1,32	0,44	0,69

Both catalysts show a reduced performance at the end of the stability testing. Glycerol's conversion, hydrogen's yield and selectivity, as well as selectivity to CO<sub>2</sub> and H<sub>2</sub>/CO ratio decrease over time, while selectivity to CO and CH<sub>4</sub>, and mole ratio CO/CO<sub>2</sub> increase. Ni/SiZr behaves better than Ni/Zr, with higher glycerol's conversion (68,2% vs 64,9%), higher H<sub>2</sub> yield (2,1 vs 1,5), higher selectivity to H<sub>2</sub> and CO<sub>2</sub> (76,7% vs 55,7%, and 57,7% vs 39,5%), as well as higher H<sub>2</sub>/CO molar ratio (4,6 vs 2,5). Moreover, it shows lower selectivity to CO and CH<sub>4</sub> (40% vs 52,3% and 2,3% vs 8,2%, respectively) and a lower molar ratio CO/CO<sub>2</sub> of 0,7 vs 1,3. Glycerol's conversion into gaseous products is about 38% for both catalysts (0,7% points higher in Ni/Zr). The quantity of carbon deposited on the surface of Ni/SiZr catalyst is estimated in 0,24 g<sub>coke</sub>/g<sub>catalyst</sub>, about half of 0,51 g<sub>coke</sub>/g<sub>catalyst</sub> estimated for Ni/Zr (Charisiou et al., 2019).

These results suggest that Ni/SiZr is more resistant to deactivation than Ni/Zr, due to its stronger metal-support interactions. It confirms that silica has high capability of stabilizing the active phase during reaction, by preventing the sintering of nickel particles through the formation of a composite structure SiO<sub>2</sub>-ZrO<sub>2</sub>. It seems that doping the ZrO<sub>2</sub> support with Si has the effect of replacing zirconia's weak acid sites with strong acid sites, lowering its basicity (Charisiou et al., 2019).

In conclusion, the nickel catalyst supported on zirconia doped with silica shows the best performances, both at the steady state test and at the stability test.

### 3.3.2 Ni catalysts supported on Zirconia-Alumina

Recently, ZrO<sub>2</sub> has been investigated both as catalyst and support, thanks to its physical and chemical properties. In addition to mechanical strength, it shows excellent redox properties that hinder the phase transition of Al<sub>2</sub>O<sub>3</sub> support, as well as thermal stability, that inhibits sintering of the metallic active sites caused by steam at high temperatures. These properties result in enhanced resistance against coke formation and deactivation (Zhao et al., 2019).

In a recent study, Zhao and co-workers prepared a series of Ni-Zr-Al mixed metal oxides, and investigated the effects of different Zr/Al ratios on catalytic performance. The catalysts were synthesized from layered double hydroxide precursors through thermal decomposition, and denoted as NiZr<sub>x</sub>Al, where x represents the Zr/Al ratio, ranging from 0,1 to 1,0. (Zhao et al., 2019). The textural properties of the catalysts (specific surface area, pore volume and average diameter) are collected in table 5.

**Table 5.** Textural properties of NiZr<sub>x</sub>Al catalysts.

Reprinted (adapted) from (Zhao et al., 2019),  
Copyright (2019), with permission from Elsevier.

Catalyst	S <sub>BET</sub> [m <sup>2</sup> /g]	v [cc/g]	D [nm]
NiAl	100,2	0,237	9,5
NiZr <sub>0,1</sub> Al	144,2	0,449	12,5
NiZr <sub>0,3</sub> Al	130,8	0,426	13,0
NiZr <sub>0,5</sub> Al	122,6	0,283	9,2
NiZr <sub>0,7</sub> Al	121,4	0,235	7,7
NiZr <sub>0,9</sub> Al	122,4	0,258	8,0
NiZr <sub>1,0</sub> Al	124,1	0,249	8,0

All samples doped with Zr show larger surface area than NiAl catalyst; the maximum increase is obtained for NiZr<sub>0,1</sub>Al. The surface area tends to decrease with further doping, for then stabilizing at Zr/Al ratio higher than 0,5. Pore volume and average diameter show a similar trend. These results suggest that Zr promotes evolution of the pore structure of the support, from sheet for Zr/Al ≤ 0,3 to ink-bottle shape for Zr/Al ≥ 0,5, improving the textural properties (Zhao et al., 2019).

The steam reforming of glycerol (10% weight in water) was performed in a fixed-bed reactor, at atmospheric pressure and 450 °C, with 200 mg of each catalyst and feed flow rate of 3 mL/h (WHSV equal to 15 h<sup>-1</sup>). The reaction was hold for 8 hours, then the relevant parameters were collected (Zhao et al., 2019). The results of test are reported in table 6.

**Table 6.** Performance of NiZr<sub>x</sub>Al catalysts.

Reprinted (adapted) from (Zhao et al., 2019), Copyright (2019), with permission from Elsevier.

Catalyst	Mole conversion to gas [%]	Selectivity [%]			
		H <sub>2</sub>	CO	CO <sub>2</sub>	CH <sub>4</sub>
NiAl	66,2	75,3	2,3	61,4	12,4
NiZr <sub>0,1</sub> Al	72,3	58,1	17,2	53,6	1,5
NiZr <sub>0,3</sub> Al	78,5	65,0	12,2	65,8	0,5
NiZr <sub>0,5</sub> Al	96,5	97,7	3,6	91,9	1,1
NiZr <sub>0,7</sub> Al	93,9	92,5	11,3	82,3	0,4
NiZr <sub>0,9</sub> Al	88,2	86,1	22,4	65,1	0,7
NiZr <sub>1,0</sub> Al	82,1	87,2	15,2	74,9	2,0

In general, the catalysts doped with Zr show higher mole conversion to gas, and a significantly lower selectivity to methane. The mole conversion to gas is function of Zr doping: it does increase from a minimum of 66,2% for NiAl catalyst, to a maximum of 96,5% for NiZr<sub>0,5</sub>Al. Further increase of Zr/Al ratio is not beneficial, as conversion rate start decreasing, down to 82,1% for NiZr<sub>1,0</sub>Al. Zirconia has a positive effect in reducing methanation: all Zr doped catalysts have a selectivity to methane 1 order of magnitude lower than NiAl. Among the doped catalysts, the most performing is NiZr<sub>0,5</sub>Al. It shows not only the highest mole conversion to gas (96,5%), but also the highest selectivity to hydrogen and carbon dioxide (97,7% and 91,9%, respectively) and the lowest selectivity to carbon monoxide (3,6%). It means that this catalyst does enhance efficiently the water gas shift reaction, while it does suppress the methanation of CO (Zhao et al., 2019).

Coke formation was investigated through thermogravimetric analysis; the results are reported in table 7.



**Table 7.** Quantification of deposited coke on the spent NiZr<sub>x</sub>Al catalysts.

Reprinted (adapted) from (Zhao et al., 2019), Copyright (2019), with permission from Elsevier.

Catalyst	Weight loss [%]	Coke [mg <sub>c</sub> /g <sub>cat</sub> .]	Ni average crystallite size [nm]		
			Before reaction	After reaction	Delta [%]
NiAl	23,0	230	—	—	—
NiZr <sub>0,1</sub> Al	10,3	103	10,1	14,7	45,5
NiZr <sub>0,3</sub> Al	9,1	91	9,5	12,1	27,4
NiZr <sub>0,5</sub> Al	3,6	36	11,5	13,2	14,8
NiZr <sub>0,7</sub> Al	4,5	45	12,0	14,5	20,8
NiZr <sub>0,9</sub> Al	5,9	59	13,1	15,9	21,4
NiZr <sub>1,0</sub> Al	10,6	106	14,2	19,6	38,0

All catalysts doped with Zr show an increased particle size of active phase after reaction. NiZr<sub>0,5</sub>Al has the best ability in suppressing the crystallite aggregation, with the lowest increment of 14,8%. All catalysts show weight loss, that occurs in two stages: first, the removal of adsorbed water at T<200 °C, and then the combustion of deposited coke at higher temperatures. The highest quantity of coke of 230 mg<sub>c</sub>/g<sub>cat</sub> is observed on NiAl. The introduction of Zr in the catalysts reduced the coke formation of at least 50%, like for NiZr<sub>0,1</sub>Al and NiZr<sub>1,0</sub>Al. Lower values are observed for intermediate doping rates: NiZr<sub>0,5</sub>Al shows the best ability in coke resistance, with 36 mg<sub>c</sub>/g<sub>cat</sub> (Zhao et al., 2019).

It can be concluded that the addition of Zr into the aluminium support with a molar ratio 0,5 improves the catalytic performances. Thanks to enhanced textural properties, it gives the best conversion to gaseous products, the highest selectivity to hydrogen, along with the lowest coke deposition. NiZr<sub>0,5</sub>Al is therefore an interesting catalyst, especially considering that these results are obtained with a reaction temperature of 450 °C, lower than the one usually applied in steam reforming with similar Ni based catalysts (Zhao et al., 2019).

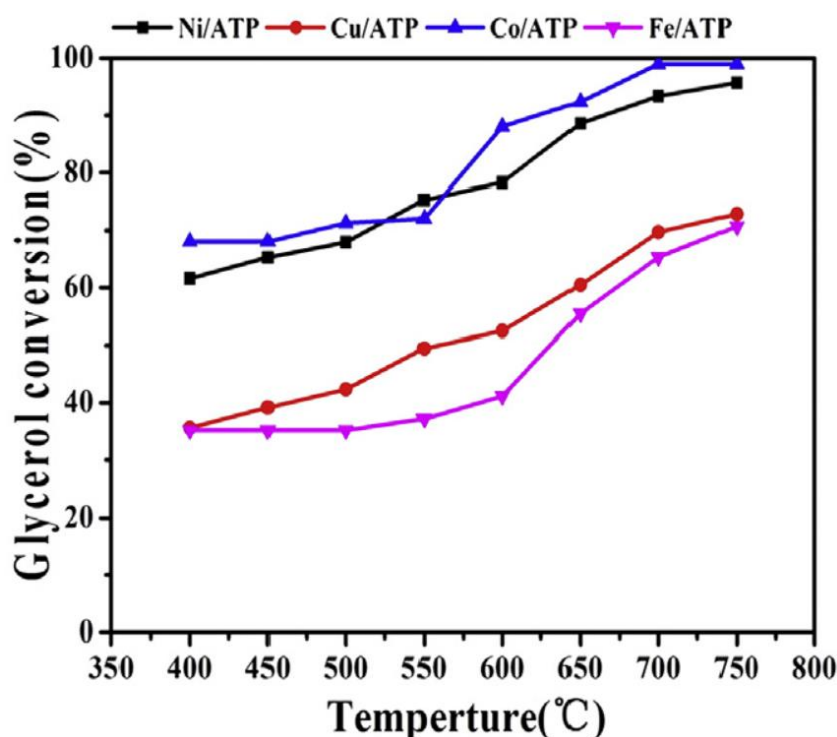
### 3.3.3 Transition metal catalysts supported on Attapulgite

Metal sintering and carbon deposition are major issues that affect the catalysts during steam reforming of glycerol. Research is playing an effort in developing more resistant catalysts in this respect. Studies have focused in regulating the surface composition of catalysts, tuning their particle sizes and shapes, enhancing metal-support interaction and fabrication of hierarchical structures, like nanoconfinement effect of the support (Chen et al., 2018).

The attapulgite is a phyllosilicate of the type 2:1 (Chen et al., 2018). The crystalline layer of a such phyllosilicate consists of 1 octahedral sheet of aluminium hydroxide between 2 tetrahedral sheets of silicon oxide, running parallel to each other (Lavikainen, 2016). The tetrahedral sheets of silica are disposed with their base periodically inverted. This geometry grants high specific surface, adsorption ability, and excellent thermal and hydrothermal stability, making it an interesting material as catalyst support (Chen et al., 2018).

In their study, Chen and co-workers investigated the catalytic behaviour of transition metals (Ni, Cu, Co and Fe) supported on attapulgite (ATP). The catalysts were synthesized with a metal loading of 10% weight by precipitation method, followed by calcination. The steam reforming was carried out in a fixed bed reactor at atmospheric pressure and at a temperature range of 400-750 °C. The WHSV was 6,46 h<sup>-1</sup> and the molar ratio water to glycerol 3, corresponding to a glycerol concentration of 57,5% in volume. A stability test of 24 hours was also conducted at constant temperature of 600 °C, with remaining parameters being unchanged. (Chen et al., 2018). The performances are calculated with equations A.6-A.8.

The glycerol's conversion of the various catalysts supported on attapulgite, as function of temperature is shown in figure 10.

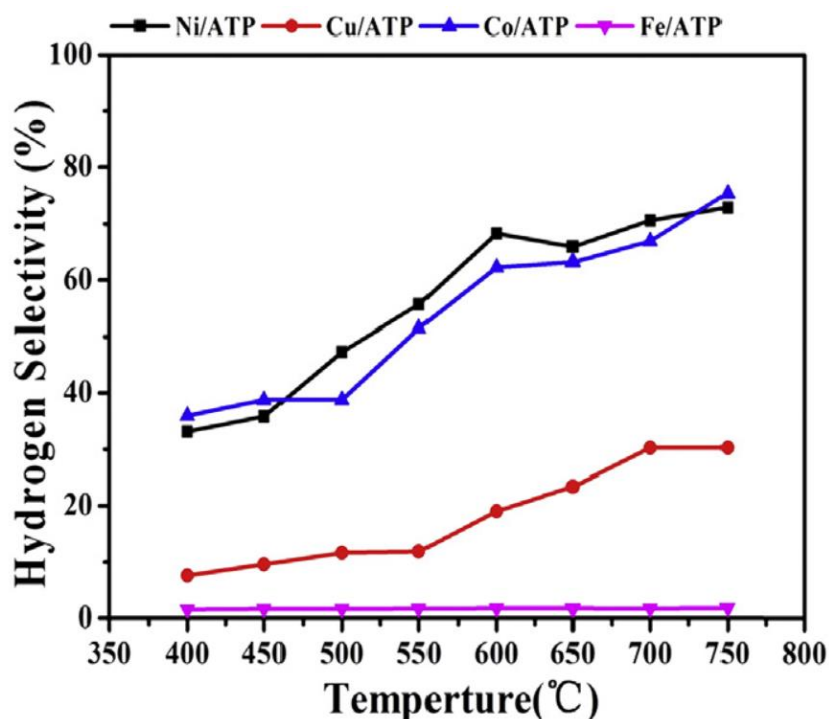


Reprinted from (Chen et al., 2018), Copyright (2018), with permission from Elsevier.

**Figure 10.** Metal catalysts supported on ATP: glycerol conversion.

Being steam reforming an endothermic process, the temperature is beneficial for the glycerol's conversion of all catalysts. The most performing one is Co/ATP, where it does increase from 67,7% at 400 °C, to 88% at 600 °C and up to 100% at 750 °C. Ni/ATP shows a conversion starting at 61,6%, increasing to 78,2% at 600 °C and 95,5% at 750 °C. Cu/ATP and Fe/ATP are less performing: their conversion, at the same temperatures is 34%-52%-72%, and 34%-41%-70%, respectively (Chen et al., 2018).

Figure 11 shows the selectivity to hydrogen as function of temperature.



Reprinted from (Chen et al., 2018), Copyright (2018), with permission from Elsevier.

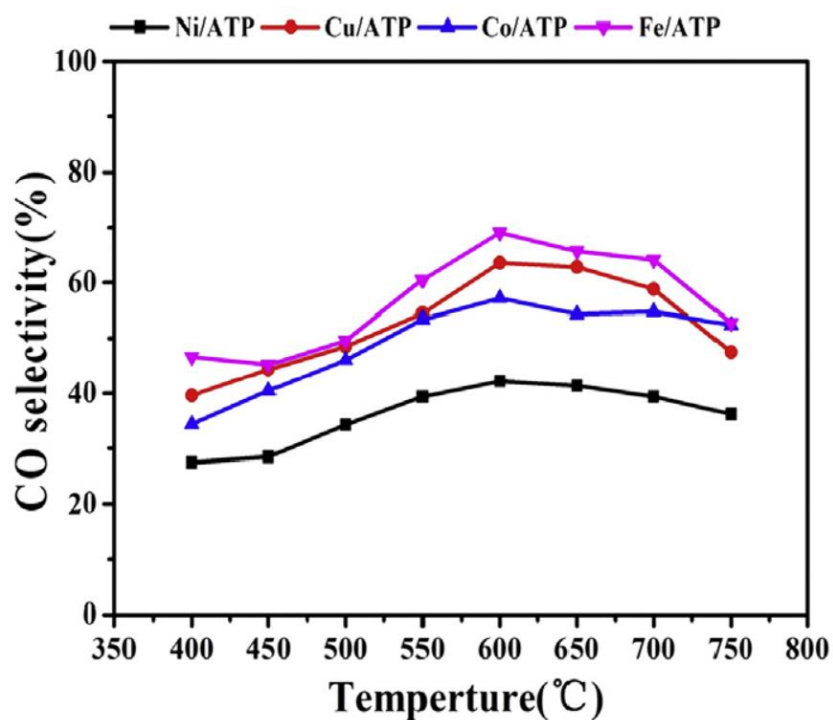
*Figure 11. Metal catalysts supported on ATP: hydrogen selectivity.*

Ni/ATP is overall the most performing catalyst, with a selectivity of 68,3% at 600 °C. Co/ATP shows a similar trend in the range, and a value of 62,2% at the same temperature. However, its selectivity at 750 °C is higher than Ni/ATP: 75% vs 73%. These catalysts are followed by Cu/ATP with a pronounced general lower performance, and 19,1% selectivity at 600 °C, while Fe/ATP has the worst behaviour, showing a flat selectivity of ~2% in the entire range. The higher performance of Ni/ATP and Co/ATP catalysts are most probably due to their higher activity in cleaving C-C and C-H bonds, accelerating the decomposition of glycerol (eq. 4) and the water gas shift reaction (eq. 2) (Chen et al., 2018).

The selectivities of the catalysts to carbon monoxide and dioxide are presented respectively in figures 12 and 13.

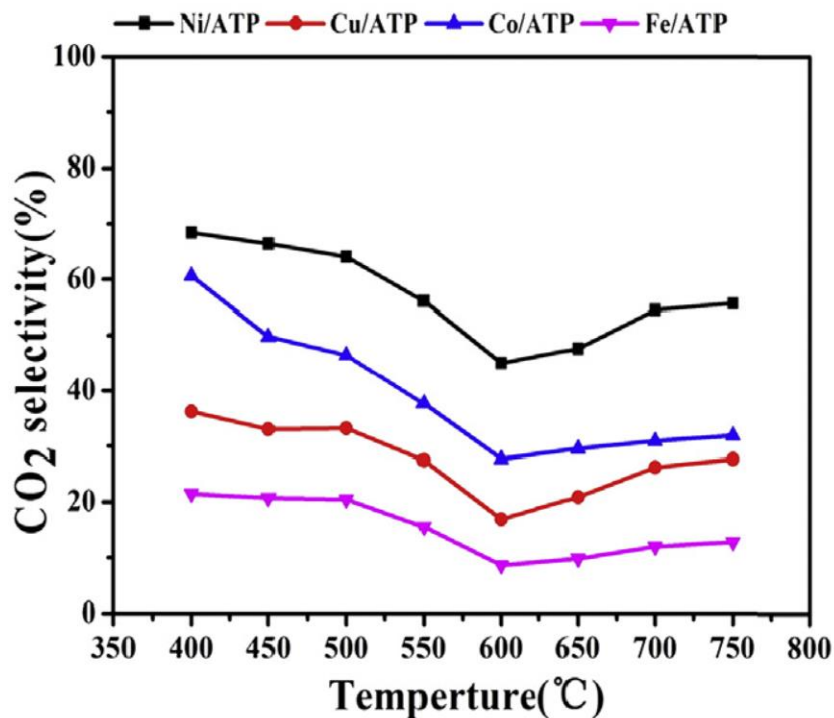
Figure 12 shows that selectivity of CO does increase with temperature for all catalysts until a maximum at 600 °C, for then stabilizing/decreasing with further temperature increase. Fe/ATP and Cu/ATP have the highest performance, followed by Co/ATP. Their selectivities at 600 °C are respectively 68,9%, 63,2% and 57,4%. Ni/ATP shows the lowest selectivity of 42,1% at the same temperature (Chen et al., 2018).

Figure 13 shows that selectivity of CO<sub>2</sub> has an opposite trend compared to CO, because for all catalysts it does decrease from a maximum at 400 °C to a minimum at 600°C, for then increasing until 750 °C. Behaviour of all catalysts is also reversed: Ni/ATP has the highest selectivity to CO<sub>2</sub>, followed by Co/ATP, Cu/ATP and Fe/ATP.



Reprinted from (Chen et al., 2018), Copyright (2018), with permission from Elsevier.

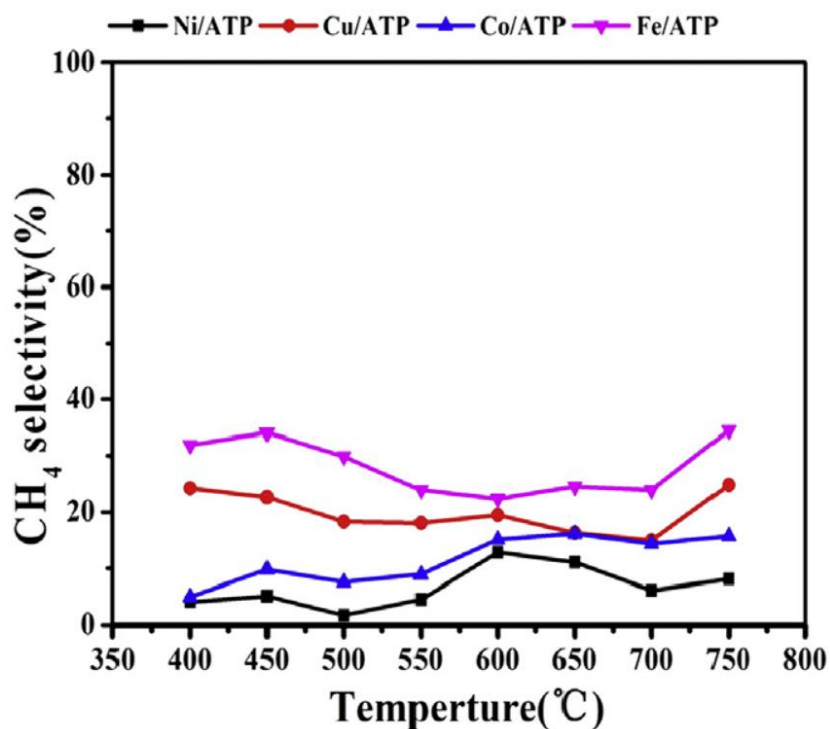
*Figure 12. Metal catalysts supported on ATP: CO selectivity.*



Reprinted from (Chen et al., 2018), Copyright (2018), with permission from Elsevier.

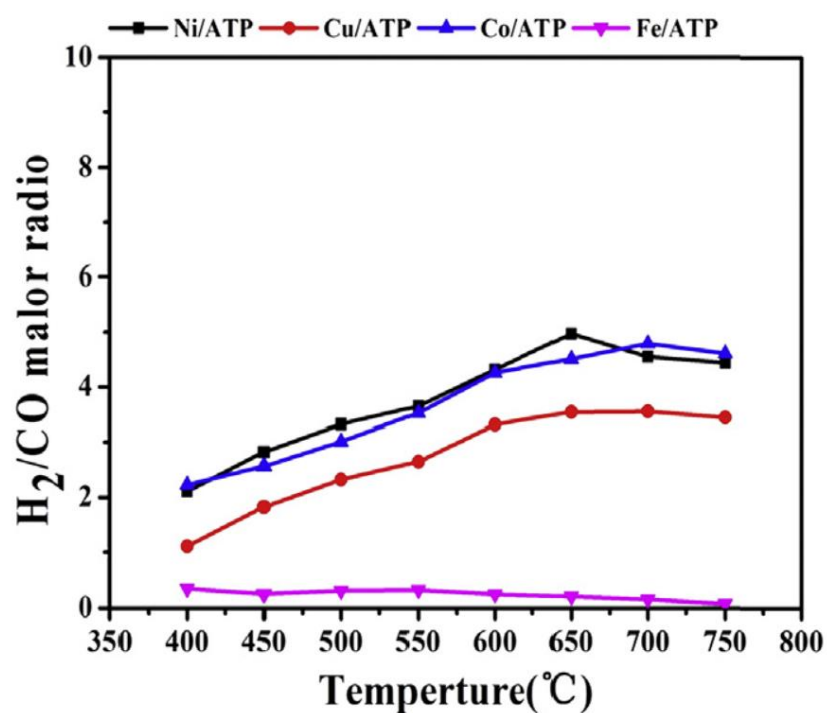
*Figure 13. Metal catalysts supported on ATP: CO<sub>2</sub> selectivity.*

The selectivity to methane and the molar ratio  $H_2/CO$  as function of temperature are shown respectively in figures 14 and 15.



Reprinted from (Chen et al., 2018), Copyright (2018), with permission from Elsevier.

Figure 14. Metal catalysts supported on ATP:  $CH_4$  selectivity.



Reprinted from (Chen et al., 2018), Copyright (2018), with permission from Elsevier.

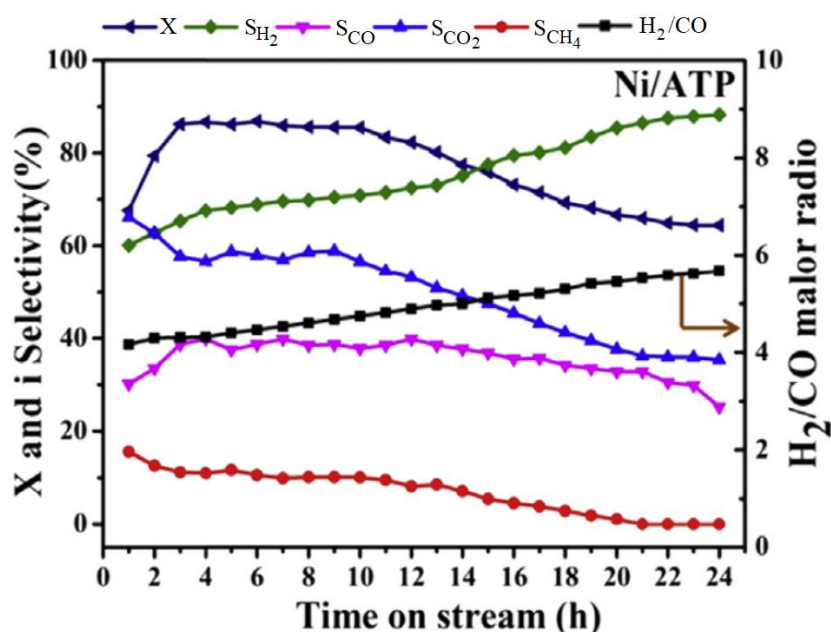
Figure 15. Metal catalysts supported on ATP: molar ratio  $H_2/CO$ .

Fe/ATP and Cu/ATP have the highest selectivity to methane, while Co/ATP and Ni/ATP the lowest. It can be noted that Ni/ATP and Co/ATP show a slight increase of selectivity at 500-600 °C. This is due to a large production of carbon monoxide at this temperature range, that undergoes the reaction of methanation (eq. 5).

As seen in figure 15, Ni/ATP and Co/ATP have a similar trend, and the highest performance: their molar ratio  $H_2/CO$  increases until about 5 at 650 °C and 700 °C, respectively. Cu/ATP approaches a molar ratio of circa 3,5 for  $T > 600^\circ C$ . Molar ratio of Fe/ATP is lower than unity and tends to zero with temperature increase. The best performances of Ni and Co reveal their higher activity for water gas shift reaction. This reaction tends to be suppressed by temperatures above 650-700 °C; this is observed especially for Ni (Chen et al., 2018).

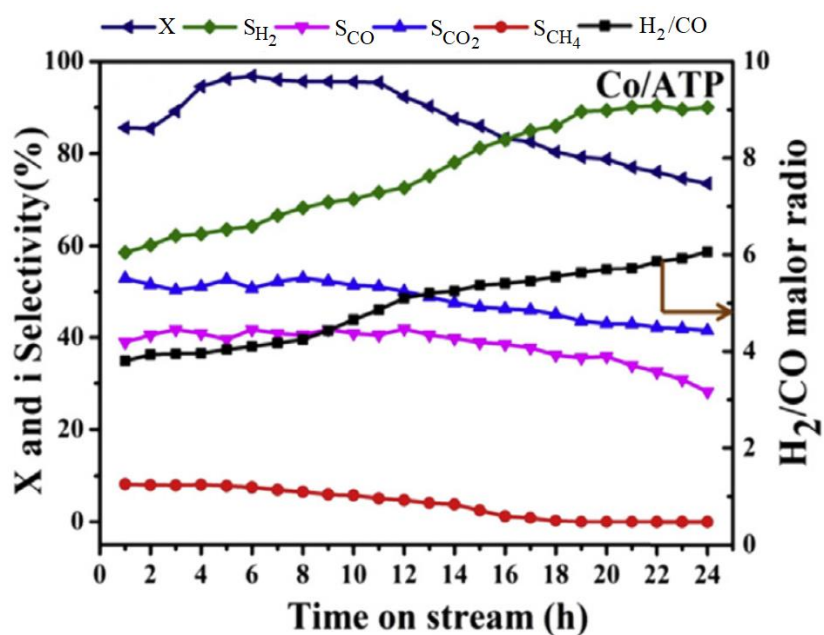
It can be concluded that formation of carbon monoxide is promoted at expense of carbon dioxide through a reverse water gas shift reaction.  $CH_4$  is produced mainly via reactions of methanation (eq. 5 and 6) and decomposition of glycerol. Methane production is promoted by low temperatures and inhibited at high temperatures, where reactions of methane steam and dry reforming take place. The lower selectivity to  $CH_4$  of Ni/ATP and Co/ATP are explained by their higher activity for these reactions (Chen et al., 2018).

The behaviour of the catalysts under stability test is reported in figures 16-19, that show glycerol's conversion, selectivity to gaseous products and molar ratio  $H_2/CO$  as function of time.



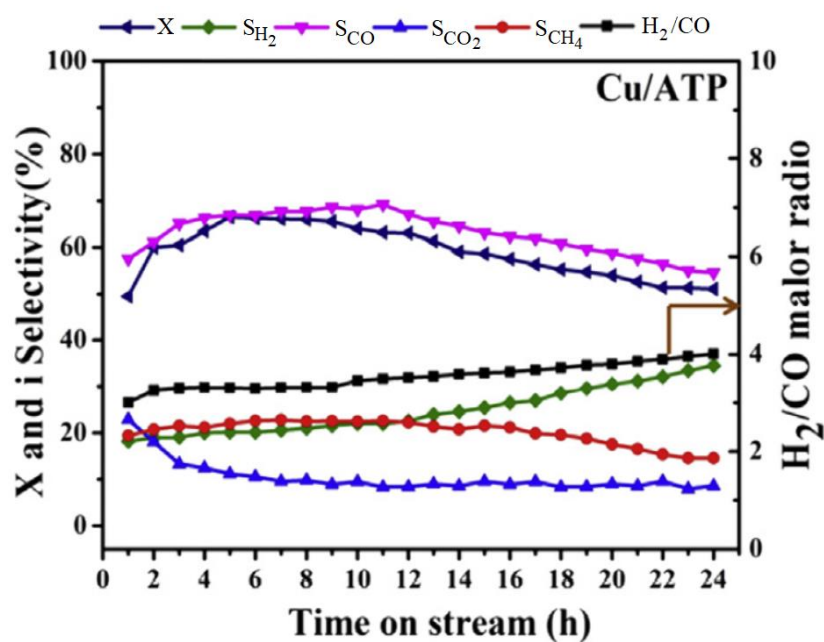
Reprinted (adapted) from (Chen et al., 2018), Copyright (2018), with permission from Elsevier.

Figure 16. Ni/ATP catalyst: performance during stability test.



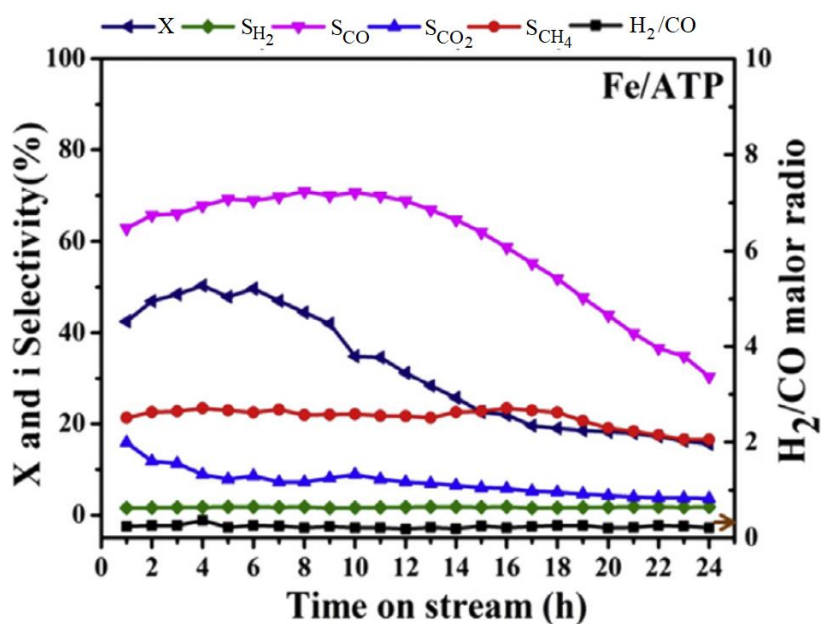
Reprinted (adapted) from (Chen et al., 2018), Copyright (2018), with permission from Elsevier.

Figure 17. Co/ATP catalyst: performance during stability test.



Reprinted (adapted) from (Chen et al., 2018), Copyright (2018), with permission from Elsevier.

Figure 18. Cu/ATP catalyst: performance during stability test.



Reprinted (adapted) from (Chen et al., 2018), Copyright (2018), with permission from Elsevier.

*Figure 19. Fe/ATP catalyst: performance during stability test.*

In general, all catalysts show a reduced glycerol's conversion at the end of the stability test, and an increased selectivity to hydrogen. As seen in figures 16 and 17, the conversions for Ni/ATP and Co/ATP decrease respectively from circa 85% and 95% at the beginning of the test, to about 65% and 73% after 24 hours. Hydrogen's selectivity shows for both catalysts a similar increase from ~60% to ~90%. Figure 18 shows that the glycerol's conversion of Cu/ATP presents a lower decrease than for other catalysts, from circa 65% to 50%. This behaviour can be attributed to the higher dispersion of copper on the support. For this catalyst, the increase in hydrogen's selectivity is from circa 20% to 30%. As seen in figure 19, the most remarkable reduction in glycerol's conversion is for Fe/ATP, where it drops from 50,3% to 15,7%; the increase in hydrogen's selectivity is instead negligible. The selectivities of remaining carbon gases tends to decrease over the time in all catalysts. It can be noted that selectivity of CH<sub>4</sub> is slightly reduced over time for Cu/ATP and Fe/ATP. Instead, the reduction is stronger in Ni/ATP and Co/ATP, where the selectivities are ~16% and 9% respectively at the beginning of the test, and they approach zero after 24 hours. The decreased selectivity to methane and carbon monoxide might be explained by decomposition of these products in carbon (eq. 9 and 10), that deposits on the surface of the catalysts (Chen et al., 2018).

Carbon deposition, deactivating the catalyst, causes the changes in glycerol's conversion and the gaseous selectivity. The carbon does encapsulate the particles of active metal, preventing further mass transfer between reactant and catalyst. The carbon deposition, its morphology, and the particles size of the catalysts before and after stability test are collected in table 8 (Chen et al., 2018).



**Table 8.** Carbon deposition and particle size of spent ATP supported catalysts.

Catalyst	Carbon deposition [%]	Morphology of deposited carbon	Dispersion of metal [%]	Catalyst's particles size [nm]	
				Before test	After test
Ni/ATP	29,15%	Filamentous	5,97	13,6	19,2
Co/ATP	23,39%	Filamentous	—	15,2	25,9
Cu/ATP	12,83%	Encapsulating	6,6	11,3	14,9
Fe/ATP	20,54%	Encapsulating	4,29	17,2	27,0

Carbon deposition and agglomeration of metal particles were found on all the spent catalysts. Carbon deposition is related to the size of metal particles and their dispersion. Larger metal particles accelerate the rate of carbon deposition on material surface. Instead, higher dispersion of metal reduces this effect. This is seen for Cu/ATP, the catalyst with highest dispersion and lowest carbon deposition. Two species of carbon were found: encapsulating and filamentous. The first type was present on Cu and Fe, causing deactivation. The second was found on Ni and Co, that remained relatively stable after the test (Chen et al., 2018).

In conclusion, Ni/ATP and Co/ATP show a better catalytic activity than Cu/ATP and Fe/ATP. Moreover, they are not deactivated by carbon deposition, keeping a stable behaviour. Attapulgite as material for catalyst's support plays a role as its higher specific area promotes dispersion of metal and thermal stability (Chen et al., 2018).

Considering the catalytic performances at steady condition and at the end of the stability test, cobalt can be assessed as the best transition metal to be supported on attapulgite.

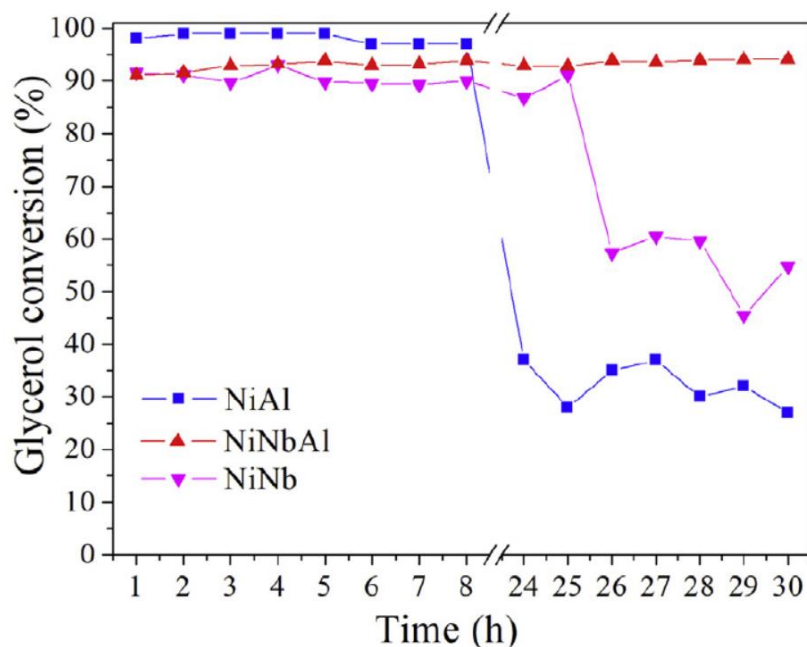
### 3.3.4 Ni catalysts supported on Niobia-Alumina

Niobia has been used as catalytic support or promoter in several reactions: dehydration of alcohols, dehydrogenation of long chain paraffins, esterification, and hydrogenation of carbon monoxide, to mention few (Nowak and Z., 1999). Niobia shows in fact interesting properties, like strong metal-support interaction and oxygen mobility. Moreover, when reduced at high temperature, it promotes the “decoration effect”: a migration of the support over the surface of dispersed metal particles. This has a great influence on the properties of metal phase, both by geometric and electronic factors. The first, through the partial covering of active sites by reducible oxide species. The second, by affecting the adsorption strength, changing the catalytic activity and resistance to coke formation (Menezes et al., 2018).

Previous literature doesn't mention niobia as supporting material for nickel in steam reforming of glycerol. In their research, Menezes and co-workers start this investigation, by studying the performance of nickel catalysts supported on alumina, niobia and niobia/alumina during glycerol's steam reforming. All the three catalysts were prepared with a quantity of active metal, nickel oxide, equal to 20% of catalyst's weight. Supports of alumina and niobia were prepared by precipitation, and the related catalysts are referred to as NiAl and NiNb. The support of niobia/alumina (where Nb accounts for 10% of support's weight) was prepared by coprecipitation, and the related catalyst referred to as NiNbAl. Coprecipitation was chosen over impregnation, the method generally applied for supports in Nb<sub>2</sub>O<sub>5</sub>/Al<sub>2</sub>O<sub>3</sub>, to obtain a higher dispersion of niobia over alumina, and a stronger metal-support interaction (Menezes et al., 2018).

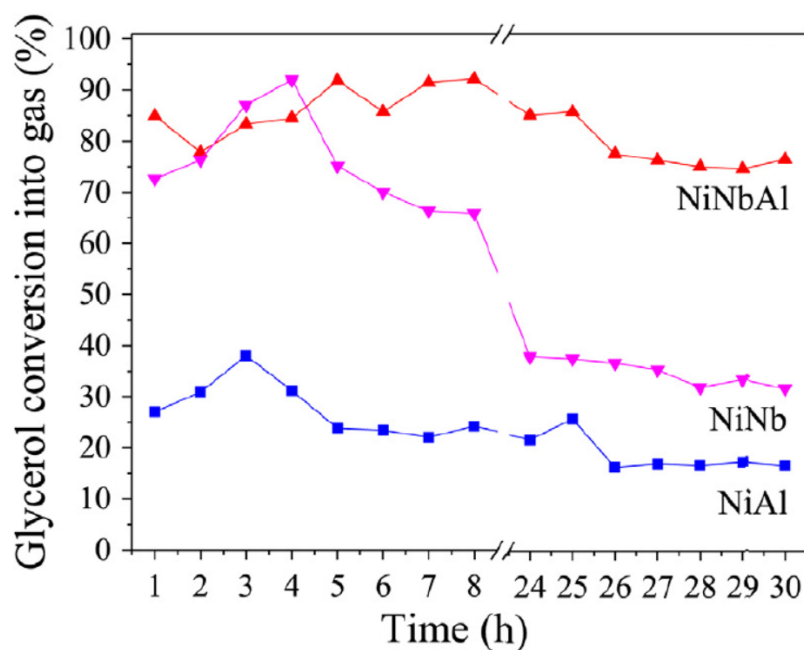
The steam reforming was carried out in a fixed bed reactor at atmospheric pressure and 500 °C, for 30 hours. The quantity of glycerol was 20% volume in water, corresponding to a molar ratio water to glycerol of 16,2. The feed flow was 0,106 mL/min, and the catalyst used 150 mg (Menezes et al., 2018). The performances are calculated with equations A.9-A.14.

Glycerol's conversions, respectively global and into gas, are presented in figures 20 and 21 as function of time, during the 30 hours of stability test.



Reprinted from (Menezes et al., 2018), Copyright (2018), with permission from Elsevier.

Figure 20. Nb supported catalysts: glycerol conversion.



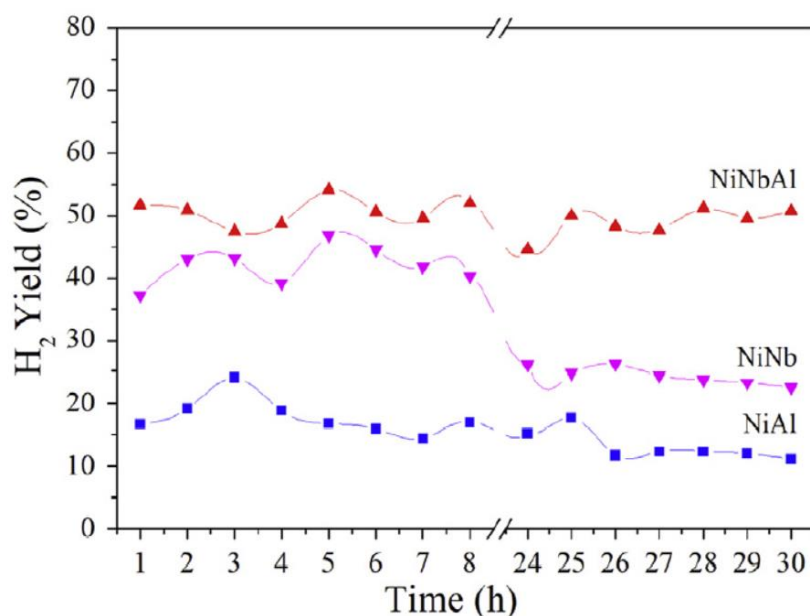
Reprinted from (Menezes et al., 2018), Copyright (2018), with permission from Elsevier.

Figure 21. Nb supported catalysts: glycerol conversion into gas.

Figure 20 shows that NiAl has a glycerol's conversion close to 100% in the first 8 hours. Then, it decreases continuously in the next 16 hours down to circa 35%. NiNb has a conversion of about 90% for the first 25 hours, then it drops to ~60% in 1 hour. Both catalysts suffered from deactivation after 24-26 hours of process. Deactivation is due to sintering of nickel and coke formation, promoted by the acid sites present both in alumina and niobia. NiNbAl is the most performing catalyst, showing a stable conversion of about 90% all time, without being affected by deactivation (Menezes et al., 2018).

As seen in figure 21, NiNbAl is the catalyst with the highest glycerol's conversion into gas, with values ranging from 80 to 90% in the first 8 hours, stabilizing to circa 75% at the end of the test. NiAl shows a max conversion of 40% at the 3<sup>rd</sup> hour of test, that then decreases over time stabilizing to circa 15% after 26 hours until the end of the test. NiNb has a conversion decreasing from a max above 90% after 4 hours, to about 35% at the end of the test (Menezes et al., 2018).

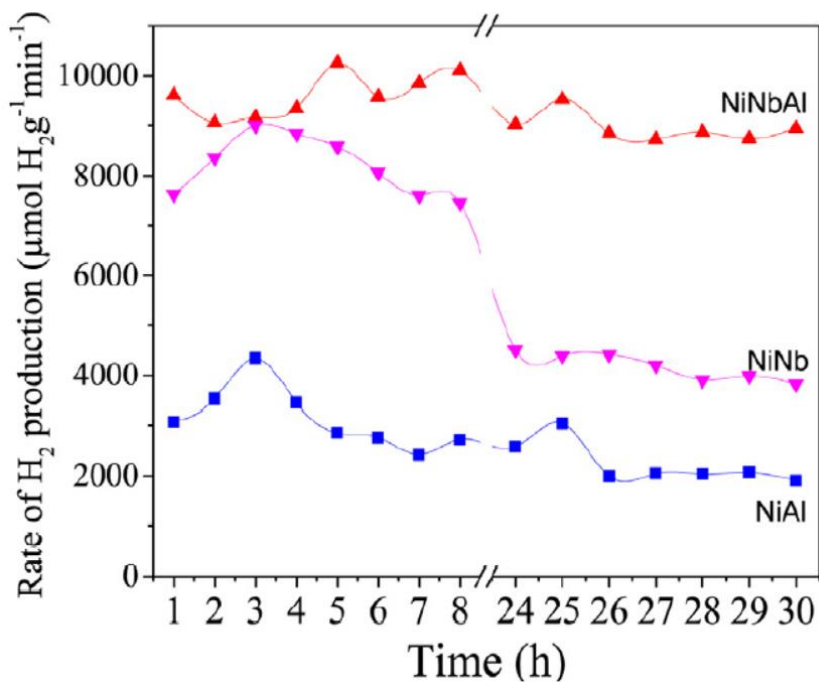
Hydrogen's yield and production as function of time are shown in figures 22 and 23.



Reprinted from (Menezes et al., 2018), Copyright (2018), with permission from Elsevier.

**Figure 22.** Nb supported catalysts: H<sub>2</sub> yield.

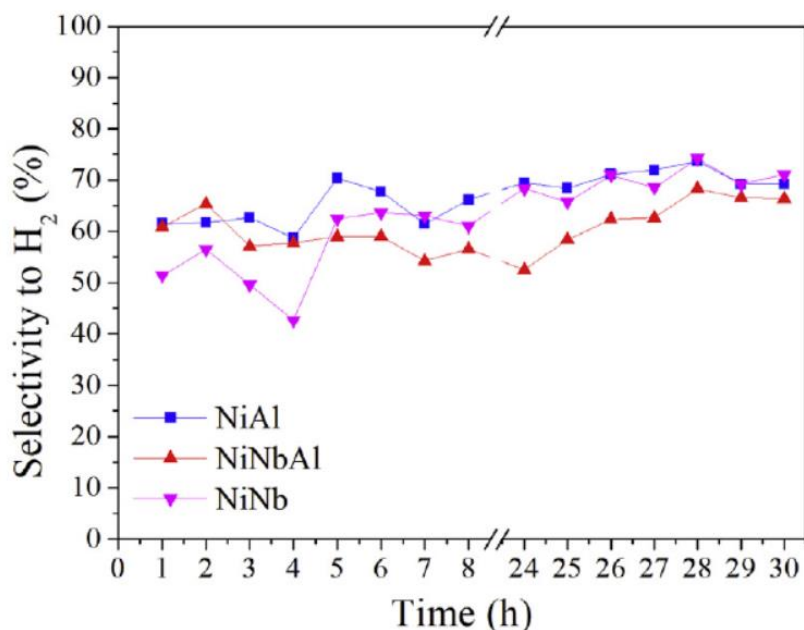
NiNbAl is the most performing catalyst, showing the highest H<sub>2</sub> yield and production rate, both relatively stable over time: their average values are respectively 50% and 9374  $\mu\text{mol g}^{-1} \text{min}^{-1}$ . This suggests that the catalyst promotes both the reactions of glycerol's reforming and water gas shift. For NiNb, both H<sub>2</sub> yield and production rate decrease after 24 hours. Their average values during the test are 34% and 6320  $\mu\text{mol g}^{-1} \text{min}^{-1}$ . NiAl has the worst performance, with an average hydrogen's yield and production rate of only 16% and 2720  $\mu\text{mol g}^{-1} \text{min}^{-1}$ . The high coke deposition on this catalyst suggests the occurrence of hydrogenation reactions of carbon monoxide and dioxide (eq. 8 and 11) (Menezes et al., 2018).



Reprinted from (Menezes et al., 2018), Copyright (2018), with permission from Elsevier.

**Figure 23.** Nb supported catalysts: H<sub>2</sub> production.

Figure 24 shows the hydrogen's selectivity of the different catalysts.

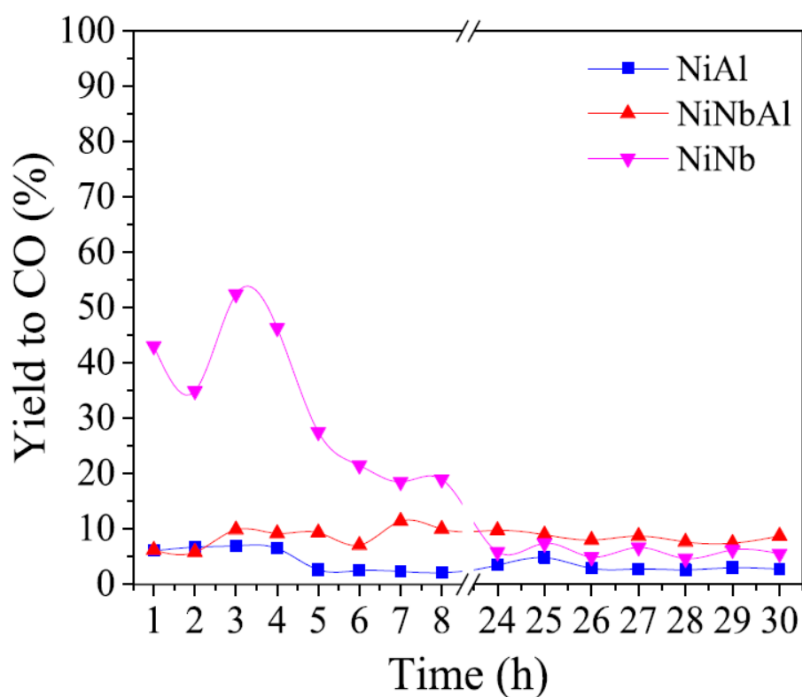


Reprinted from (Menezes et al., 2018), Copyright (2018), with permission from Elsevier.

**Figure 24.** Nb supported catalysts: selectivity to H<sub>2</sub>.

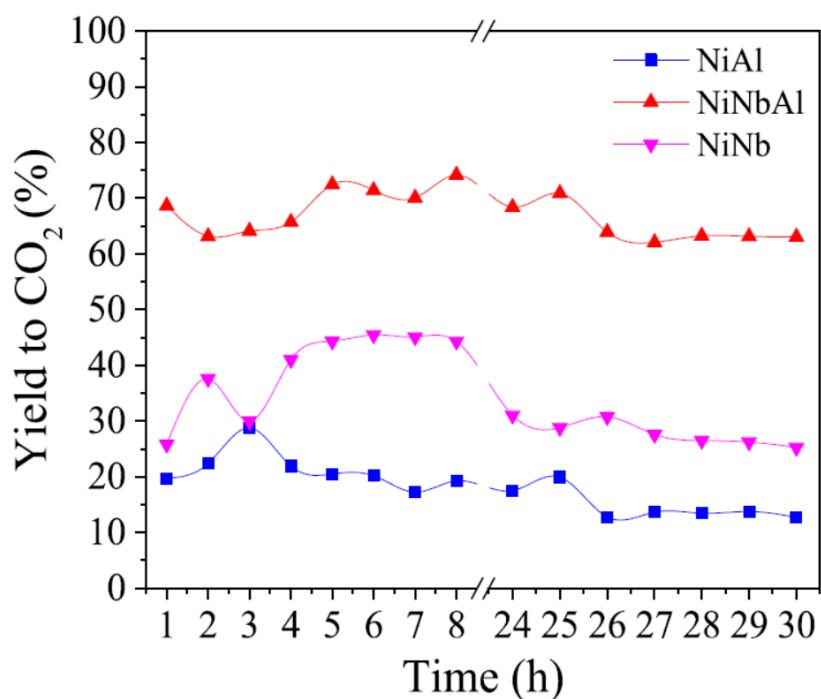
At the beginning of the test, NiAl and NiNbAl have a selectivity slightly above 60%, while NiNb slightly above 50%. After 30 hours, NiAl and NiNb stabilize their selectivity to about 70%, while NiNbAl to circa 65%.

The catalytic yields to carbon monoxide and dioxide are presented in figures 25 and 26.



Reprinted from (Menezes et al., 2018), Copyright (2018), with permission from Elsevier.

Figure 25. Nb supported catalysts: yields to CO.



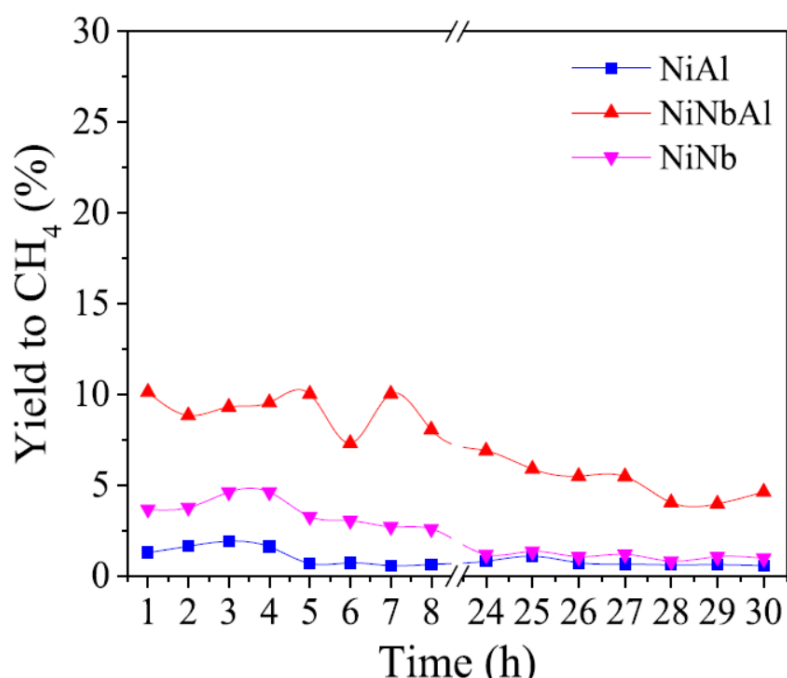
Reprinted from (Menezes et al., 2018), Copyright (2018), with permission from Elsevier.

Figure 26. Nb supported catalysts: yields to CO<sub>2</sub>.

As seen in figure 25, NiNbAl and NiAl have a stable trend over time, and an average yield to CO of circa 10% and 5%, respectively. The yield of NiNb reaches a max of 55% after 3 hours, for then decreasing and stabilizing between the values of the other two catalysts at the end of the test. This means that for NiNb the water gas shift reaction is promoted over the time. Low yield to CO is due not only to water gas shift, but also to the disproportionation reaction of carbon monoxide (equation 10) (Menezes et al., 2018).

As shown in figure 26, NiNbAl has the highest yield to CO<sub>2</sub> of about 65% at the end of the test. This confirms the high activity of this catalyst in steam reforming and water gas shift reactions. NiNb and NiAl follow, with a yield respectively of circa 25% and 15% towards the end of the stability test (Menezes et al., 2018).

Figure 27 shows the catalytic yield to methane.



Reprinted from (Menezes et al., 2018), Copyright (2018), with permission from Elsevier.

**Figure 27.** Nb supported catalysts: yields to CH<sub>4</sub>.

NiNbAl has the highest yield to methane, decreasing from 10% to 5% at the end of the test. Since this catalyst has the highest glycerol's conversion and yield to hydrogen, this means that methane has a preferential formation by methanation of carbon monoxide released from glycerol's decomposition (reaction 4 followed by reaction 5). NiAl and NiNb show instead a low methane yield (it stabilizes in both to circa 1% after 24 hours) indicating a low activity in side reactions of methanation (eq. 5 and 6) (Menezes et al., 2018).

Relevant data for the analysis of the spent catalysts are collected in table 9.

**Table 9.** Carbon deposition and particle size of spent Nb supported catalysts.

Reprinted (adapted) from (Menezes et al., 2018), Copyright (2018), with permission from Elsevier.

Catalyst	Catalyst's mass loss [%]	Morphology of deposited carbon	Ni dispersion [%]		Ni average crystallite size [nm]	
			Before test	After test	Before test	After test
NiAl	70%	Amorphous	15,0	12,3	6,7±0,8	8,2±2,0
NiNb	70%	Amorphous	8,5	5,7	11,9±1,4	17,7±4,1
NiNbAl	40%	Filamentous	16,8	13,1	6,0±0,6	7,7±1,3

The addition of niobia as promoter in the alumina support has beneficial effects for the catalyst. NiNbAl shows the highest nickel dispersion and the lowest crystallite size. Nickel has also the strongest interaction with NbAl support, so the metal particles are not easily detachable from the support. The combination of these properties results in a high resistance to sintering and low carbon deposition, as shown by the lowest mass loss of the catalyst. Instead, when the metal-support interaction is weak like in NiAl and NiNb, the nickel particles can be separated from the support. These released particles promote carbon nucleation that encapsulates them, deactivating the nickel. These results are coherent with the type of deposited carbon found on the three catalysts: filamentous on NbAl support, and amorphous on Al and Nb supports (Menezes et al., 2018).

It can be concluded that the addition of niobia in the aluminium support improves strongly the behaviour of Ni catalyst. Further studies could investigate the performance of NiNbAl catalyst as function of Nb doping. If the beneficial effects of niobia are still maintained by decreasing its amount, the cost of the catalyst could be reduced (Menezes et al., 2018).

### 3.3.5 Comparison of catalysts analysed

Table 10 summarizes the main process conditions and performances obtained with the latest catalysts developed for steam reforming of glycerol into hydrogen. Reactor type and pressure are the same in all processes. The glycerol's conversion reported is the conversion into gas for all catalysts in except of Co/ATP, where only the global conversion was provided. NiSiZr and Co/ATP were evaluated by the authors both at steady state condition and in a stability test, while the other two catalysts were assessed directly in a stability test. The comparison is therefore made evaluating the performances shown in the stability tests.

*Table 10. Performance of latest catalysts for steam reforming of glycerol.*

Catalyst	Ni/SiZr	NiZr <sub>0,5</sub> Al	Co/ATP	NiNbAl
Reactor	fixed bed			
Glycerol vol. in feed [%]	31	8	57,5	20
WHSV [h <sup>-1</sup> ]	39 <sup>a</sup>	15	6,5	44,6 <sup>b</sup>
Temperature [°C]	600	450	600	500
Pressure	atmospheric			
Glycerol conversion [%]	37,9	96,5	73	75
Selectivity to H <sub>2</sub> [%]	76,7	97,7	90	65
Test duration [h]	20	8	24	30
COP [1/°C]	0,12	0,02	0,10	0,26

Calculated considering a density of the feed of: <sup>a</sup>1,081 g/ml; <sup>b</sup>1,052 g/ml.

A straight assessment of the best performance in terms of highest conversion and selectivity is not possible, because relevant parameters like feed composition, WHSV, temperature and test duration are quite different among the catalysts. The evaluation shall consider that high glycerol concentration in the feed and high WHSV mean higher workload for the catalyst. Longer duration of the test means higher possibility of catalyst deactivation. In addition, lower reaction temperature means cheaper process operation. Given these considerations, the comparison is performed through a global coefficient of performance, defined according equation A.15.

NiNbAl shows the highest COP and is assessed as the best catalyst: its relatively high values of conversion and selectivity are achieved at the longest test duration, the highest WHSV along with a high glycerol concentration, and at moderate temperature. Ni/SiZr is the second-best catalyst: even if its conversion and selectivity are lower than ones of Co/ATP, the product of its feed concentration by WHSV and test duration is 2,7 times higher. NiZr<sub>0,5</sub>Al shows the highest conversion and selectivity at the lowest reaction temperature. However, they are achieved at the shortest test duration, the lowest glycerol's concentration and the second lowest WHSV. Therefore, this is the least performing catalyst.

Further work is needed to correctly assess the best catalyst for an industrialization of the process. At first, all catalysts should be tested in identical conditions. Then, their production cost should be estimated. A balance of performance and costs can finally identify the most suitable catalyst to be employed at industrial level.



### 3.4 Techno-economic assessment of steam reforming plant

As introduced in paragraph 3.1, steam reforming of glycerol is considered the most promising route to valorize this by-product of biodiesel production. The required process technology and infrastructure is essentially the one already in use for steam reforming of methane. Moreover, compared to other conversion processes of glycerol into hydrogen, steam reforming is found to be the most effective and convenient (Chen et al., 2018).

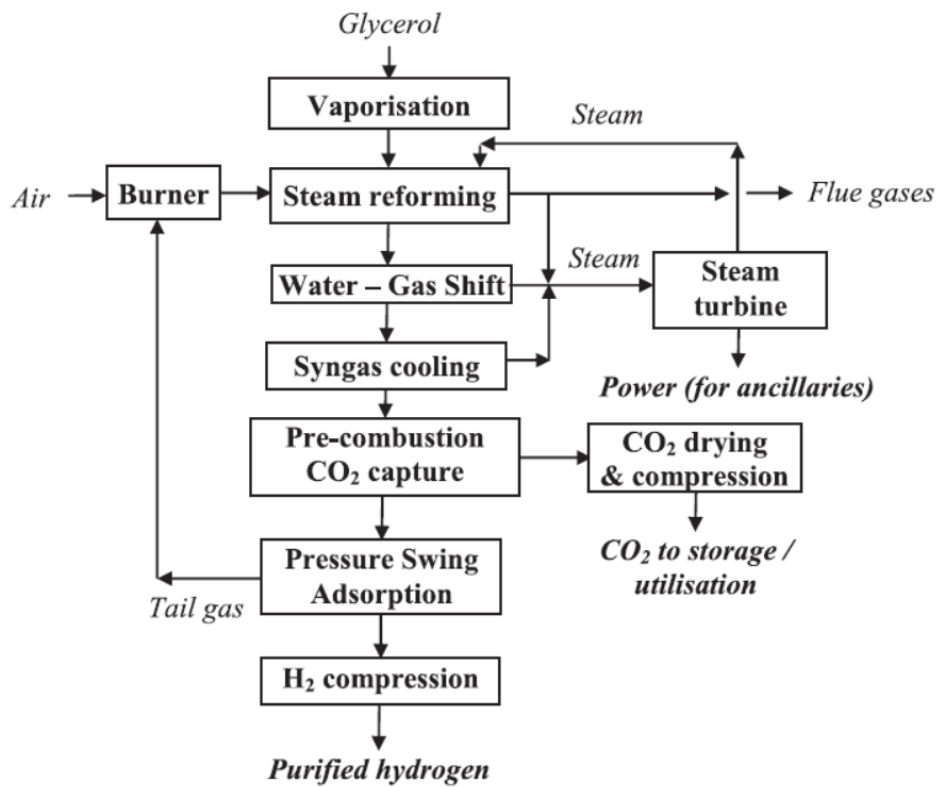
A techno-economic study of catalytic reforming at industrial scale is reported in the research article from Ana Maria and Calin Cristian Cormos, where the authors evaluate the thermo-chemical conversion of glycerol into hydrogen and power, by conventional steam reforming and oxygen autothermal reforming, with and without CO<sub>2</sub> capture. Their analysis investigates three categories of design concepts: hydrogen production plants (cases 1), power generation plants (cases 2), and a flexible hydrogen and power co-generation plant, based on conventional steam reforming with CO<sub>2</sub> capture (case 3). The catalyst considered for glycerol reforming is nickel-based in all cases. The plants are sized for production rates comparable with existing industrial applications: for cases 1, the hydrogen output is set to 10<sup>5</sup> Nm<sup>3</sup>/h, while the net power output for cases 2 is set to 500 MW<sub>e</sub>. The design cases are summarized in table 11 (Cormos, 2017).

*Table 11. Design cases of glycerol reforming plants.*

GLYCEROL REFORMING PLANT CONCEPTS	1. HYDROGEN PRODUCTION	2. POWER GENERATION	3. FLEXIBLE H <sub>2</sub> + POWER COGEN.
a. Steam reforming without CO <sub>2</sub> capture.	1.a	2.a	—
b. Steam reforming with CO <sub>2</sub> capture.	1.b	2.b	X
c. Autothermal reforming without CO <sub>2</sub> capture.	1.c	2.c	—
d. Autothermal reforming with CO <sub>2</sub> capture.	1.d	2.d	—

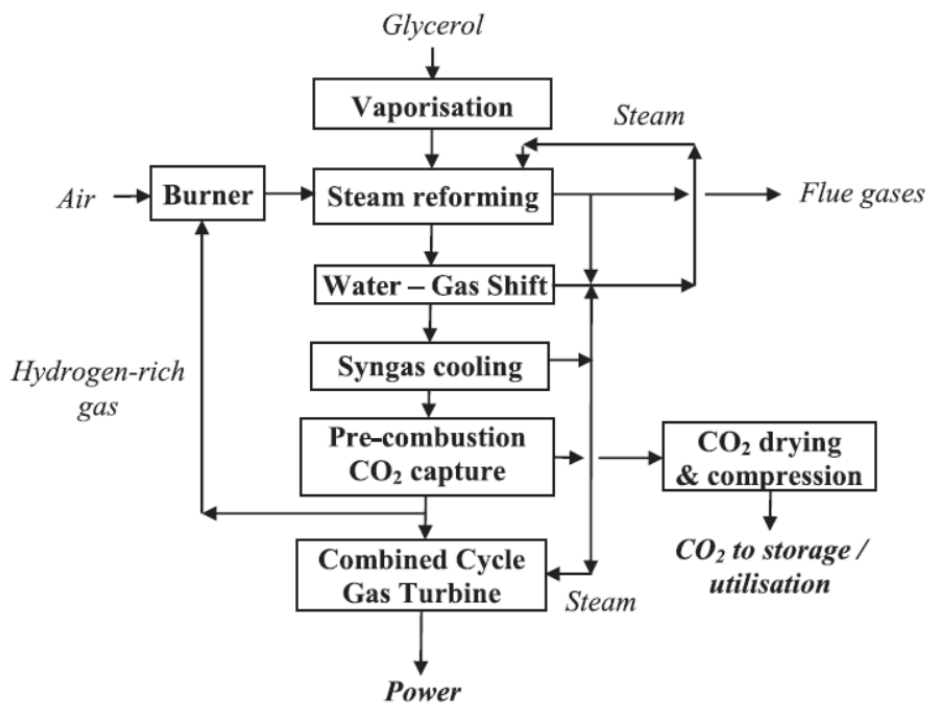
Figure 28 shows a schematic of case 1.b: hydrogen production by steam reforming with CO<sub>2</sub> adsorption. Following glycerol's decomposition and water gas shift reactions, the syngas is cooled and sent to the carbon capture unit, featured by a gas-liquid absorption-desorption cycle. The CO<sub>2</sub> captured is then dried employing triethylene glycol in an absorption-desorption cycle and compressed for transportation or storage. The gas enriched in hydrogen is purified in a Pressure Swing Adsorption unit; finally, it is compressed and stored for customers. The source of energy to drive the process is the tail gas from PSA unit, which is combusted in a burner and provides heat to produce steam. This is utilized both in reforming process and to drive a steam turbine, which generates the power required to drive the ancillary units (Cormos, 2017).

Figure 29 shows a schematic of case 2.b: power generation by steam reforming with CO<sub>2</sub> adsorption. This configuration doesn't need the PSA unit. Following the CO<sub>2</sub> capture, the hydrogen rich gas is employed both as working fluid in a gas turbine cycle for power generation, and in the burner for steam generation (Cormos, 2017).



Reprinted from (Cormos, 2017), Copyright (2017), with permission from Elsevier.

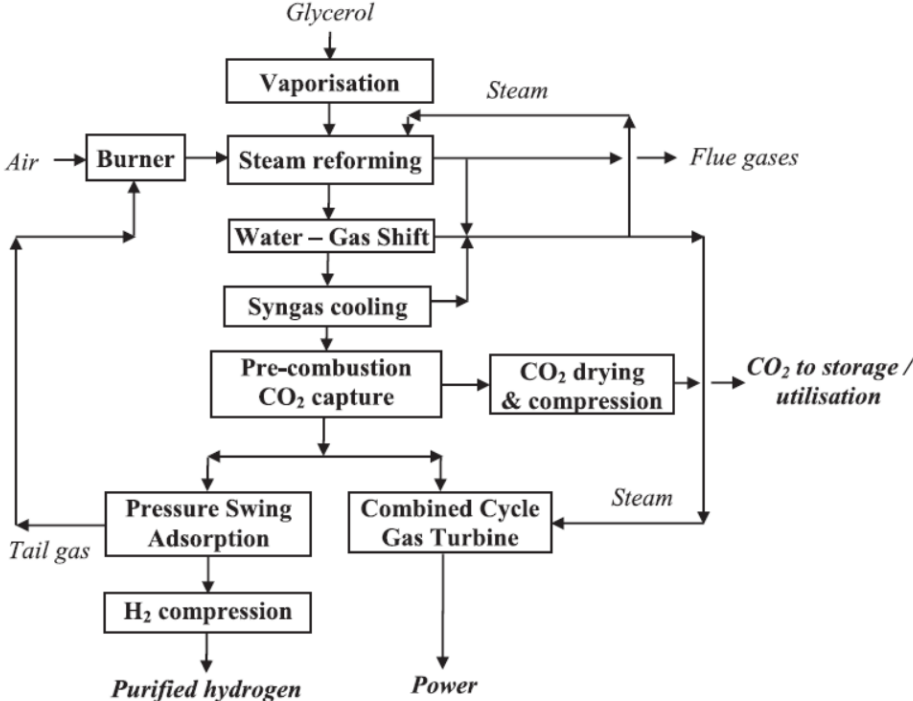
*Figure 28. Schematic of steam reforming plant: H<sub>2</sub> production with CO<sub>2</sub> capture.*



Reprinted from (Cormos, 2017), Copyright (2017), with permission from Elsevier.

*Figure 29. Schematic of steam reforming plant: power generation with CO<sub>2</sub> capture.*

Figure 30 shows a schematic of case 3: flexible hydrogen and power co-generation. It can be observed that this configuration is a combination of the previous setups: after CO<sub>2</sub> capture, the hydrogen rich gas is sent both to the PSA unit for hydrogen production, and to the gas turbine for power generation. The steam turbine is now not required.



Reprinted from (Cormos, 2017), Copyright (2017), with permission from Elsevier.

**Figure 30.** Schematic of steam reforming plant: H<sub>2</sub> and power cogeneration with CO<sub>2</sub> capture.

### 3.4.1 Technical assessment

The different concepts of reforming plants are simulated with software ChemCad, optimizing glycerol's conversion and yield to hydrogen, as well as heat and energy integration. The technical parameters are calculated with equations A.16-A.21. The plants are designed in a thermal integrated mode: the only energy input is the glycerol, and all the heating duties are fed by heat recovery from available hot streams. The conversion rate obtained is higher than 98%, with a yield of circa 80%; these results are found consistent with experimental data presented in literature (Cormos, 2017).

Relevant design parameters of the plants are reported in table 12.

**Table 12.** *Glycerol reforming plants: main design parameters.*

Reprinted (adapted) from (Cormos, 2017), Copyright (2017), with permission from Elsevier.

PLANT UNIT	DESIGN PARAMETERS
Glycerol composition [% wt.]	52,5% glycerol, 10% methanol, 14,5% methyl oleate, 23% water.
Glycerol vaporization	Vaporizer outlet temperature: 350 °C
Glycerol reforming process	Fuel pre-heating: 500 °C Water/glycerol ratio: 10/1 Catalyst: Ni/Al <sub>2</sub> O <sub>3</sub> Operating pressure: 30 bar Operating temperature: 900 °C
Water Gas Shift conversion	Catalyst: Fe-Cr Steam/CO ratio: 2,5/1 Two adiabatic fixed bed reactors Operating temperature: 300-450 °C
Heat Recovery Steam Generation & Steam turbine	Pressure levels: 120 bar/34 bar/3 bar One medium pressure steam re-heat Steam turbine isentropic efficiency: 85%
Pressure Swing Adsorption	Purified hydrogen: >99,95% (vol.) Tail gas pressure: 1,5 bar
CO <sub>2</sub> capture (absorption-desorption cycle)	Solvent: Methyl-diethanol-amine (MDEA) Solvent regeneration: pressure flash & thermal Heat duty for regeneration: ca 0,65 MJ/kg CO <sub>2</sub>
Gas turbine	Mitsubishi Hitachi Power Systems – M701G2 Net power output: 334 MW Net power efficiency: 39,5% Pressure ratio: 21 Turbine outlet temperature: 588 °C
Heat exchangers	$\Delta T_{\min}$ =10 °C Pressure drop: 3-5% of inlet pressure

The performance indicators of hydrogen production concepts are reported in table 13.

**Table 13.** Plants performance indicators:  $H_2$  production.

Reprinted (adapted) from (Cormos, 2017), Copyright (2017), with permission from Elsevier.

PROCESS PARAMETER		DESIGN CASES			
		1.a	1.b	1.c	1.d
Glycerol flowrate	[t/h]	110,44	110,44	136,42	136,42
Glycerol thermal energy (A)	[MW <sub>th</sub> ]	468,14	468,14	578,29	578,29
Gross power output (B)	[MW <sub>e</sub> ]	25,36	13,54	62,52	45,28
ASU power consumption	[MW <sub>e</sub> ]	—	—	11,25	11,25
Reformer power consumption	[MW <sub>e</sub> ]	0,11	0,11	0,13	0,13
CO <sub>2</sub> drying and compression	[MW <sub>e</sub> ]	—	7,25	—	9,04
Hydrogen compression	[MW <sub>e</sub> ]	3,88	3,88	3,86	3,86
Power island consumption	[MW <sub>e</sub> ]	0,25	0,25	0,44	0,43
Total power consumption (C)	[MW <sub>e</sub> ]	4,24	11,49	15,68	24,71
Hydrogen output (D)	[MW <sub>th</sub> ]	300	300	300	300
Net power output (E=B-C)	[MW <sub>e</sub> ]	21,12	2,05	46,84	20,57
Hydrogen efficiency (D/A*100)	[%]	64,08	64,08	51,87	51,87
Net power efficiency (E/A*100)	[%]	4,51	0,43	8,10	3,55
Cumulative energy efficiency	[%]	68,59	64,51	59,97	55,42
Carbon capture rate	[%]	—	71,20	—	75,48
Specific CO <sub>2</sub> emissions	[kg/MWh]	446,73	136,75	503,61	135,38

The main result is that steam reforming is more energy efficient than autothermal reforming, both in designs with and without carbon capture. Comparing the cumulative energy efficiency of the two technologies, case 1.a is about 8,6 percentage points more efficient than case 1.c, while case 1.b is about 9,1 percentage points more efficient than case 1.d. The reason is a higher thermal efficiency of steam reforming due to a higher fraction of combustible gases (CO, H<sub>2</sub> and CH<sub>4</sub>) available in the syngas. Moreover, autothermal reforming requires an Air Separation Unit which is an important source of power consumption. Carbon capture rate is instead 4,3 percentage points higher in autothermal reforming. The lower performance in steam reforming is due to the combustion of the tail gas in the burner, which releases CO<sub>2</sub> that is not recovered (Cormos, 2017).

The performance indicators of power production concepts are reported in table 14.

**Table 14.** *Plants performance indicators: power production.*

Reprinted (adapted) from (Cormos, 2017), Copyright (2017), with permission from Elsevier.

PROCESS PARAMETER		DESIGN CASES			
		2.a	2.b	2.c	2.d
Glycerol flowrate	[t/h]	275,56	275,56	325,38	325,38
Glycerol thermal energy (A)	[MW <sub>th</sub> ]	1168,06	1168,06	1379,24	1379,24
Gas turbine output	[MW <sub>e</sub> ]	334	334	334	334
Steam turbine output	[MW <sub>e</sub> ]	209,47	192,59	227,75	210,96
Expander power output	[MW <sub>e</sub> ]	5,22	3,77	6,45	4,82
Gross power output (B)	[MW <sub>e</sub> ]	548,69	530,36	568,20	549,78
ASU power consumption	[MW <sub>e</sub> ]	—	—	13,58	13,58
Reformer power consumption	[MW <sub>e</sub> ]	0,80	0,80	0,95	0,95
CO <sub>2</sub> drying and compression	[MW <sub>e</sub> ]	—	20,15	—	24,75
Power island consumption	[MW <sub>e</sub> ]	10,63	11,05	13,10	13,78
Total power consumption (C)	[MW <sub>e</sub> ]	11,43	32,00	27,63	53,06
Net power output (D=B-C)	[MW <sub>e</sub> ]	537,26	498,36	540,57	496,72
Gross power efficiency (B/A*100)	[%]	46,97	45,40	41,19	39,86
Net power efficiency (D/A*100)	[%]	45,99	42,66	39,19	36,01
Carbon capture rate	[%]	—	79,05	—	81,25
Specific CO <sub>2</sub> emissions	[kg/MWh]	668,49	152,57	784,62	180,90
SPECCA	[MJ/kg]	—	1,18	—	1,34

Also the power production concepts are more energy efficient with steam reforming than autothermal reforming, both in designs with and without carbon capture. Comparing the net power efficiency of the two technologies, case 2.a is about 6,8 percentage points more efficient than case 2.c, while case 2.b is about 6,6 percentage points more efficient than case 2.d. Carbon capture rate is closer, but 2,2 percentage points higher in autothermal reforming. Steam reforming has instead a lower specific primary energy consumption for CO<sub>2</sub> avoided (Cormos, 2017).

The third plant concept is evaluated as a flexible energy conversion system that can be profitably integrated in the electrical net, adapting to the irregular time-dependent demand from grid and market. According to the need, the glycerol can be fully converted into electrical power, or partially or totally into hydrogen, by gradually turning down the gas turbine. The plant is designed in the range 0-200 MW<sub>th</sub> (Cormos, 2017). The related performance indicators are reported in table 15.

*Table 15. Plant performance indicators: flexible H<sub>2</sub> and power co-generation.*

Reprinted (adapted) from (Cormos, 2017), Copyright (2017), with permission from Elsevier.

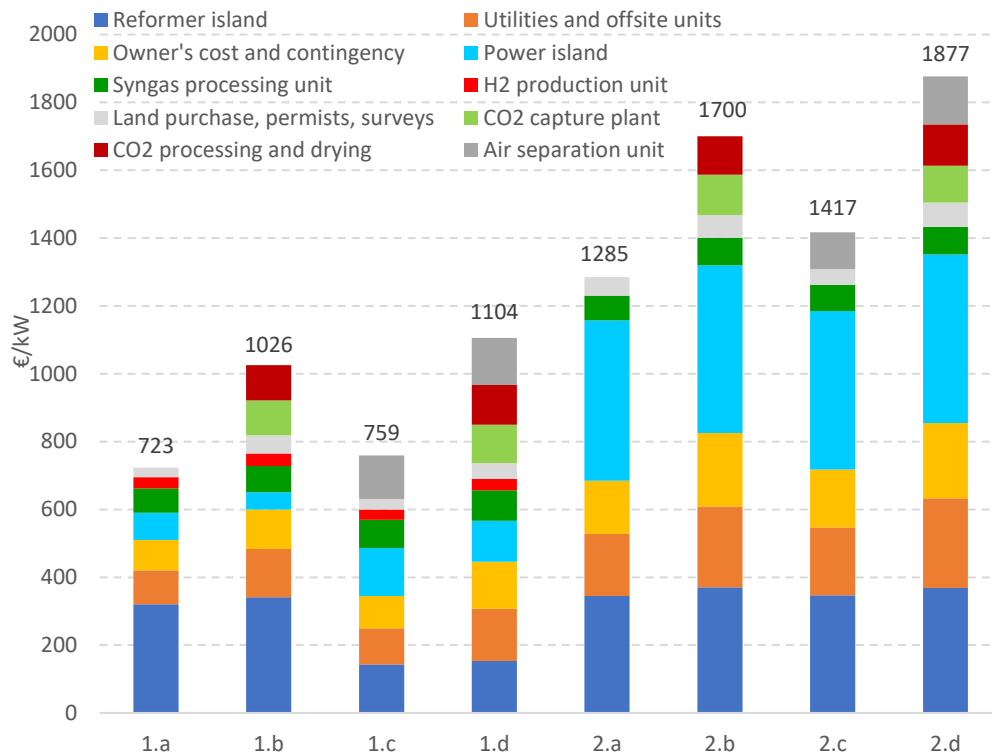
PROCESS PARAMETER		OPERATING MODE		
		100% power	50% H <sub>2</sub>	100% H <sub>2</sub>
Glycerol flowrate	[t/h]	275,56		
Glycerol thermal energy (A)	[MW <sub>th</sub> ]	1168,06		
Gas turbine output	[MW <sub>e</sub> ]	334,00	292,41	254,32
Steam turbine output	[MW <sub>e</sub> ]	192,59	171,05	154,10
Expander power output	[MW <sub>e</sub> ]	3,77	3,77	3,77
Gross power output (B)	[MW <sub>e</sub> ]	530,36	467,23	412,19
Reformer power consumption	[MW <sub>e</sub> ]	0,80	0,80	0,80
CO <sub>2</sub> drying and compression	[MW <sub>e</sub> ]	20,15	20,15	20,15
Hydrogen compression	[MW <sub>e</sub> ]	0	1,32	2,64
Power island consumption	[MW <sub>e</sub> ]	11,05	10,51	10,02
Total power consumption (C)	[MW <sub>e</sub> ]	32,00	32,78	33,61
Hydrogen thermal output (D)	[MW <sub>th</sub> ]	0	100	200
Net power output (E=B-C)	[MW <sub>e</sub> ]	498,36	434,45	378,58
Hydrogen efficiency (D/A*100)	[%]	0	8,56	17,12
Net power efficiency (E/A*100)	[%]	42,66	37,19	32,41
Cumulative energy efficiency	[%]	42,66	45,75	49,53
Carbon capture rate	[%]	79,05	79,05	79,05
Specific CO <sub>2</sub> emissions (H <sub>2</sub> & power)	[kg/MWh]	152,57	142,26	131,41

The total power consumption at full thermal output is slightly higher (5%) than at full electrical output. However, the cumulative energy efficiency increases with H<sub>2</sub> production, while specific CO<sub>2</sub> emissions tend to decrease. Carbon capture rate remains constant. Therefore, this system is intrinsically suitable as a flexible power generation unit. When the electrical demand from the grid is lower, the plant doesn't lose glycerol's energy but instead converts and stores it into hydrogen with an increased efficiency (Cormos, 2017).

### 3.4.2 Economic assessment

The economic assessment of the plants is performed through estimation of capital costs, operational and maintenance costs, hydrogen and power production costs and cumulative cash flow analysis (Cormos, 2017). The economic parameters are calculated with equations A.22-A.25.

Figures 31 and 32 report respectively the specific capital investment costs per net kW and the specific operational and maintenance costs per MWh, by design cases.

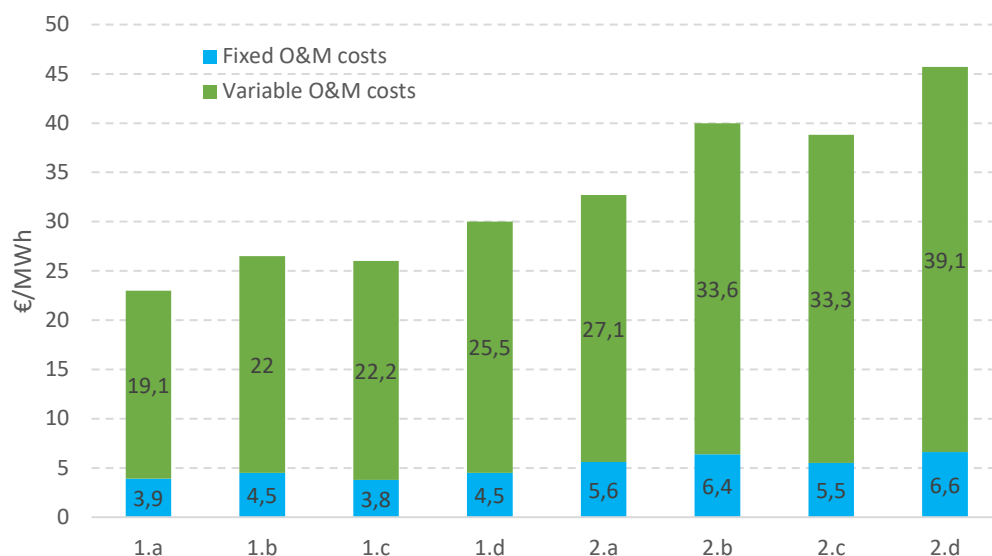


Reprinted (adapted) from (Cormos, 2017), Copyright (2017), with permission from Elsevier.

**Figure 31.** Glycerol reforming plants: specific investment costs.

As shown in figure 31, hydrogen production cases are in general cheaper than power generation ones, and autothermal reforming is more expensive than steam reforming. Within the same technology, the designs with carbon capture are more expensive than without carbon capture. In detail, the investment costs of autothermal design are between 5% and 7,6% higher than steam reforming in hydrogen production, and circa 10% higher in power production. The carbon capture feature in steam reforming bears an incremental capital cost of 42% and 32%, respectively for hydrogen production and power production cases. The corresponding incremental cost in autothermal reforming cases is respectively 45% and 32% (Cormos, 2017).





Reprinted (adapted) from (Cormos, 2017), Copyright (2017), with permission from Elsevier.

**Figure 32.** Glycerol reforming plants: specific O&M costs.

The operational and maintenance costs shown in figure 32 are detailed by their fixed and variable components. The fixed costs are not dependent on the energy generated: for example, taxes, insurances, administration, annual overhaul. The variable costs are instead proportional to the energy generated: for example, costs of fuels and catalysts, waste disposal, unscheduled repairs. The O&M costs of autothermal design are circa 13% higher than steam reforming in hydrogen production, and 19-14% higher in power production. The incremental O&M costs due to the carbon capture feature is in steam reforming of 15% and 22%, respectively for hydrogen production and power production cases. The corresponding incremental cost in autothermal reforming cases is respectively 15% and 18% (Cormos, 2017).

The levelized production costs of hydrogen and electricity, as well as capture costs of CO<sub>2</sub> are reported in table 16.

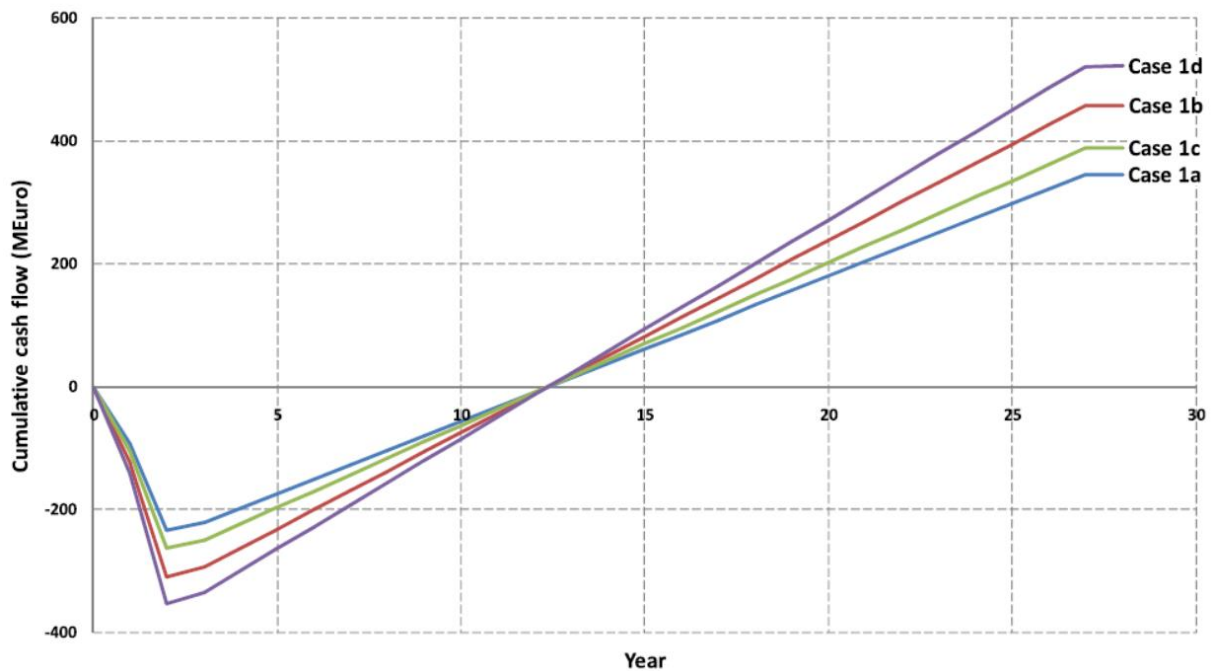
**Table 16.** Production costs of H<sub>2</sub> and electricity and capture costs of CO<sub>2</sub>.

Reprinted (adapted) from (Cormos, 2017), Copyright (2017), with permission from Elsevier.

COST		DESIGN CASES							
		1.a	1.b	1.c	1.d	2.a	2.b	2.c	2.d
Hydrogen	[€/MWh]	31,61	40,26	34,08	41,68	—	—	—	—
Electricity	[€/MWh]	—	—	—	—	49,84	65,86	54,71	72,29
CO <sub>2</sub> removal	[€/t]	—	25,41	—	20,27	—	28,19	—	26,75
CO <sub>2</sub> avoided	[€/t]	—	30,71	—	25,94	—	31,05	—	29,12

Compared to autothermal reforming, steam reforming is 3-7% cheaper in production of hydrogen and 9% cheaper in production of electricity. Autothermal reforming has instead a lower capture cost of CO<sub>2</sub>, thanks to its higher carbon capture rate. Removal of carbon dioxide increases the production cost of hydrogen by 27% and 22%, respectively in steam and autothermal reforming, and the cost of electricity by 32% in both technologies.

Figure 33 shows the cumulative cash flow analysis of hydrogen production cases. The analysis takes as assumption 2 years for construction of the plant, 25 years of operation and 1 year for recovery of the working capital (Cormos, 2017).



Reprinted (adapted) from (Cormos, 2017), Copyright (2017), with permission from Elsevier.

**Figure 33.** Glycerol reforming plants: cumulative cash flow analysis of  $H_2$  production cases.

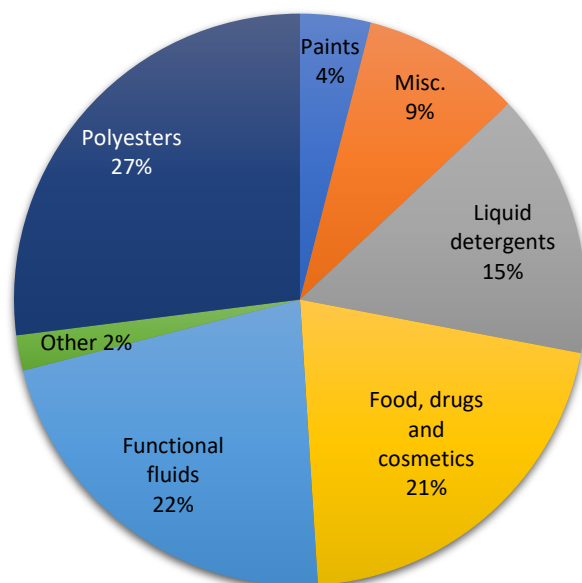
The highest cashflow is obtained for autothermal reforming and steam reforming with  $CO_2$  capture (cases 1.d and 1.b), followed by their corresponding configurations without  $CO_2$  capture (cases 1.c and 1.a) (Cormos, 2017).

### 3.4.3 Conclusions

The assessment shows that steam reforming technology is more energy efficient and cheaper than autothermal reforming, in both configurations of hydrogen production and power production. Autothermal reforming achieves instead higher carbon capture rates. The hydrogen and power co-generation plant is a flexible solution to supply electrical power to the grid, because capable of adapting to its variable needs: at lower power demands, the production is switched from electricity to hydrogen.

## 4 Valorization of glycerol into propylene glycol

Propylene glycol, also identified as 1,2-propanediol, is a chemical with molecular formula  $C_3H_8O_2$  (NCBI, 2019<sup>b</sup>). It has an isomer called 1,3-propanediol (NCBI, 2019<sup>c</sup>). Propylene glycol is a non-toxic compound which finds wide application in several fields. It is employed as a monomer for polyester resins, as an antifreeze agent, in liquid detergents, in paints, cosmetics and food, as detailed in figure 34. Currently, worldwide production of propylene glycol accounts for 2,2 million tonnes per year, with a global market growing at a yearly rate of 4,5% (Nanda et al., 2016).

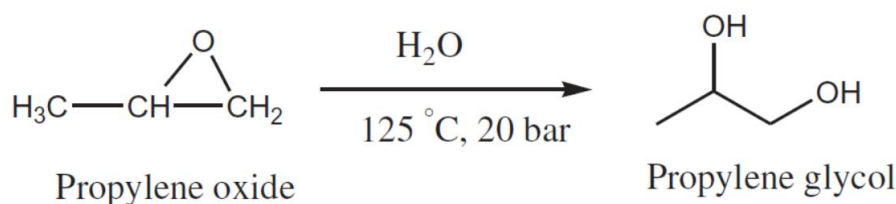


Reprinted (adapted) with permission from (Nanda et al., 2016). Copyright (2016) Taylor & Francis.

**Figure 34.** Commercial applications of propylene glycol.

Miscellaneous: tobacco humectants, flavours and fragrances, animal feed.

The conventional route to produce propylene glycol is by hydrolysis of propylene oxide derived from petroleum sources, as shown in figure 35.



Reprinted (adapted) with permission from (Nanda et al., 2016). Copyright (2016) Taylor & Francis.

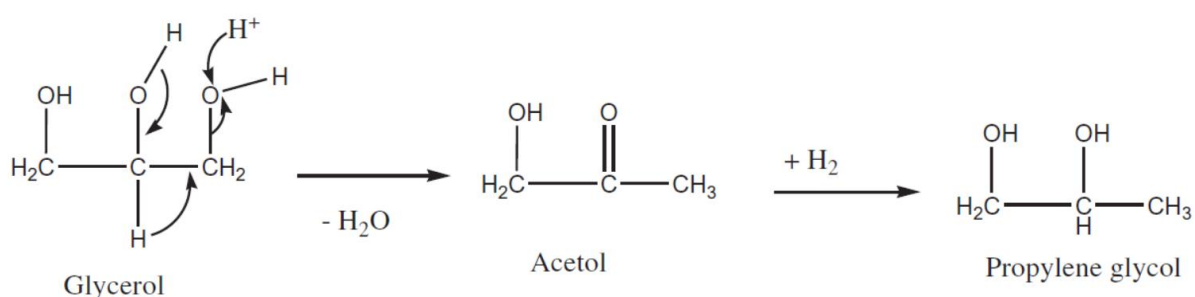
**Figure 35.** Hydrolysis reaction of propylene oxide into propylene glycol.

This process is usually non-catalytic, occurs at temperatures of 150-250 °C, pressures higher than 7 bar and employs large excess of water. The latter leads to the presence of di and tri-propylene glycol as co-products and the need for a separation unit, reducing the global efficiency and profitability (Nanda et al., 2016).

Therefore, hydrogenolysis of glycerol has recently attracted focus as a promising alternative to produce propylene glycol: it's not only a greener process but also a way to recycle a waste product on large scale, reducing the production costs (Nanda et al., 2016).

## 4.1 Hydrogenolysis - Reactions

Hydrogenolysis is a selective process to remove one atom of oxygen from a chemical, in two steps. The first is a reaction of dehydration of the feedstock, the second is a reaction of hydrogenation of the intermediate product. In hydrogenolysis of glycerol, its molecule is dehydrated into acetol in a highly endothermic reaction; then, acetol is hydrogenated into propylene glycol, as shown in figure 36. Dehydration of glycerol's molecule is the challenging part of the process, as it shall fulfil a selective scission of one of the primary C-O bonds only. If secondary C-O bonds or C-C bonds are cleaved, the scission results in the formation of degradation products like ethylene glycol, ethanol, methanol and methane, or 1,3-propanediol, respectively (Nanda et al., 2016).



Reprinted with permission from (Nanda et al., 2016). Copyright (2016) Taylor & Francis.

**Figure 36.** Hydrogenolysis reaction of glycerol into propylene glycol.

Conversion of glycerol by hydrogenolysis is carried out in batch or continuous flow reactors, in presence of metallic catalysts and hydrogen. The process was initially developed with homogeneous catalysts in batch reactors. However, homogeneous catalysis of glycerol presents some economic and environmental issues, like separation and recovery of the catalyst from the products, the use of expensive and toxic solvents in the reaction, and corrosion. Batch reactors instead require long reaction times and extended down time for maintenance, resulting in high specific labour cost and hindering the scale up to industrial level. Therefore, current research is focusing on heterogeneous catalysts and continuous flow reactors. The purpose is to increase the heat and mass transfer efficiency, as well as the surface to volume ratio, making the process more efficient and economical and easing its industrialization (Nanda et al., 2016).

## 4.2 Hydrogenolysis - Catalysts

Heterogeneous catalysts for glycerol's conversion into propylene glycol can be prepared through several methods: impregnation, ion-exchange, precipitation, gel-based processes, hydrothermal treatment, solid fusion and carbon microsphere template. Glycerol's conversion and selectivity to propylene glycol are strongly affected by preparation and activation methods. They both influence the structural and physicochemical properties of the catalysts, like metal dispersion and thermal stability. Proper preparation and activation can enhance the reducibility of the metal, minimizing metal sintering at the steps of reduction and calcination, and during

the reaction. Moreover, they can reduce the adsorption of water on the surface of the catalyst during reaction, improving the formation of the product. Studies report that calcination for a long period followed by reduction in a flow environment (air/H<sub>2</sub>) lead to higher active sites for hydrogenolysis of glycerol (Nanda et al., 2016).

The performances of heterogeneous catalysts - glycerol's conversion and selectivity to propylene glycol - are reported in table 17 by preparation method.

**Table 17.** Hydrogenolysis to propylene glycol: performance of catalysts by preparation method.

Reprinted (adapted) with permission from (Nanda et al., 2016). Copyright (2016) Taylor & Francis.

Catalyst	Method	Surface area [m <sup>2</sup> /g]	Reactor type / Process conditions	Glycerol X [%]	1,2PD S [%]
Cu-Al <sub>2</sub> O <sub>3</sub>	CP	57	Batch reactor / 20% wt aq glycerol, 0,01 g/mL cat, 493 K, 5,2 MPa H <sub>2</sub> , 5 h	58	88
	SF	127		5	74
Cu-SiO <sub>2</sub>	IM	38,6 (Cu)	Batch reactor / 80% aq glycerol, 453 K, 6 MPa, 4 g cat, 12 h	83	99
	PG	198,9		50	98
CuO-ZnO	OG	30,1 (Cu)	Batch reactor / 140 mL pure glycerol, 473 K, 3 g cat, 5 MPa H <sub>2</sub> , 7 h	46	90
	CP	16,7		17	87
Cu-Cr <sub>2</sub> O <sub>3</sub>	IM	15,1	Batch reactor / 50 g glycerol, 1 g cat, 8 MPa, 493 K	32	41
	Pre	19,3		80	85
CuO/MgO	CP	26,2	Batch reactor / 75% wt aq glycerol 8,0 mL, 1,0 g cat, 3,0 MPa H <sub>2</sub> , 453 K, 20 h	72	98
	IM	N.D.		30	93
Ru-TiO <sub>2</sub>	IM	2,4	Batch reactor / 20% wt aq glycerol, 6 MPa H <sub>2</sub> , 453 K, catalyst loading 6% wt of solution, 8 h	31	59
	CP	7,2		44	58
Cu-ZnO/Al <sub>2</sub> O <sub>3</sub>	IM	145	Flow reactor / 80% wt aq glycerol, 523 K, 3,2 MPa H <sub>2</sub> , 2,8 h <sup>-1</sup>	100 <sup>a</sup>	95 <sup>a</sup>
	CP	182		20 <sup>a</sup>	76 <sup>a</sup>
	SG	175		76 <sup>a</sup>	78 <sup>a</sup>
Ni-ZnO	IM	5	Flow reactor / 10% wt aq glycerol, W <sub>cat</sub> =0,5 g, 508 K, 3,1 MPa H <sub>2</sub> , 6 h	45	44
	CP	11		80	46
	HT	24		84	50
	CT	32		88	55
Cu-ZnO/Al <sub>2</sub> O <sub>3</sub>	IM	25	Flow reactor / 80% wt aq glycerol, 523 K, 0,05 h <sup>-1</sup> , 0,1 MPa	64	68
	CP	75		86	85

CP: co-precipitation, CT: carbon microsphere template, HT: hydrothermal treatment, IE: ion-exchange, IM: impregnation, OG: oxalate gel, PG: gel precipitation, Pre: precipitation, SF: solid fusion, SG: sol-gel.

<sup>a</sup>After 12 hours on stream.

In general, co-precipitation leads to better catalytic performances than impregnation, thanks to a larger surface area of the catalyst and a higher dispersion of Cu obtained with this method. Moreover, once reduced, the co-precipitated catalysts have higher total acidity, which promotes dehydration of glycerol to acetol. However, the highest conversion and selectivity, respectively of 100% and 95%, are observed for Cu-ZnO/Al<sub>2</sub>O<sub>3</sub> prepared by impregnation. Compared to the other preparation methods, the resulting catalyst shows higher activity and stability, thanks to lower levels of coke deposition (2,3%, against 3,9% for the catalyst prepared by sol gel, and 5,5% for the one prepared by co-precipitation) (Nanda et al., 2016).

### 4.3 Catalytic development

Noble metals have the capacity of adsorbing hydrogen and facilitating the reaction of hydrogenation. Several studies have investigated the performance of elements like Rh, Ru, Pd and Pt in hydrogenolysis of glycerol. In general, noble metals without an acid or basic additive exhibit a low selectivity to propylene glycol. A high selectivity to propylene glycol of 83%, along with a moderate glycerol's conversion of 35%, was found only with a Pt/C catalyst, in a batch reactor at 200 °C and 200 psi, after 24 hours of reaction. Some studies have demonstrated the positive effects of adding inorganic solid acids into a Ru/C catalyst. The presence of niobia tungstophosphoric acid leads to a conversion of 63% and a selectivity to propylene glycol of 67%. Others demonstrated that bases like LiOH enhance performance of Ru/TiO<sub>2</sub> up to a glycerol's conversion of 90% and a selectivity to propylene glycol of 87%. Values of 92% conversion and 93% selectivity are obtained with Pt supported on hydrotalcite (Nanda et al., 2016).

Recently, catalysts based on 3d transition metals are gaining interest in hydrogenolysis, because cheaper than noble metals and easily available. Copper is an attracting material due to its intrinsic ability in selectively cleaving the C-O bonds of glycerol's molecule rather than the C-C bonds. Cu/SiO<sub>2</sub>, a copper catalyst highly dispersed on silica support, prepared by ion-exchange method and reacted in 40% wt aqueous glycerol solution at 255 °C and 15 bar, achieved 100% conversion and 87% selectivity. Studies analysed the effects of boron oxide as promoter for Cu/SiO<sub>2</sub> catalyst. The simple catalyst reacted in 10% wt aqueous glycerol solution at 200 °C and 50 bar, showed 62% conversion and 90% selectivity. The doping with 3% wt boron under same reaction conditions improved the conversion to 100% and selectivity to 98%. Further studies investigated the effects of different kinds of zeolite ( $\gamma$ -Al<sub>2</sub>O<sub>3</sub>, HY, 13X, HZSM-5, H $\beta$ ) as support for Cu based catalysts. Alumina, a well-known support for dehydration reactions, exhibits the highest activity, thanks to its suitable acidity to catalyse the dehydration of glycerol into acetol. The latest catalytic advancements involve the combination of noble and transition metals, like oxides of Cu, Zn, Cr and Zr. By varying the proportions of different metals, it is possible to achieve a glycerol's conversion of 100% and very high selectivity to propylene glycol. Cu-Ru and Ru-Cu/ZrO<sub>2</sub> showed a selectivity of 84% and 87%. A Cu:Zn:Cr:Zr catalyst, with a molar ratio of 3:2:1:3, achieved a selectivity of 97% (Nanda et al., 2016).

All catalysts are affected by deactivation, that leads to decreased activity over time. There are several causes: mainly sintering, coke deposition and leaching of the metals. Sintering leads to an increased size of metal particles; coke deposition plugs the pores of the catalyst. Both phenomena lead to a reduction of the active surface of the catalyst. Leaching of active metal during the reaction contributes instead to a significant loss of catalytic activity. The deactivation caused by coke deposition can be partially recovered through combustion (calcination) of the spent catalyst at high temperature, followed by reduction. However, if deactivation is caused by sintering, heat treatment is not sufficient to regain the original properties of the catalyst (Nanda et al., 2016).

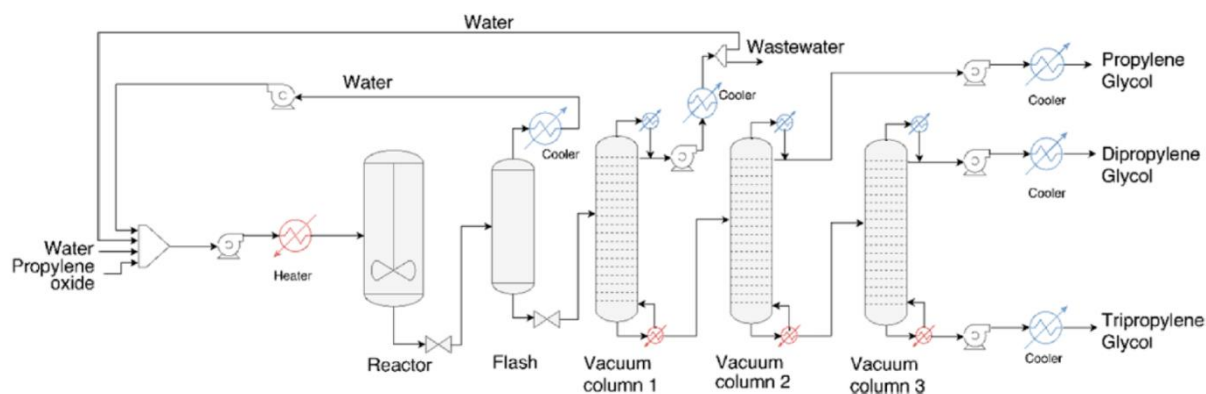
In conclusion, the most promising catalysts for scaling up glycerol's hydrogenolysis at industrial level are the Cu based, because cheaper than ones based on noble metals and high performing. However, prior to their commercial application, research shall investigate further the deactivation phenomena and regeneration of the spent catalysts (Nanda et al., 2016).

## 4.4 Techno-economic assessment of hydrogenolysis plant

The increasing global demand of propylene glycol along with the surplus of glycerol supply from biodiesel production, make hydrogenolysis an appealing and sustainable route to convert a waste product into a valuable chemical. Techno-economic analysis play an important role in evaluating a process at industrial level, because they account for economic and environmental aspects at the early design stage. In their study, Gonzalez-Garay and co-workers analyse different routes to produce propylene glycol and assess their economic and environmental aspects under uncertainty. In detail, they compare the conventional industrial process based on petrochemical propylene oxide, against three different hydrogenolysis routes based on glycerol. Two of them are processes with supply of external hydrogen: one isothermal at high pressure, the other non-isothermal at ambient pressure. The third hydrogenolysis route is an isothermal process at high pressure with hydrogen generated in situ. The feedstock utilized is purified crude glycerol, in a solution of 90% wt glycerol and 10% wt water. Unless otherwise specified, propylene glycol and by-products are produced with a purity of 99,5% wt in all cases (Gonzalez-Garay et al., 2017).

### 4.4.1 Process description

Conversion of propylene oxide into propylene glycol is the route named “Business as Usual” (BAU); the related process flow diagram is shown in figure 37.



Reprinted with permission from (Gonzalez-Garay et al., 2017). Copyright (2017) American Chemical Society.

**Figure 37.** PFD: non-catalytic hydrolysis of propylene oxide.

This process is non-catalytic and occurs in liquid phase. Propylene oxide is mixed with water in a molar ratio 1:15; then, the stream is pressurised to 18,25 bar and heated to 190 °C. In the reactor, the hydrolysis of propylene oxide produces propylene glycol, according equation 12.

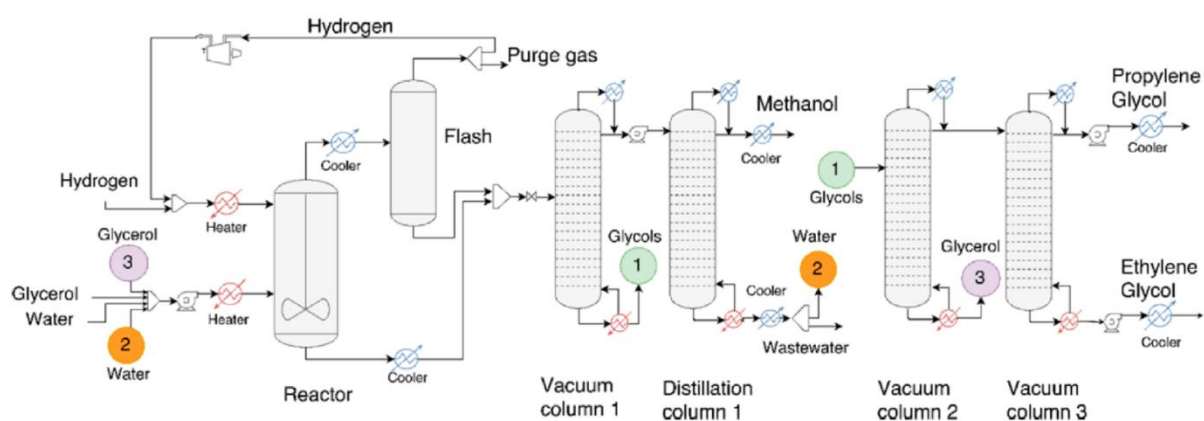


Secondary reactions take place according equations 13 and 14. Part of propylene glycol reacts with propylene oxide producing dipropylene glycol; the latter reacts in turn with propylene oxide, releasing tripropylene glycol.



Propylene oxide is converted 100% into products, with a yield of 85% to propylene glycol, 10% to dipropylene and 5% to tripropylene glycol. The high excess of water is required to limit the generation of these by-products. The mixture of water and products leaves the reactor, and after its pressure is reduced to 1 bar, the stream is sent to a flash separator. The vapour phase is recovered from the top and cooled to recycle water in the process. The liquid mixture of water and glycols undergoes a further pressure reduction to 0,1 bar, then it's sent to a train of distillation columns, which operate under vacuum condition to avoid decomposition of the products. In the first distillation column the glycols are separated from the remaining water, which is recycled in the process. The bottom products are sent to the second column: here, propylene glycol is recovered as overhead product. The remaining glycols leaving the second column feed the third one, where they are separated from each other in dipropylene and tripropylene glycol (Gonzalez-Garay et al., 2017).

The first hydrogenolysis route, named “Glycerol Based 1” (GB-1), is an isothermal process at high pressure with supply of external hydrogen. Its process flow diagram is shown in figure 38.



Reprinted with permission from (Gonzalez-Garay et al., 2017). Copyright (2017) American Chemical Society.

**Figure 38.** PFD: isothermal hydrogenolysis at high pressure with external  $H_2$ .

The reactor, loaded with a  $Cu/Al_2O_3$  catalyst, is fed by two streams: one is a solution of 75% wt glycerol in water, the other is pure hydrogen. Both streams are earlier pressurized to 20 bar and heated to 205 °C. The molar ratio hydrogen to glycerol is 5:1. The main reactions occurring in the reactor are the dehydration of glycerol into acetol, and acetol's hydrogenation into propylene glycol, according equations 15 and 16.



Part of glycerol reacts with hydrogen before dehydration, producing ethylene glycol and methanol, according equation 17.

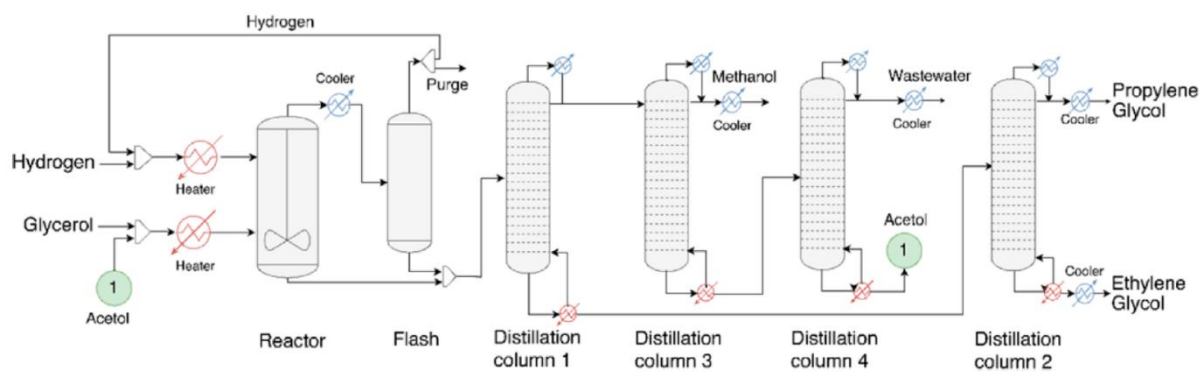


The performances achieved are a glycerol's conversion of 88,7% and a selectivity to propylene glycol of 94,3%.



The overhead stream from the reactor is cooled to 30 °C and sent to a flash unit, where hydrogen is separated from the liquid phase and recycled in the process. The liquid products from the bottom of the reactor and the flash unit are mixed into one stream. After its pressure is reduced to 0,1 bar, this stream is sent to the first distillation system. Methanol and water are the overhead products of the vacuum column 1, while glycols the bottom products. The overhead stream is sent to the distillation column 1 (atmospheric): methanol is separated from water and recovered; water is partly recycled in the process. The glycols are instead sent to the second distillation system, operated at 0,05 bar. Glycerol is recovered at the bottom of the vacuum column 2 and recycled in the process. The remaining glycols at the top of vacuum column 2 are sent to the vacuum column 3, where propylene glycol and ethylene glycol are recovered as overhead and bottom products, respectively (Gonzalez-Garay et al., 2017).

In the hydrogenolysis route “Glycerol Based 2” (GB-2), the conversion of glycerol is atmospheric, with supply of external hydrogen and a gradient of temperature between the top and bottom of the reactor. The purpose of the gradient is to promote the glycerol’s conversion by Cu/Al<sub>2</sub>O<sub>3</sub>, favoured at temperatures above 200 °C, and the hydrogenation of acetol, favoured between 100 and 150 °C. The process flow diagram is shown in figure 39.

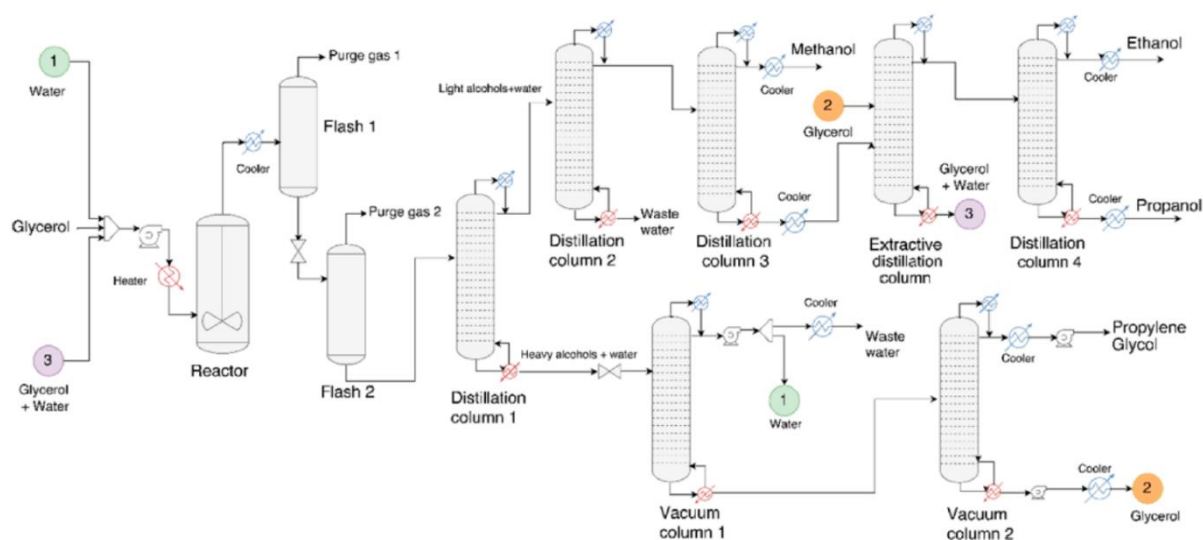


Reprinted with permission from (Gonzalez-Garay et al., 2017). Copyright (2017) American Chemical Society.

**Figure 39.** PFD: non-isothermal hydrogenolysis at ambient pressure with external H<sub>2</sub>.

The reactor is fed by a stream of hydrogen and a stream of glycerol, in a molar ratio 5:1, both heated to 200 °C. The temperatures are set to 200 °C at the top and 120 °C at the bottom of the reactor, because they lead to 100% conversion of glycerol along with the highest yield to propylene glycol of 96,9%. At these conditions, the conversion of glycerol is not dependent on its concentration, so glycerol’s stream is not diluted. The gaseous phase from the reactor is cooled to 30 °C and sent to a flash unit. From here, the hydrogen rich gas separated is mostly recycled back in the process, while a part is discharged to avoid gas accumulation. The liquid streams from the reactor and the flash unit are mixed and sent to the first distillation column. The bottom products, propylene and ethylene glycol, are separated and recovered in the distillation column 2. The overhead stream consisting of water, acetol and methanol is instead sent to a third column. Here, methanol is recovered from the top, while the bottom stream, a mixture of water and acetol, is sent to the fourth column for separation. The acetol recovered is recycled back to the reactor, the water is sent to a wastewater treatment unit (Gonzalez-Garay et al., 2017).

The third route, named “Glycerol Based 3” (GB-3), is an isothermal hydrogenolysis at high pressure with hydrogen generated in situ. The related process flow diagram is shown in figure 40.



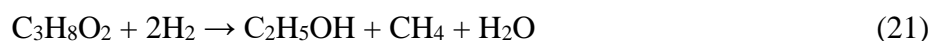
Reprinted with permission from (Gonzalez-Garay et al., 2017). Copyright (2017) American Chemical Society.

**Figure 40.** PFD: isothermal hydrogenolysis at high pressure with  $H_2$  generated in situ.

Fresh glycerol is diluted with water released in the process to get an aqueous solution of 50% wt glycerol. Once the stream is pressurized to 20 bar and heated to 240 °C, it feeds the reactor loaded with a Nickel-Raney catalyst. In the reactor, glycerol’s conversion proceeds as in routes GB-1 and GB-2: glycerol is dehydrated into acetol, which is then hydrogenated in propylene glycol (equations 15 and 16). However, in the current alternative hydrogen is produced in the reactor itself by two reactions. In the first one, acetol reacts with water producing hydrogen and carbon dioxide (equation 18). In the second, glycerol reacts with water producing hydrogen, methanol and carbon dioxide (equation 19).



There are also side reactions, where propylene glycol reacts with hydrogen to produce propanol and water (eq. 20) or ethanol, methane and water (eq. 21).



The glycerol’s conversion achieved is 96%, with a yield to propylene glycol of 33%.

The stream leaving the reactor is cooled to 30 °C prior its inlet to flash unit 1, where gases are released to atmosphere. The liquid phase, after its pressure is reduced to 1 bar, is sent to flash unit 2 to purge the remaining gases. From here, the liquid stream is sent to the distillation column 1, to separate the heavy alcohols (acetol, propylene glycol and glycerol) from the light ones (methanol, ethanol and propanol). Heavy alcohols are recovered from the bottom and proceed their treatment in vacuum columns, to avoid degradation of the glycols. In the first one, acetol and water are recovered as overhead products and partly recycled in the process. The

bottom products, glycerol and propylene glycol, are instead sent to the second vacuum column for separation, and recovered at the bottom and the top, respectively.

Separation of light alcohols recovered from the top of distillation column 1 is more complex. This is due to the low relative volatility between the components, and because the mixture of ethanol/propanol/water is an azeotrope. At first, the stream is sent to the distillation column 2 to achieve the azeotropic point. The water recovered at the bottom is sent to treatment, while the overhead mixture of alcohols and water proceeds to a third distillation column. Here, methanol is separated from the azeotrope and recovered from the top. The azeotrope is processed further in an extractive distillation column, adding glycerol from vacuum column 2 as separating agent (in a molar ratio glycerol to azeotrope of 0,45:1). The glycerol removes 94% of the water from the azeotrope; then, glycerol and water are recycled back in the reactor. The remaining mixture of ethanol and propanol proceeds to distillation column 4, where the alcohols are separated and recovered (ethanol with a purity of 99,3% wt) (Gonzalez-Garay et al., 2017).

#### 4.4.2 Technical assessment

The four processes are simulated with Aspen-HYSYS, addressing heat integration. Design of reactors is based on stoichiometric data. The energy and mass balances of each route per kg of propylene glycol produced are reported in table 18 (Gonzalez-Garay et al., 2017).

**Table 18.** Production of propylene glycol: specific mass and energy balances per route.

Reprinted (adapted) with permission from (Gonzalez-Garay et al., 2017). Copyright (2017) American Chemical Society.

Process parameters / kg propylene glycol		Route			
		BAU	GB-1	GB-2	GB-3
Raw materials [kg]	propylene oxide	0,9034	—	—	—
	glycerol solution 90% wt	—	1,4238	1,3707	3,7300
	hydrogen	—	0,0297	0,0321	—
	water	0,2165	0,0093	—	0,5687
Waste streams [kg]	gas purge	—	0,0052	0,0071	2,7926
	wastewater	—	0,4305	0,3798	0,3205
By-products [kg]	ethylene glycol	—	0,0178	0,0146	—
	dipropylene glycol	0,1326	—	—	—
	tripropylene glycol	0,0087	—	—	—
	methanol	—	0,0111	0,0080	0,0325
	ethanol	—	—	—	0,1316
	propanol	—	—	—	0,0165
Energy consumption	electricity [kW]	0,1229	0,0578	0,0582	0,1214
	heating demand [MJ]	11,231	4,635	4,819	16,707
	cooling demand [MJ]	12,640	5,970	6,157	12,288

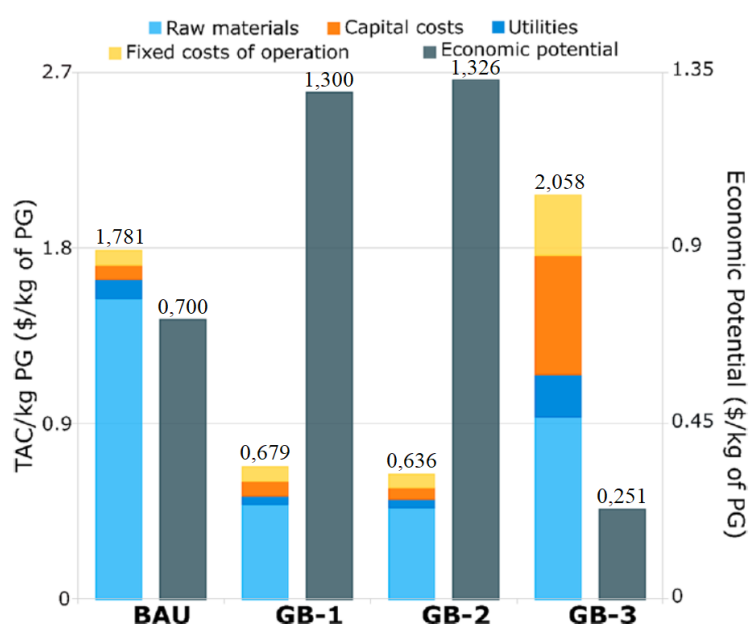
In terms of raw materials, route GB-2 shows the lowest glycerol's consumption, followed by GB-1 (+4%) and GB-3 with the highest (+172%). Hydrogen consumption is slightly higher in route GB-2 than GB-1 (+8%). In terms of energy, the lowest electricity and cooling demand

is for routes GB-1 and GB-2, about half of BAU and GB-3. Routes GB-1 and GB-2 show also the lowest heating demand, followed by cases BAU and GB-3.

### 4.4.3 Economic assessment

The economic performance of the four alternatives is evaluated with two parameters: the Total Annualized Cost and the Economic Potential. As detailed in equations A.26 and A.27, TAC is the sum of operational costs (fixed and variable) and an annual capital charge, EP is the net profit after taxes. Capital costs are evaluated with equations A.28 and A.29. The evaluation considers 330 days of operation per year, along with a price of 0,25 \$/kg and 1,70 \$/kg, respectively for glycerol and propylene oxide. (Gonzalez-Garay et al., 2017).

The economic parameters of each route, normalized per kg of propylene glycol produced, are displayed in figure 41.



Reprinted (adapted) with permission from (Gonzalez-Garay et al., 2017).  
Copyright (2017) American Chemical Society.

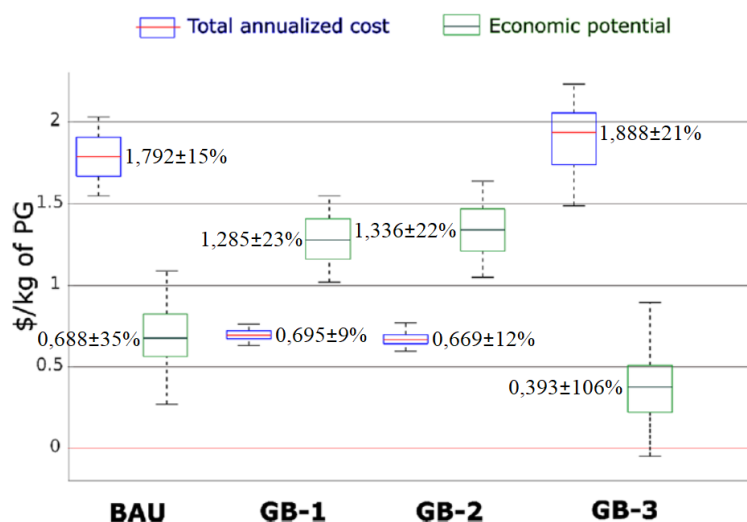
**Figure 41.** Production of propylene glycol: specific TAC and EP per route.

The highest economic potential is achieved with routes GB-2 and GB-1. Thanks to the lower cost of glycerol compared to propylene oxide, these processes have a TAC respectively 64% and 62% lower than the BAU case, leading to a profit up 86-89% higher. Route GB-3 instead is the alternative with highest TAC and lowest EP, and it is less profitable than BAU case. The reason is the low yield to propylene glycol achieved in this process (Gonzalez-Garay et al., 2017).

The performance of the four processes is affected by several uncertainties. A sensitivity analysis over the process parameters (technical and economic) identifies as most critical the prices of products and raw materials, the process conversions and the flow rates of raw materials. These parameters are modelled through normal distributions.

The uncertainty analysis is then performed via Monte Carlo simulations to generate set of samples of the uncertain parameters. With respect to mass and energy flows, variables like by-products and waste streams show fluctuations from 5% to 70%, while production of propylene glycol and utilities consumption at most up to 10% (Gonzalez-Garay et al., 2017).

The specific TAC and EP of the four processes under uncertainty are shown in figure 42. The central mark of the box plots indicates the mean value, the bottom and top edges indicate respectively the 25<sup>th</sup> and 75<sup>th</sup> percentiles; the whiskers display the  $\pm 2,7$  standard deviations.



Reprinted (adapted) with permission from (Gonzalez-Garay et al., 2017).  
Copyright (2017) American Chemical Society.

**Figure 42.** Production of propylene glycol: specific TAC and EP under uncertainty.

The uncertainty analysis confirms routes GB-2 and GB-1 as the best performing. Their EP have not only a higher mean value, but also the lowest variability. Instead, the high fluctuation of GB-3 reveals unpredictable profits, making this process comparable to BAU in best scenarios, but unviable in worst ones (Gonzalez-Garay et al., 2017).

#### 4.4.4 Conclusions

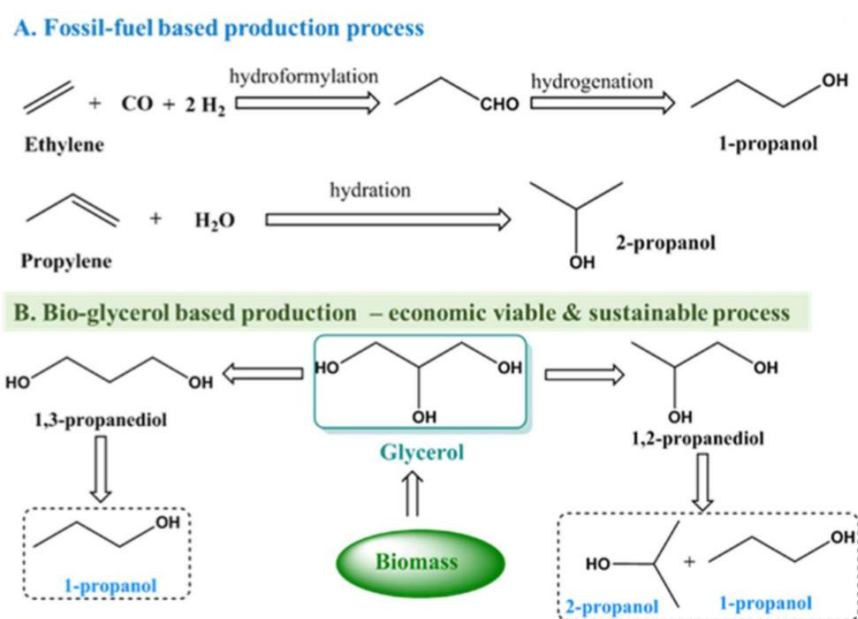
The assessment shows that the economic performance of the processes is highly dependent on raw material like propylene oxide and glycerol, while hydrogen has a low contribution. The two routes converting glycerol with an external source of hydrogen are assessed as the best processes both by the deterministic and the uncertainty analysis. They are cheaper and more sustainable than the conventional process based on propylene oxide, as they utilize a low-cost bio-feedstock. Their development at industrial level is therefore attractive. Instead, the glycerol's conversion with hydrogen generated in situ is the process with worst performance. The plant configuration is complex and expensive, and the low yield to propylene glycol is not compensated by the production of hydrogen and the valuable by-products (Gonzalez-Garay et al., 2017).



# 5 Valorization of glycerol into propanols

## 5.1 Introduction

Propanol (propyl alcohol), also identified as 1-propanol or n-propanol, is an alcohol with molecular formula  $C_3H_8O$  (NCBI, 2019<sup>d</sup>). It has an isomer called isopropanol (isopropyl alcohol) or 2-propanol (NCBI, 2019<sup>e</sup>). Both these chemicals are valuable commodities which find several applications. 1-propanol is primarily utilized as solvent in different industries (pharmaceutical, paint, cosmetics, cellulose ester) and as organic intermediate for synthesis of chemicals. Moreover, it is a suitable automotive fuel and is considered a future substitute of gasoline. 2-propanol is widely used as disinfectant and solvent mainly in the pharmaceutical and automotive industry. Propanols are usually produced from fossil-based feedstocks: 1-propanol from ethylene, via the process of hydroformylation-hydrogenation; 2-propanol by hydration of propylene. A new possibility recently investigated is the production via the double dehydration-hydrogenation reactions of glycerol. The two routes are shown in figure 43 (Samudrala and B., 2018).



Reprinted with permission from (Samudrala and B., 2018). © 2018 by MDPI.

**Figure 43.** Synthetic routes to propanols: fossil and glycerol based.

In the second half of the 1970s, the annual world production of 1-propanol accounted for 0,09 million tonnes (IPCS, 1990<sup>a</sup>), while production of 2-propanol for more than 1,1 Mt (IPCS, 1990<sup>b</sup>). More recently, the global market of propanols was estimated to reach 2,7 million tonnes by 2018, with an annual growth rate of 3,9% (Markets and Markets, 2013). At this increasing demand, the production process based on glycerol becomes attractive, because more sustainable than one based on chemicals derived from petroleum (Samudrala and B., 2018).

Studies on direct conversion of glycerol into propanols are still limited in number, compared to the large research on conversion into propanediols. Most of them investigate catalysts based on expensive noble metals. However, there are few studies about cheaper

elements like nickel and alumina (Lin et al., 2014). These catalytic systems are more promising for a future industrialization of the process.

## 5.2 Double layer catalysts

Considering that hydrogenolysis of glycerol consists mainly of dehydration and hydrogenation steps, some researchers have developed bifunctional catalysts “acid-metal”. The acid sites of one catalyst are to promote the dehydration, while the metallic sites on the other are in charge of hydrogenation (Lin et al., 2014).

In their study, Lin and co-workers analysed the conversion of glycerol into 1-propanol in a fixed bed reactor (in down-flow mode) using a zeolitic and a Ni based catalysts. The novelty of their work is the sequential packing of the catalysts in the reactor, where the zeolitic layer is packed prior to the Ni one. This ensures that dehydration step occurs before hydrogenation and improves the selectivity to 1-propanol compared to the case of single catalyst. The zeolite employed is of the type H- $\beta$ , with a ratio Si/Al of 15,8. Before use, it was dried and calcinated. NiO/Al<sub>2</sub>O<sub>3</sub> was prepared by wetness impregnation followed by calcination. Both catalysts were crushed and sieved into particles of mesh 20-40, then packed in the reactor as two layers in contact each other (zeolite at the upstream side). The reactants used are an aqueous solution of 40% glycerol in volume at a flow rate of 0,2 mL/min (LHSV of 3 h<sup>-1</sup>) and hydrogen at a rate of 96 mL/min. Following stabilization of the reactant flows, the temperature of catalytic layers was increased from ambient condition to 220 °C, and the pressure of the reactor reached 2 MPa. Glycerol’s conversion and selectivity to the products are calculated with equations A.30 and A.31 (Lin et al., 2014).

The performances of the double layer catalyst and the single nickel catalyst are reported in table 19.

**Table 19.** Hydrogenolysis into propanols: performance of single and double layer catalysts.

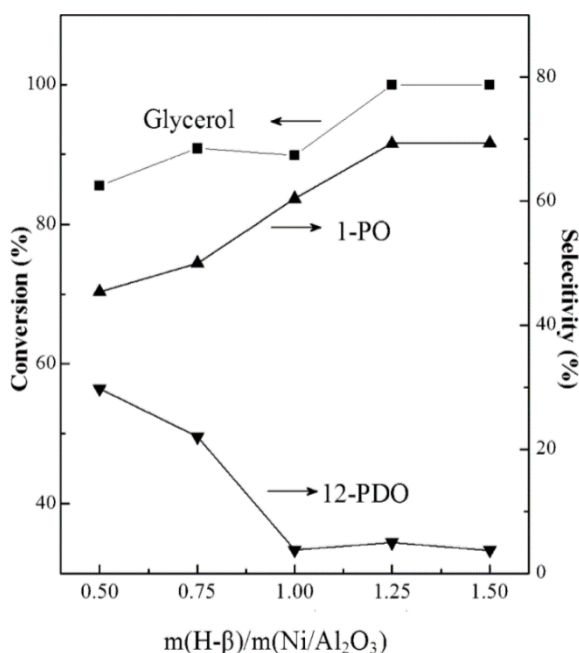
Reprinted (adapted) with permission from (Lin et al., 2014). Copyright (2014) American Chemical Society.

Catalyst <sup>a</sup>		Ni/Al <sub>2</sub> O <sub>3</sub>	H- $\beta$ +Ni/Al <sub>2</sub> O <sub>3</sub>
Conversion of glycerol [%]		60,5	89,9
Selectivity to [%]	1,2-propanediol	51,7	3,7
	1,3-propanediol	0,2	2,6
	Ethylene glycol	2,4	1,5
	1-propanol	0,2	60,3
	Acetol	32,7	1,1
	Acrolein	—	0,2
	Propanal	0,9	0,2
	Acetone	—	10,3
	Ethanol	8,0	11,6
	Methanol	1,5	0,9
	Unidentified	2,4	7,6

<sup>a</sup> The mass of each single catalyst employed in the tests is 1 g.



The single layer catalyst Ni/Al<sub>2</sub>O<sub>3</sub> achieves a 60% conversion into glycerol with 52% selectivity to propylene glycol. The main by-products are acetol and ethanol, with a selectivity respectively of 33% and 8%. Selectivity to 1-propanol is instead basically null. The presence of H-β catalyst in addition to the layer of Ni/Al<sub>2</sub>O<sub>3</sub> increases the glycerol's conversion by 29% and changes significantly the distribution of the products. 1-propanol shows the highest selectivity of 60%, while the ones of propylene glycol and acetol are instead reduced to 4% and 1%, respectively. The main by-products are now ethanol and acetone. These results show clearly that zeolite does enhance hydrodeoxygenation of glycerol, addressing the products distribution to 1-propanol (Lin et al., 2014).



Reprinted with permission from (Lin et al., 2014).  
Copyright (2014) American Chemical Society.

**Figure 44.** Hydrogenolysis into propanols: performance by ratio Hβ/NiAl<sub>2</sub>O<sub>3</sub>.

These results are compared with the research conducted by Friedrich and co-workers, who studied the direct conversion of glycerol to 1-propanol utilizing two commercial Ni based catalysts: Ni/Al<sub>2</sub>O<sub>3</sub> and Ni/SiO<sub>2</sub>. In a continuous fixed bed reactor, at 320 °C and a LHSV of 3 h<sup>-1</sup>, they reported for both catalysts a glycerol's conversion of 99%, along with a selectivity of 35,3% for Ni/Al<sub>2</sub>O<sub>3</sub> and 42,8% for Ni/SiO<sub>2</sub> (Lin et al., 2014).

The two-layers catalytic system from Lin et al. presents higher selectivity, at the same LHSV and a similar conversion, but at a temperature 100 °C lower. This is therefore the most performing catalyst based on non-noble metals to convert glycerol to 1-propanol. However, the single layer catalyst Ni/Al<sub>2</sub>O<sub>3</sub> proved a relatively stable performance over 72 hours while the double layer catalyst shows a poor stability over time. As reported in table 20, taking as example a ratio H-β to Ni/Al<sub>2</sub>O<sub>3</sub> equal to 1, the performance decreases quite fast (Lin et al., 2014).

**Table 20.** Hydrogenolysis into propanols: performance over time of H- $\beta$ /NiO/Al<sub>2</sub>O<sub>3</sub>.

Catalyst [1 g / 1 g]	H- $\beta$ / NiO/Al <sub>2</sub> O <sub>3</sub>		
Time on stream [min]	30	60	100
Glycerol conversion [%]	100	92	70
Selectivity to 1-propanol [%]	60	52	43

X-ray diffraction measurements found that the crystal structure of H- $\beta$ -zeolite was quite stable after the test. The instability might be then attributed to carbon deposits on the layer of H- $\beta$  catalyst (Lin et al., 2014).

Therefore, the promising results achieved with the sequential double layer catalyst shall be supported by further research to enhance the resistance against coke deposition and improve the stability over time.

### 5.3 Noble metal-based catalysts

Catalysts based on noble metals are highly effective in hydrogenolysis of glycerol and have good selectivity to propanols (Samudrala and B., 2018), (Lin et al., 2014). Table 21 reports the performance of three of them found in recent literature.

**Table 21.** Hydrogenolysis into propanols: performance of noble metal-based catalysts.

Catalyst	Pt-H <sub>4</sub> SiW <sub>12</sub> O <sub>40</sub> /ZrO <sub>2</sub>	2,5%Pt/Zr <sub>0,7</sub> Al <sub>0,3</sub> O <sub>y</sub>	2%Pd/MoO <sub>3</sub> -Al <sub>2</sub> O <sub>3</sub>
Reactor	—	Autoclave	Fixed bed
Reactants and time of reaction	LHSV 0,045 (0,18) h <sup>-1</sup>	30 g 10% glycerol solution, 0,3 g catalyst, 35 ml H <sub>2</sub> , 8 h	0,5 mL/h 10% wt aqueous glycerol, 0,5 g catalyst, 100 mL/min H <sub>2</sub> , 6 h
Temperature [°C]	200	240	210
Pressure H <sub>2</sub> [bar]	50	60	1
Glycerol conversion [%]	99,7 (50)	81,2	88,4
Selectivity [%]	1-propanol	80 (40)	52
	2-propanol	11 (—)	39
Reference	(Zhu et al., 2012) cited by (Lin et al., 2014), (Samudrala and B., 2018)	(Li et al., 2018)	(Samudrala and B., 2018)

In absolute terms, the most performing catalyst is the platinum based supported on zirconia from Zhu and co-workers, with the highest glycerol's conversion of 99,7% along with a total selectivity to propanols of 91%. The second most performing is the one based on 2% palladium from Samudrala and Bhattacharya, with a glycerol's conversion and a total selectivity to propanols of 88% and 91%, respectively. A strong asset of this system is the low supply pressure of hydrogen (atmospheric). The platinum catalyst supported on Zr-Al from Li and co-workers is instead the one with the lowest glycerol's conversion (81%), but the highest selectivity to 1-propanol (86%).

In general, these catalysts show higher selectivity to propanols than nickel-based ones. However, it can be noted that the results of the best performing catalyst from Zhu et al. are achieved at a LHSV of  $0,045 \text{ h}^{-1}$ , relatively low compared to the  $3 \text{ h}^{-1}$  of the double layer zeolitic system. Moreover, when the LHSV is increased from  $0,045$  to  $0,18 \text{ h}^{-1}$ , both conversion and selectivity drop by 50% (Lin et al., 2014).

Therefore, also the catalysts based on noble metals need further development and study, and in addition they have the drawback of high cost that prevents their commercialization on large scale.



## 6 Discussion of literature review

### 6.1 Potential of bio-processes

As mentioned in the introduction, the global amount of glycerol released as by-product of biodiesel processing has reached 3,8 Mt in 2018, exceeding by 3,3 million the annual market of glycerol, evaluated in half million tonnes. The literature review has identified two catalytic processes, steam reforming and hydrogenolysis, that might convert this excess (waste) in three different valuable products: hydrogen, propylene glycol and propanols.

There is abundant research on steam reforming of glycerol into hydrogen, and on hydrogenolysis into propylene glycol. Techno economic analysis show that the production of these commodities from glycerol can generate profit. Studies about conversion into propanols are instead still limited; the process is not yet ready for being commercialized.

The bio-production of any of these commodities could absorb alone the annual excess of crude glycerol. Hydrogen is a clear example: as mentioned in paragraph 3.1, its global market accounts for 57 million tonnes per year, 1 order of magnitude higher than the glycerol to be disposed. From table 13, the steam reforming plant analysed can produce hydrogen with an efficiency of 64,1%. If all the waste from 2018 was processed in such plants, the net output of hydrogen would result in 2,1 million tonnes, about 3,7% of its annual production.

Propylene glycol holds a lower market: as seen in chapter 4, its global production is 2,2 million tonnes per year, yet with an annual growth rate of 4,5%. From table 18, the most performing route analysed converts 1,371 kg of 90% refined glycerol into 1 kg of propylene glycol, therefore with an efficiency of 72,9%. At the composition of crude glycerol given in table 12, the quantity of refined glycerol obtainable from waste is 1,92 million tonnes. Processing the excess of glycerol in these plants would result in 1,4 Mt of propylene glycol: 64% of its market could be bio-based.

Propanols, with a total production of 2,7 million tonnes per year, could soon represent a third chemical capable of valorizing alone the global excess of glycerol.

### 6.2 Catalytic development of bio-processes

The literature review has identified common features in the conversion process into the three chemicals. The catalyst and the process conditions are the critical elements to achieve a successful conversion of glycerol into the desired product. Their suitable choice can promote the main chemical reactions over side reactions, resulting in high conversion and selectivity to the final product. The side reactions might lead to other valuable by-products; however, this is not necessarily beneficial. Their presence requires additional equipment (distillation columns, separators) to recover the distinct chemicals, increasing the overall cost of the plant and complicating the process operation.

In general, catalysts based on noble metals have shown to be efficient and resistant to coke deposition, but their cost hinder the industrialization of the process on large scale. Therefore, the latest research is focusing on cheaper materials, especially transition metals.

Nickel is the element most widely utilized as active metal in catalysts for steam reforming. Higher catalytic performances and resistance against deactivation can be achieved by associating nickel with different compounds as supports. Among the latest catalysts developed, there are nickel based supported on niobia and alumina, and on silica and zirconia.

Copper is the promising metal to catalyse the hydrogenolysis of glycerol into propylene glycol. Similarly, the combination with silica, alumina and zirconia as supports results in the best performances.

In hydrogenolysis of glycerol into propanols, nickel plays again an important role as active metal, supported on alumina or silica. The latest development involves the use of double layer catalysts, one zeolitic and one in nickel/alumina.

Tests at laboratory level show good performances in terms of conversion and selectivity, but deactivation is a common issue. In this respect, there are larger research and results achieved on catalysts for steam reforming than on those for hydrogenolysis. However, it shall be noted that the catalytic tests described in the articles reviewed are performed with solutions of pure glycerol. The glycerol released as by-product of biodiesel production is instead crude glycerol, that in addition to water contains several impurities like alcohols, fatty acids, salts. On one side, the direct utilization of this feedstock in a conversion process would remove the cost of glycerol purification, making its valorization more sustainable. On the other side, the impurities might have detrimental effects on the reaction, by further deactivating the catalyst or plugging the reactors (Menezes et al., 2018), (Nanda et al., 2016).

As exception, Hoşgün and co-workers investigated the production of propylene glycol both from crude and pure glycerol, comparing the results of the two processes. In a batch reactor loaded with a Nickel Raney catalyst and under the same process conditions, they reported equal conversion and selectivity, respectively 77% and 25%, with both feedstocks. The positive performance of crude glycerol was attributed to the presence of alkali impurities that acted as co-catalysts (Hoşgün et al., 2012) cited by (Nanda et al., 2016). The study doesn't include a stability test to analyse the deactivation of the catalyst over time. Moreover, it is performed in a batch reactor. Since the continuous flow reactor is the most suitable type for industrialization of the process, it would be useful to investigate the use of crude glycerol on the latter type.

Therefore, the effects of the impurities from biodiesel processing shall be investigated further in both processes of steam reforming and hydrogenolysis of glycerol, in terms of reaction performance, stability of the catalysts and of the reactors (Menezes et al., 2018), (Nanda et al., 2016).

## 6.3 Comparison of techno-economic assessments

The literature review has identified a techno-economic study both for steam reforming of glycerol into hydrogen and for its hydrogenolysis into propylene glycol. It is therefore possible to compare the two technologies at technical and economical level, to identify the most profitable conversion process of valorization. The most efficient configurations of each technology are chosen for the comparison. These are: case 1.a of steam reforming plant (hydrogen production without CO<sub>2</sub> capture) and route GB-2 of hydrogenolysis plant (non-isothermal process, at ambient pressure and with supply of external hydrogen).

The market prices of hydrogen and propylene glycol are very close: 2,68 \$/kg and 2,65 \$/kg, respectively (Gonzalez-Garay et al., 2017). Therefore, the higher profitability of one of the plants will depend on several factors, like: production capacity, conversion efficiency, capital and operational costs.

The annual production of propylene glycol in the hydrogenolysis plant is 43780 tonnes (Gonzalez-Garay et al., 2017). The production rate of hydrogen in the reforming plant is 10<sup>5</sup> Nm<sup>3</sup>/h, that corresponds, with a density of 0,0893 Kg/m<sup>3</sup> at standard conditions, to 8930 kg/h. Since the plant is operated 7500 hours per year (Cormos, 2017), the annual production of hydrogen is calculated in 66975 tonnes. The production capacity of the two plants is therefore in the same order of magnitude, but 53% higher in the steam reforming plant.

Performance of glycerol's conversion is higher in hydrogenolysis process. Hydrogen is produced with an efficiency of 64,1%, that becomes 68,6% considering the power contribution (refer table 13); glycerol is converted into propylene glycol with an efficiency of 72,9%. However, the main feedstock utilized in the two processes is different in quality and cost. Steam reforming is based on crude glycerol, with a cost of 50 €/tonne (Cormos, 2017). Hydrogenolysis plant employs refined glycerol, purchased at 0,25 \$/kg (Gonzalez-Garay et al., 2017). At an exchange rate of 1,18 \$/€ based on the average of 2018 (IRS, 2019), the raw material utilized in steam reforming is 4 times cheaper than refined glycerol utilized in hydrogenolysis.

The biggest difference between the technologies is in their capital cost. The one of the hydrogenolysis plant is estimated in 8,2 million dollars (Gonzalez-Garay et al., 2017). The capital cost of the steam reforming plant can be calculated in 255,9 M\$, based on the specific investment cost of 723 €/kW reported in figure 31, the thermal output of 300 MW reported in table 13, and the previous exchange rate \$/€. Therefore, the gap between the initial investments of the two plants is 247,7 M\$. This large value can be explained by the different process conditions at which the systems operate, more moderate in hydrogenolysis plant. Production of propylene glycol is a process run at atmospheric pressure and at a maximum temperature of 200 °C (refer page 47). The steam reforming plant is instead operated at a temperature of 900 °C, a pressure of 30 bar in the reformer and 120 bar in the steam turbine (refer table 12), requiring more expensive equipment.

Considering all these factors, it is decided to compare the plants through their economic parameters: the total annualized cost and the economic potential. For hydrogenolysis plant, they are available from figure 42, and equal for case GB-2 respectively to 0,669 and 1,336 \$ per kg of propylene glycol. These parameters are not given in the assessment of steam reforming plant; however, they can be calculated through the other information available.

From table 16, the cost of hydrogen production is 31,61 €/MWh. At a thermal output of 300 MW (refer table 13) and 7500 hours of operation, the total annualized cost is calculated as

$$TAC = 31,61 \frac{\text{€}}{\text{MWh}} * 1,18 \frac{\text{\$}}{\text{€}} * 300 \text{ MW} * 7500 \frac{\text{h}}{\text{year}} = 83,92 \frac{\text{M\$}}{\text{year}} \quad (22)$$

Normalizing this value to the annual production of hydrogen, the specific TAC is calculated as

$$\frac{TAC}{\text{kg H}_2} = \frac{83,92 \frac{\text{M\$}}{\text{year}}}{7500 \frac{\text{h}}{\text{year}} * 8930 \frac{\text{kg}}{\text{h}}} = 1,253 \frac{\text{\$}}{\text{kg}} \quad (23)$$

The yearly revenue is calculated as

$$Revenue = 2,68 \frac{\text{\$}}{\text{kg}} * 8930 \frac{\text{kg}}{\text{h}} * 7500 \frac{\text{h}}{\text{year}} = 179,49 \frac{\text{M\$}}{\text{year}} \quad (24)$$

Considering that the taxes are already included by Cormos in the fixed costs of operation, the economic potential is therefore calculated with equation A.27 in

$$EP = 179,49 \frac{\text{M\$}}{\text{year}} - 83,92 \frac{\text{M\$}}{\text{year}} = 95,57 \frac{\text{M\$}}{\text{year}} \quad (25)$$

Normalizing this value to the annual production of hydrogen, the specific EP is calculated as

$$\frac{EP}{\text{kg H}_2} = \frac{95,57 \frac{\text{M\$}}{\text{year}}}{7500 \frac{\text{h}}{\text{year}} * 8930 \frac{\text{kg}}{\text{h}}} = 1,427 \frac{\text{\$}}{\text{kg}} \quad (26)$$

The specific total annualized cost and economic potential of the two plants can be now reported in a chart for comparison, as shown in figure 45.

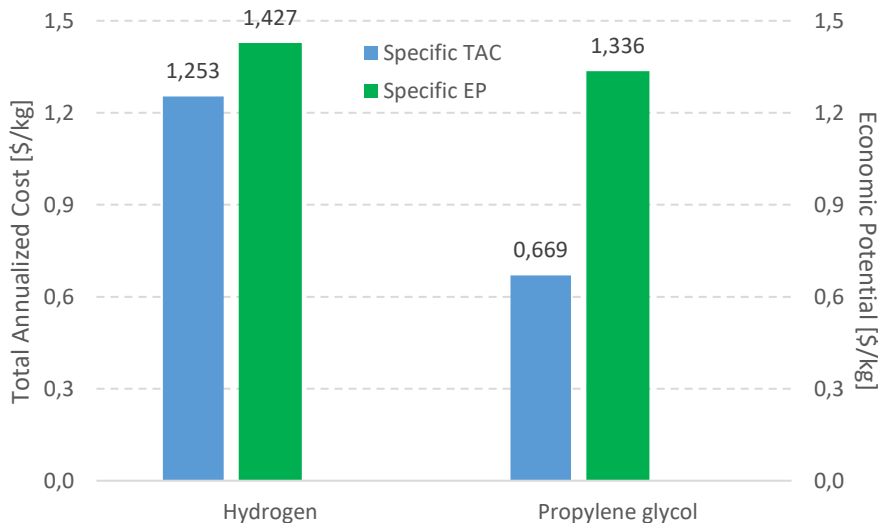


**Figure 45.** Specific TAC and EP: hydrogen vs propylene glycol.



The steam reforming plant shows the best economic potential, 7% higher than in hydrogenolysis. However, the larger capital costs make its total annualized cost 87% greater. Therefore, the production of propylene glycol is considered the best route to valorize glycerol, by providing a net profit slightly lower than hydrogen, but at a much more affordable investment.

Both studies do not explicitly mention the rate of catalyst deactivation; it is assumed that this has been considered under maintenance operations and costs. As comparison, the annual cost of the catalyst in steam reforming plant is evaluated in 2,5 M€/year (Cormos, 2017), that normalized to the TAC of 71,1 M€/year, accounts for 3,5% of the total production costs. The annual costs of the catalyst in hydrogenolysis plant is evaluated under uncertainty in 1,95 M\$/year, that normalized to the total annualized cost of 29,27 M\$/year (Gonzalez-Garay et al., 2017) accounts for 6,7% of the total production costs.

## 6.4 Suggestions for future work

The comparison of valorization technologies has considered the investments required to build brand-new plants. Steam reforming is penalized in the assessment because of its larger capital cost. However, steam reforming plants are already in use for production of hydrogen from methane. Therefore, it would be interesting to evaluate at technical and economical level the conversion of a such existing plant to reforming of glycerol. This option might not only be more profitable than production of hydrogen from methane, but also show larger profitability than hydrogenolysis into propylene glycol, at a closer investment. Moreover, since the temperatures required in glycerol reforming are ~200 °C lower than the ones needed in reforming of methane, this might also be a possibility to extend the design lifetime of an old reforming plant.

The catalyst utilized in simulations of steam reforming plant is Ni/Al<sub>2</sub>O<sub>3</sub>. It would be interesting to study the techno-economic assessment of the plant with one of the latest catalyst developed, like nickel supported on niobia and alumina. The conversion and selectivity are lower than Ni/Al<sub>2</sub>O<sub>3</sub>, however, the reaction is promoted at 500 °C instead of 900 °C, hence at more economical condition.

The production of propylene glycol from glycerol is assessed as profitable at a moderate investment compared to production of hydrogen. The system achieves profit by utilizing purified glycerol and Cu/Al<sub>2</sub>O<sub>3</sub> as catalyst. A possibility for larger profit would be the use of crude glycerol as feedstock. This option should be supported by technical and economical evaluations. Process simulations should evaluate if the efficiency of conversion is still acceptable or is decreased by the presence of by-products. Techno-economic studies should evaluate the benefit of cheaper raw material against the drawback of more frequent replacement of deactivated catalysts. This option would be of course even more valuable, if further catalytic tests show equal stability of the catalyst with use of crude glycerol, as found by Hoşgün and co-workers for Nickel Raney.

Finally, it shall be reminded that the prices of crude and refined glycerol are direct function of their availability. In a scenario where they are extensively converted into valuable chemicals, their value might rise again, with a lower profitability of their valorization process. Therefore, economic studies should evaluate the different investments under variability in the market prices of feedstocks, as function of quantity of converted products.



## 7 Conclusion

This thesis has identified two processes, steam reforming and hydrogenolysis, to convert glycerol into three bulk chemicals: hydrogen, propylene glycol and propanols. The bio-production of any of these commodities could absorb the excess of glycerol released from biodiesel processing. The review has shown that the available catalysts and process equipment are suitable for the bio-production of hydrogen and propylene glycol at industrial level, achieving a similar profit. Instead, hydrogenolysis of glycerol into propanols requires further development in the catalysts prior to industrialization of the process. The capital cost for the construction of a glycerol's steam reforming plant is 31 times higher than the cost for an hydrogenolysis plant. Therefore, conversion into propylene glycol is assessed as the best route to valorize glycerol, by leading to profit at the lowest investment. Further work might identify as profitable option the conversion to glycerol of an existing steam reforming plant based on methane.



## 8 Appendix

Glycerol's global conversion:

$$X_{C_3H_8O_3} \% = \frac{\text{Glycerol in} - \text{Glycerol out}}{\text{Glycerol in}} * 100 \quad (\text{A. 1})$$

Glycerol's conversion into gaseous products:

$$X_{C_3H_8O_3 \text{ gaseous products}} \% = \frac{\text{C atoms in the gas products}}{\text{total C atoms in the feedstock}} * 100 \quad (\text{A. 2})$$

Yield to hydrogen:

$$Y_{H_2} = \frac{\text{H}_2 \text{ moles produced}}{\text{moles of glycerol in the feedstock}} \quad (\text{A. 3})$$

Selectivity to hydrogen:

$$S_{H_2} \% = \frac{\text{H}_2 \text{ moles produced}}{\text{C atoms produced in the gas phase}} * \frac{1}{RR} * 100 \quad (\text{A. 4})$$

where RR is the reforming ratio (7/3), defined as the ratio of moles of H<sub>2</sub> to CO<sub>2</sub> formed.

Selectivity to i:

$$S_i \% = \frac{\text{C atoms in species } i}{\text{C atoms produced in the gas phase}} * 100 \quad (\text{A. 5})$$

where species i refers to CO, CO<sub>2</sub> and CH<sub>4</sub>.

Glycerol's conversion:

$$\text{Glycerol conversion, \%} = \frac{\text{Glycerol in} - \text{Glycerol out}}{\text{Glycerol in}} * 100 \quad (\text{A. 6})$$

Selectivity to hydrogen:

$$H_2 \text{ selectivity, \%} = \frac{\text{H}_2 \text{ moles produced}}{\text{C atoms in gas products}} * \frac{1}{RR} * 100 \quad (\text{A. 7})$$

where RR is the reforming ratio (7/3), defined as the ratio of moles of H<sub>2</sub> to CO<sub>2</sub> formed.

Selectivity to i:

$$\text{Selectivity of } i, \% = \frac{C \text{ atoms in species}}{C \text{ atoms in gas products}} * 100 \quad (\text{A. 8})$$

where species i refers to CO, CO<sub>2</sub> and CH<sub>4</sub>.

Glycerol's conversion:

$$X[\%] = \frac{N_{Glycerol}^{In}[\text{mol h}^{-1}] - N_{Glycerol}^{Out}[\text{mol h}^{-1}]}{N_{Glycerol}^{In}[\text{mol h}^{-1}]} * 100 \quad (\text{A. 9})$$

Glycerol's conversion into gas:

$$X_G[\%] = \frac{C \text{ moles in gas products}}{C \text{ moles in the feed}} * 100 \quad (\text{A. 10})$$

Hydrogen yield:

$$Y_{H_2}[\%] = \frac{N_{H_2}^{Out}[\text{mol h}^{-1}]}{7N_{Glycerol}^{In}[\text{mol h}^{-1}]} * 100 \quad (\text{A. 11})$$

Selectivity to hydrogen:

$$S_{H_2}[\%] = \frac{\text{Molecules of } H_2 \text{ produced}}{C \text{ atoms in gas product}} * \frac{1}{RR} * 100 \quad (\text{A. 12})$$

where RR is the H<sub>2</sub>/CO<sub>2</sub> reforming ratio of 7/3 for glycerol.

Yield to CO, CO<sub>2</sub> and CH<sub>4</sub>:

$$Y_i[\%] = \frac{C \text{ moles in specie } i}{C \text{ moles in feed}} * 100 \quad (\text{A. 13})$$

where i species are CO, CO<sub>2</sub> and CH<sub>4</sub>.

Hydrogen production rate:

$$H_2 \text{ production rate} \left[ \frac{\mu\text{mol}}{g_{cat} \text{ min}} \right] = \frac{N_{Glycerol}^{In}[\text{mol min}^{-1}] * X_G * y_{H_2} * 10}{m_{catalyst}[\text{g}]} * 10^6 \quad (\text{A. 14})$$

where  $X_G$  is glycerol's conversion to gas and  $y_{H_2}$  is the hydrogen molar fraction in gaseous products.

Coefficient of performance:

$$COP [1/^\circ C] = \frac{X_G * S_{H_2} * v_f * WHSV * t}{T} \quad (A. 15)$$

where  $v_f$  [%] is the glycerol volume in the feed,  $t$  [h] is the test duration and  $T$  [ $^\circ C$ ] is the reaction temperature.

Hydrogen efficiency:

$$\eta_{H_2} = \frac{\text{Hydrogen thermal energy [MW}_{th}]}{\text{Glycerol thermal energy [MW}_{th}]} * 100 \quad (A. 16)$$

Net electrical efficiency:

$$\eta_{net} = \frac{\text{Net power output [MW}_e]}{\text{Glycerol thermal energy [MW}_{th}]} * 100 \quad (A. 17)$$

Cumulative energy efficiency:

$$\eta_{cumulative} = \eta_{net} + \eta_{H_2} \quad (A. 18)$$

Carbon capture rate:

$$CCR = \frac{\text{Captured CO}_2 \text{ molar flow [kmole/h]}}{\text{Glycerol carbon molar flow [kmole/h]}} * 100 \quad (A. 19)$$

Specific CO<sub>2</sub> emission:

$$SE_{CO_2} = \frac{\text{Emitted CO}_2 \text{ mass flow [kg/h]}}{\text{Net power output [MW}_e] + \text{Hydrogen energy [MW}_{th}]} \quad (A. 20)$$

Specific primary energy consumption for CO<sub>2</sub> avoided:

$$SPECCA = \frac{\text{Heat rate}_{CO_2 \text{ capture}} [MJ/MWh_e] - \text{Heat rate}_{no \text{ capture}} [MJ/MWh_e]}{\text{SE}_{CO_2 \text{ no capture}} [kg/MWh_e] - \text{SE}_{CO_2 \text{ capture}} [kg/MWh_e]} * 100 \quad (A. 21)$$

Capital costs:

$$C_E = C_B * \left(\frac{Q}{Q_B}\right)^M \quad (\text{A. 22})$$

where  $C_E$  is the capital cost of the plant sub-system with capacity  $Q$ ,  $C_B$  is the capital cost of the plant sub-system with capacity  $Q_B$ ,  $M$  is a constant that depends on equipment type.

Specific Capital Investment costs per kW net energy:

$$SCI_{net\ kw} = \frac{\text{Total investments costs}}{\text{Net power output} + \text{Hydrogen thermal output}} \quad (\text{A. 23})$$

Cost of removed carbon dioxide:

$$CO_2\ removal\ cost = \frac{LCOH/LCOE_{with\ CCS} - LCOH/LCOE_{without\ CCS}}{CO_2\ removed} \quad (\text{A. 24})$$

Cost of avoided carbon dioxide:

$$CO_2\ avoided\ cost = \frac{LCOH/LCOE_{with\ CCS} - LCOH/LCOE_{without\ CCS}}{CO_2\ emissions_{without\ CCS} - CO_2\ emissions_{with\ CCS}} \quad (\text{A. 25})$$

where LCOH and LCOE are the levelized costs of hydrogen and electricity.

Total annualized cost:

$$TAC = FCOP + VCOP + ACC \quad (\text{A. 26})$$

where FCOP, VCOP and ACC stands respectively for: Fixed Cost of Production, Variable Cost of Production, Annual Capital Charge.

Economic potential:

$$EP = Revenue - TAC - taxes \quad (\text{A. 27})$$

where Revenue is calculated from the sales of the product.

Capital cost:

$$C_e = a + b * S^n \quad (\text{A. 28})$$

where  $C_e$  is the purchase cost of the equipment,  $a$  and  $b$  are cost related constants,  $S$  is a constant related to the size of the equipment and  $n$  is an exponent depending on the type of equipment.



Total capital cost:

$$TCC = \sum_i C_{e,i} * f_i \quad (\text{A. 29})$$

where  $f_i$  is the installation factor of the individual equipment  $i$ .

Glycerol's conversion:

$$\text{Conversion} = 1 - \frac{[\text{Glycerol}]_{\text{product}}}{[\text{Glycerol}]_{\text{reactant}}} * 100 \quad (\text{A. 30})$$

Selectivity to product X:

$$\text{Sel. to X} = \frac{[X]}{[\text{Glycerol}]_{\text{reactant}} - [\text{Glycerol}]_{\text{product}}} * \frac{\text{no. of C atoms in X}}{3} * 100 \quad (\text{A. 31})$$



## 9 References

Anitha M., Kamarudin S.K., Kofli N.T. (2016). The potential of glycerol as a value-added commodity. *Chemical Engineering Journal*, 295: 119–130.

Avasthi K.S., Reddy R. N. and Patel, S. (2013). Challenges in the production of hydrogen from glycerol-a biodiesel byproduct via steam reforming process. *Procedia Engineering*, 51: 423–429.

Badwal S., Giddey S., Munnings C. (2013). Hydrogen production via solid electrolytic routes. *Wiley Interdisciplinary Reviews: Energy and Environment*, 2(5): 473–487.

Charisiou N.D., Siakavelas G., Papageridis K.N., Baklavaridis A., Tzounis L., Polychronopoulou K., Goula M.A. (2017). Hydrogen production via the glycerol steam reforming reaction over nickel supported on alumina and lanthana-alumina catalysts. *International Journal of Hydrogen Energy*, 42: 13039–13060.

Charisiou N.D., Papageridis K.N., Siakavelas G., Sebastian V., Hinder S.J., Baker M.A., Polychronopoulou K., Goula M.A. (2019). The influence of SiO<sub>2</sub> doping on the Ni/ZrO<sub>2</sub> supported catalyst for hydrogen production through the glycerol steam reforming reaction. *Catalysis Today*, 319: 206–219.

Chen M., Zhou Z., Wang Y., Liang T., Li X., Yang Z., Chen M., Wang J. (2018). Effects of attapulgite-supported transition metals catalysts on glycerol steam reforming for hydrogen production. *International Journal of Hydrogen Energy*, 43: 20451–20464.

Cormos, C.C. and A.M. (2017). Techno-economic and environmental performances of glycerol reforming for hydrogen and power production with low carbon dioxide emissions. *International Journal of Hydrogen Energy*, 42: 7798–7810.

Gonzalez-Garay A., Gonzalez-Miquel M., Guillen-Gosalbez G. (2017). High-value propylene glycol from low-value biodiesel glycerol: A techno-economic and environmental assessment under uncertainty. *ACS Sustainable Chemistry & Engineering*, 5: 5723–5732.

Hoşgün H.L., Yıldız M., Gerçel H.F. (2012). Hydrogenolysis of Aqueous Glycerol over Raney Nickel Catalyst: Comparison of Pure and Biodiesel By-Product. *Industrial & Engineering Chemistry Research*, 51(10): 3863–3869.

International Programme on Chemical Safety (1990<sup>a</sup>). *Environmental Health Criteria 102: 1-propanol*. [online] Available at: <http://www.inchem.org/documents/ehc/ehc/ehc102.htm> [accessed 30 March 2019]

International Programme on Chemical Safety (1990<sup>b</sup>). *Environmental Health Criteria 103: 2-propanol*. [online] Available at: <http://www.inchem.org/documents/ehc/ehc/ehc103.htm> [accessed 30 March 2019]

Internal Revenue Service (2019), *Yearly average currency exchange rates*. [online] Available at: <https://www.irs.gov/individuals/international-taxpayers/yearly-average-currency-exchange-rates> [accessed 28.03.2019]

Lavikainen, L. (2016). *The structure and surfaces of 2:1 phyllosilicate clay minerals*. Ph.D. thesis. Joensuu, University of Eastern Finland. [online] Available at: [http://epublications.uef.fi/pub/urn\\_isbn\\_978-952-61-2122-2/urn\\_isbn\\_978-952-61-2122-2.pdf](http://epublications.uef.fi/pub/urn_isbn_978-952-61-2122-2/urn_isbn_978-952-61-2122-2.pdf) [accessed 19.02.2019]

Li C., He B., Ling Y., Tsang C.W., Liang C. (2018). Glycerol hydrogenolysis to n-propanol over Zr-Al composite oxide-supported Pt catalysts. *Chinese Journal of Catalysis*, 39: 1121–1128.

Lin, Yu-Chuan (2013). Catalytic valorization of glycerol to hydrogen and syngas. *International Journal of Hydrogen Energy*, 38: 2678–2700.

Lin X., Lv Y., Xi Y., Qu Y., Phillips D.L., Liu C. (2014). Hydrogenolysis of Glycerol by the Combined Use of Zeolite and Ni/Al<sub>2</sub>O<sub>3</sub> as Catalysts: A Route for Achieving High Selectivity to 1-Propanol. *Energy&Fuels*, 28: 3345–3351.

Markets and Markets (2013). *Propanol market by applications & geography - Trends and forecasts to 2018*. [online] Available at: <https://www.marketsandmarkets.com/Market-Reports/isopropyl-alcohol-and-n-propanol-market-1113.html> [accessed 30 March 2019]

Menezes J.P., Manfro R.L., Souza M.M.V.M. (2018). Hydrogen production from glycerol steam reforming over nickel catalysts supported on alumina and niobia: Deactivation process, effect of reaction conditions and kinetic modeling. *International Journal of Hydrogen Energy*, 43: 15064–15082.

Nanda M.R., Yuan Z., Xu W.Q. & C. (2016). Recent advancements in catalytic conversion of glycerol into propylene glycol: A review. *Catalysis Reviews*, 58(3): 309–336.

National Center for Biotechnology Information (2019<sup>a</sup>). *Glycerol*, CID=753. [online] Available at: <https://pubchem.ncbi.nlm.nih.gov/compound/753> [accessed 09 February 2019]

National Center for Biotechnology Information (2019<sup>b</sup>). *Propylene glycol*, CID=1030. [online] Available at: <https://pubchem.ncbi.nlm.nih.gov/compound/1030> [accessed 07 April 2019]

National Center for Biotechnology Information (2019<sup>c</sup>). *1,3-Propanediol*, CID=10442. [online] Available at: <https://pubchem.ncbi.nlm.nih.gov/compound/10442> [accessed 07 April 2019]

National Center for Biotechnology Information (2019<sup>d</sup>). *1-Propanol*, CID=1031. [online] Available at: <https://pubchem.ncbi.nlm.nih.gov/compound/1031> [accessed 30 March 2019]

National Center for Biotechnology Information (2019<sup>e</sup>). *Isopropyl alcohol*, CID=3776. [online] Available at: <https://pubchem.ncbi.nlm.nih.gov/compound/3776> [accessed 30 March 2019]

Nowak I. and Ziolk M. (1999). Niobium Compounds: Preparation, Characterization, and Application in Heterogeneous Catalysis. *Chemical Reviews*, 99: 3603–3624.

OECD-FAO (2017). *Agricultural Outlook 2017-2026*. [online] Available at: <https://stats.oecd.org/index.aspx?queryid=76849#> [Data extracted 07 February 2019]

Sad M.E., Duarte H.A., Vignatti C., Padró C.L., Apesteguía C.R. (2015). Steam reforming of glycerol: Hydrogen production optimization. *International Journal of Hydrogen Energy*, 40: 6097–6106.

Samudrala S.P. and Bhattacharya S. (2018). Toward the Sustainable Synthesis of Propanols from Renewable Glycerol over MoO<sub>3</sub>-Al<sub>2</sub>O<sub>3</sub> Supported Palladium Catalysts. *Catalysts*, 8(9): 385.

Schwengber C.A., Alves H.J., Schaffner R.A., da Silva F.A., Sequinel R., Bach V.R., Ferracin R.J. (2016). Overview of glycerol reforming for hydrogen production. *Renewable and Sustainable Energy Reviews*, 58: 259–266.

van Ryneveld E., Mahomed A.S., van Heerden P.S., Green M.J., Friedrich H.B. (2011). A catalytic route to lower alcohols from glycerol using Ni-supported catalysts. *Green Chemistry*, 13: 1819–1827.

Zhao Y., Shuzhuang L., Yuanyuan Z., Ting W., Shizhong L., Wei C., Fangli J. (2019). The role of Zr in NiZrAl oxides catalyst and the evaluation on steam reforming of glycerol for hydrogen product. *Catalysis Today*, 319: 229–238.

Zhu S., Zhu Y., Hao S., Zheng H., Mo T., Li Y. (2012). One-step hydrogenolysis of glycerol to biopropanols over Pt-H<sub>4</sub>SiW<sub>12</sub>O<sub>40</sub>/ZrO<sub>2</sub> catalysts. *Green Chemistry*, 14(9): 2607–2616.







**Norges miljø- og biovitenskapelige universitet**  
Noregs miljø- og biovitenskapelige universitet  
Norwegian University of Life Sciences

Postboks 5003  
NO-1432 Ås  
Norway